IMPACT OF CLIMATE CHANGE ON SEDIMENT FLOWS BY USING SPATIAL DISTRIBUTED MODELING FOR SELECTED CATCHMENTS IN UPPER INDUS BASIN

By:

MOIEN AHSAN
(2014-Ph.D-WRE-02)

FOR THE DEGREE OF

DOCTOR OF PHILOSOPHY

IN

WATER RESOURCES ENGINEERING

FACULTY OF CIVIL ENGINEERING

CENTRE OF EXCELLENCE IN WATER RESOURCES ENGINEERING

University of Engineering and Technology, Lahore, Pakistan

2019

This thesis was evaluated by the following national and international examiners:

External Examiners:

From Abroad:

1. Professor Tan Minggao, Professor, Research Centre of Fluid Machinery Engineering and Technology, Jiangsu University, 301 Xuefu Lu.Zhenjinag Shi, Jiangsu, P. R. China Email: tmgwxf@ujs.edu.cn

2. Prof. Dr. Harald Kachele, Associate Professor, Scientific Staff in Research Area 2 "Land Use and Governance", Leibniz-Centre for Agricultural Landscape Research (ZALF), Muncheberg, Germany Email: Harald.Kaechele@zalf.de

3. Dr. Hj. Khamaruzaman b Hj. Wan Yusof, Associate Professor, Civil Engineering Department, Universiti Teknologi PETRONAS, Bandar Seri Iskandar, 31751, Perak Danul Ridzuan, Malaysia Email: kzaman.wyusof@gmail.com

From Pakistan:

1. Prof. Dr. Hashim Nisar Hashmi, Vice Chancellor, University of Engineering and Technology, Taxila Email: hashim.nisar@uettaxila.edu.pk

2. Prof. Dr. Iftikhar Ahmad, Professor, College of Earth & Environmental Sciences Punjab University, Lahore Email: hydromod@yahoo.com

Internal Examiner:

Prof. Dr. Abdul Sattar Shakir, Dean, Faculty of Civil Engineering, University of Engineering and Technology, Lahore Email: shakir@uet.edu.pk

ABSTRACT

Climate is globally changing at an alarming rate and the river flows are directly affected by the rainfall patterns and snowmelt. The discharge in river, rainfall intensity and erodibility affects the soil erosion and sedimentation. The soil which erodes from one place is transported to another with the water and settles down which adversely affects the water availability, reducing the storage capacity of reservoirs. As per IPCC (2013) earth's general temperature has been increased up to 0.89 °C from 1901 to 2012. The increase in temperature has significant effect on precipitation and glacier melts which may cause increase or decrease in discharge and sediment yield of any basin so it is very important to access the relationship between the climatic parameters and their impact on discharge & sediment yield. This study investigated the assessment of hydro-meteorological parameters in upper Indus Basin using the available historical data and their impact on snow cover and glaciers of Gilgit & Ghorband river basins. Furthermore, the climate model SDSM was applied on seven stations for projection of the future climate at the end of 21th century (2099). The output of the model was fed into SWAT model to access the impact of climate change on discharge and sediment.

Statistical test has been applied on historical climate data and result has indicated that in upper region (snow covered) of UIB the annual maximum temperature is increasing whereas, in lower region it is decreasing. Tmax is increasing more than Tmin. Temperature in Winter and Spring season is also increasing at most of the stations. Annual and seasonal precipitation in the region is increasing; it

increases with the increase in elevation and decreases with decrease in elevation. Average Annual flows in highly elevated areas (Snow Cover)/ tributaries is increasing and in low elevated region it has decreased whereas, during the winter and spring season monthly flow has been increased due to the increase in temperature (earlier melt of snow), during the summer it has decreased due the decrease in temperature,. Annual and seasonal snow cover area has decreased in Ghorband river catchment, annual and seasonal snow cover area has also increased in Gilgit river basin. At the end of 21st century in Gilgit river basin annual temperature estimated to be increased by 2.33 ^{0}C, which may increase surface runoff and sediment yield 14 and 24 % respectively. In Ghorband river catchment annual temperature estimated to increase 1.99 ^{0}C, may increase in surface runoff and sediment yield 13 and 20 % respectively by the end of 21st century which lead to the primary outcome of this research.,

Furthermore, Options for the reduction of erosion and consequent sediment origination control were simulated and compared. The provision of sediment basin for management of sediment yield in the Gilgit and Ghorband river basin can reduce sediment yield upto 65%. Analysis of temperature, precipitation and stream flow that the phenomenon of the climate change has been occurring in the upper Indus basin and has significant effect on mountainous watershed, as aforesaid situation is alarming for the planner and water experts to guide and adopt the Integrated Watershed Management to fulfill the fore coming food and water demands. Thus, it is recommended that climate change study should preferably be made prior to the construction of water resources & agriculture related projects

.

ACKNOWLEDGEMENTS

All the acclamation and appreciation are for ALMIGHTY ALLAH, the most compassionate and merciful, who knows whatever is there in the universe, hidden or evident and is entire source of all knowledge and wisdom to mankind. I offer my humblest thanks to HOLY PROPHET HAZRAT MUHAMMAD (peace be upon him), who enabled me to recognize our Creator and declared it to be an obligatory duty of every Muslim to seek knowledge.

I feel highly privileged in taking this opportunity to express my sincerest thanks to my esteemed supervisor Prof. Dr. Abdur Sattar Shakir for his dexterous supervision, impetus guidance, valuable and expert suggestions, and sympathetic attitude throughout the progress of my study. He always remained a great source of inspiration and motivation to me, and provided me with all the resources I needed.

I am also very grateful to the Director, Prof. Dr. Habib Ur Rahman for providing me such a wonderful and learning environment at CEWRE.

I owe debt of gratitude to Dr. Ghulam Nabi, Co-Supervisor for his constant interest, invigorating encouragement and valuable suggestions during my thesis work.

The author is gratefully acknowledged to Higher Education Commission of Pakistan for providing financial support for this research. Furthermore, the PMD, WAPDA for providing the time series of data for this study

It is great privilege for me to record my heartiest and sincerest thanks to my better half Miss Sonia Zafar (Assistant Director Technical, BS-18) for her sincerest encouragement, data typing and valuable suggestions.

My sincere thanks also goes to Muhammad Tanveer (Junior Engineer MMP), Arslan Arshad and Tahira khurshid (PhD Scholar, PU) for giving me time on a number of occasions and valueable concepts regarding my research.

I am indebted to Dr. Muhammad Ijaz Ahmad (Assistant Professor CEWRE) and Dr. Muhammad Yasin (Assistant Professor CIMR, PU) for the stimulating discussions and the sleepless nights when we were working together before deadlines, for all the fun and for very silly fights we had in the last 4 years.

A heartiest thanks goes to my loving and sweet mother Hameeda Bibi for her moral and financial assistance, Love you my sweat mother. My affectionate and loving brothers Mr. Amar Aziz, Tariq Aziz , Abdullah Aziz and Sajid Aziz for their prayers, amicable attitude and their inspiration which happens to be the sprinkling candle in the darkness. They always encouraged me whenever I was demoralized during my academic career.

Last but not least, my sincere thanks to my beloved daughter Hareem Fatima and those whom I could not name but their prayer and love always holds me in my difficult times.

May Allah almighty bless us all!

(**Engr. Moien Ahsan)**

0334-4415225

DEDICATION

THE THESIS IS DEDICATED

TO MY FATHER (LATE)

TABLE OF CONTENTS

Chapter No. Description **Page #**

Table of Contents (Continued)

Table of Contents (Continued)

Table of Contents (Continued)

LIST OF TABLES

LIST OF FIGURES

LIST OF ABBREVIATIONS

AOGCMs	Atmosphere Ocean General Circulation Models
ASTER	Advanced Space borne Thermal Emission & Radiometer
BC	Bias Correction
CEWRE	Centre of Excellence in Water Resource Engineering
DEM :	Digital Elevation Model
ET	Potential evapotranspiration
FDC	Flow Duration Curve
GCM :	General Circulation Model
GDP	Gross domestic product
GIS	Geographic Information System
HEC-HMS	Hydrological Modeling System
HKH	Hindu Kush-Karakoram-Himalayan
HRUs	Hydrologic Response Units
IPCC	Intergovernmental Panel of on Climate Change
IRS	Indus River System
IRS	Indus River System
IRSA	Indus River System Authority
MODIS	Moderate Resolution Imaging Spectro radiometer
NCEP	National Centre for Environmental Prediction
NESPAK	National Engineering Services Pakistan Limited
OPPB	One Peak Precipitation basin
PMD	Pakistan Meteorological Department
RMSE	Root Mean Square Error

SDSM	Statistical Down Scaling Model
SRTM	Shuttle radar topographic mission
SWAT	Soil and Water Assessment Tool
SWHP	Surface Water hydrology Project
Tmax	Maximum Temperature
Tmin	Minimum Temperature
TPPB	Two Peak Precipitation basin
UET	University of Engineering and Technology, Lahore-Pakistan
UIB	Upper Indus Basin
WAPDA	Water and Power development Authority
WMO	World meteorological Organization

Chapter 1
INTRODUCTION

1.1 GENERAL

Pakistan is located in the Northwest of the South Asian subcontinent, lying between 24° to 37° north latitude and 61° to 75° east longitude. It borders with Iran in the west, Afghanistan in the northwest, China in the northeast, and India in the east. On the south side lies the Arabian Sea. The total land area is estimated to be 804,000 km^2.

Pakistan is among the countries most vulnerable to climate change impacts. Changing temperature, precipitation, flows, Sediments, humidity concentrations and extreme weather conditions pose serious threats to natural ecosystem of the country disrupting the performance of various sectors of the economy-agriculture being the most affected. Water availability has been reduced from 5600 m3 to 1000 m3 since 1947 (Kahlown et al., 2007).

Climatologically, most parts of Pakistan are arid to semi-arid with significant spatial and temporal variability in climatic parameters. The country has a long latitudinal extent stretching from the Arabian Sea in the south to the Himalayan Mountains in north. It is located in sub-tropics and partially in temperate region. There are the homes of about 180 Million people and probably a larger portion of those is most vulnerable to climate change. Large numbers of residents live in low coastal areas or river deltas where sea level rise and flooding are the likeliest devastating consequences of rise in global temperatures as the climate shifts(Farooqi et al., 2005).

Climate change may cause significant impacts on water resources by resulting changes in the hydrological cycle. Increasing temperature will lead to greater amounts of water vapour in the atmosphere and the hydrological cycle will be intensified with more precipitation. The extra precipitation will not be equally distributed around the globe. Some parts of the world may see significant reductions in precipitation or alterations in the timing of wet and dry seasons and would lead to increases in both floods and droughts. The extra precipitation will not be equally distributed around the globe. Some parts of the world may see significant reductions in precipitation or alterations in the timing of wet and dry seasons and would lead to increases in both floods and droughts. Quantitative estimates of the hydrological effects of climate change at local and regional scales are essential for understanding and solving the potential water resource management problems associated with water supply for domestic and industrial water use, power generation, and agriculture.

Global mean surface temperature is projected to increase by 1.4-5.8oC over the period 1990-2100. The global mean sea-level is also projected to rise in the range of 9-88 cm during the same period of time. Glacier and snow covered area plays an important role in the hydrology of glaciered basin. Climate change is likely to change the snow cover area and alter the water availability, making long term water management more challenging in future.

Fresh water resources in Pakistan are based on snow/ glacier-melt and monsoon rains, both are highly sensitive to climate change. Country specific climate change projections strongly suggest the following future trends in Pakistan:

i. Decrease in glacier volume and snow cover leading to alterations in the seasonal flow pattern of the Indus River System (IRS).

ii. Increased annual flows for a few decades followed by decline in flows in subsequent years.

iii. Increase in the formation and outburst of glacial lakes

iv. Higher frequency and intensity of extreme climate events coupled with irregular monsoon rains causing frequent floods and droughts.

v. Greater demand on water due to higher evapotranspiration rates at elevated temperatures.

These trends will have a significant impact on the spatial and temporal distribution of water resources on both annual and inter-annual basis in the country.

As per Report published by Ministry of Climate Pakistan (2012) agriculture is central to human survival and is probably the human enterprise, most vulnerable to climate change. The agriculture sector, as the single largest sector of Pakistan's economy, is its lifeline. It accounts for 45% of the labor force, 21% of GDP and 70% of total export earnings. Agriculture in Pakistan is greatly affected by short-term climate variability and could be significantly impacted by long-term climatic changes. As the duration of crop growth cycle is related to temperature, an increase in temperature will speed up crop growth and shorten the time between sowing and harvesting. This shortening could have an adverse effect on productivity of crops and fodder for livestock. The hydrological cycle is similarly likely to be influenced by global warming, necessitating the agriculture and livestock sectors particularly in rain-fed areas to adapt to climate change.

Climate change is likely to have multi-faceted adverse effects on the ecosystem as a whole particularly on the already vulnerable forestry sector in Pakistan. The most likely impacts of climate change are decreased productivity, changes in species composition, reduced forest area, unfavorable conditions for

biodiversity, higher flood risks and increase in sediment load in the river due to intense rainfall events.

The most likely climate change risks to the mountain areas of Pakistan are increase in frequency and intensity of precipitation, resulting in more frequent flash floods and landslides. Increase in intensity of wind storms and lightning, resulting in top soil erosion and forest fires, Increase in temperature, resulting in rapid glacier melting and glacial lake outburst floods (GLOFs) and change in cropping patterns. Sedimentation in river basins should be closely monitored due to its negative effects on the rivers, reservoirs, hydropower and the surrounding community residing in these areas. Sediments can be reduces by proper watershed management. The sediment load of a river is sensitive to both, climate change and a wide range of human activities within its drainage basin. The potential future changes in sediment load is considered as an important requirement for sound river basin management (Walling, 2008). Climate variability may influence hydro-sediment logical processes, given that the main climate variables such as precipitation, radiation and temperature, affect stream flow and sediment dynamics.

1.2 CATCHMENT MODELING

The relationship between direct runoff and rainfall may be considered to have three aspects:

- The relation between the volume of rainfall in a given storm and resulting volume of direct runoff.
- The relation between the hydrograph of direct runoff and time distribution.
- The relation between rainfall frequency and discharge frequency (Vijay, 1988).

1.2.1 Lumped Models

A Lumped model considers the whole catchment as a single unit. Hydrological parameters are averaged for the watershed. For example, Slope elevation, soil type, land cover and all other associated properties. Lumped parameter models don't explicitly take into account the spatial variability of inputs, output or parameters. They take all the data for sub-catchment and combine it into a single number or set of numbers, that define the response of the basin to certain inputs. This model is not suitable for spatial GIS database. However, GIS-based spatial parameters can be lumped to run lumped parameter watershed models. Examples of Lumped Model are the Stanford Watershed Model (SWM) and Hydrological Modeling System (HEC-HMS).

1.2.2 Distributed Models

Distributed models consider spatial variation in inputs and parameters in general, the watershed area is divided into a number of elements and water balance component are first calculated separately for each element. Data for each element inside the watershed is used to compute surface and subsurface flows within that element accumulative at outlet. These are calculated by accumulating and routing upslope flows. These models are suited with spatial database (GIS databases).The example of distributed model is System Hydrological European Model (SHE).

1.2.3 Semi-Distributed Models

In this type of model some parameters are lumped and some parameters are distributed and these models use conceptual functional relationships for different hydrological processes applied to a number of relatively homogeneous subareas of the

catchment which are treated as lumped units. Semi distributed model widely used is TOPMODEL.

The study is conducted in the selected sub catchments of Upper Indus Basin. The Indus river carries a highest sediment load in the world. It is necessary to reduce the sediment flows from the catchment. In this study impact of the climate change on the sediment flows and climate parameters i.e precipitation and temperature will be accessed and than watershed management techniques will be suggested to increase the life of dams on the basis of future forecasting/ under the climate change Scenarios.

1.3 PROBLEM STATEMENT

In recent decades, extreme climatic events have been a major issue worldwide. Regional assessments on various climates and geographic regions are needed for understanding uncertainties in extreme events' responding to global warming.

As a country particularly vulnerable to the adverse impacts of climate change, Pakistan cannot afford to ignore the threat it poses to its economy and socio-political stability. To date, despite overwhelming evidence of this threat, Pakistan’s response has been poor. The issue of climate change is not captured in the country’s overall economic planning. Integrating climate change concerns in our national economic strategies necessitates both a national climate change policy and institutional arrangements, for its implementation.

Pakistan is one of the countries most vulnerable to the effects of climate change in the future. From the Himalayas to the Indus River Basin, deserts and coastal areas of Sindh & Baluchistan, the people of Pakistan will pay a heavy price if resolute action is not taken here and on a global scale. Climate change is expected to increase seasonal/ annual rainfall and temperature in future. As per National Climate Change Policy (2012) the climate change threats to the Pakistan are considerably increased in the frequency and intensity of extreme weather events coupled with erratic monsoon rains causing frequent and intense floods and droughts. Projected recession of the Hindu Kush-Karakoram-Himalayan (HKH) glaciers due to global warming and carbon soot deposits from trans-boundary pollution sources, threatening water inflows into the Indus River System (IRS). Increased siltation of major dams caused by more frequent and intense floods; Rising temperatures resulting in enhanced heat and water-stressed conditions, particularly in arid and semi-arid regions, leading to reduced agricultural productivity; Further decrease in the already scanty forest cover, from too rapid change in climatic conditions to allow natural migration of adversely affected plant species; Increased intrusion of saline water in the Indus delta, adversely affecting coastal agriculture, mangroves and the breeding grounds of fish; Threat to coastal areas due to projected sea level rise and increased cyclonic activity due to higher sea surface temperatures; Increased stress between upper riparian and lower riparian regions in relation to sharing of water resources.

It is very important to develop guidelines for evaluating climate change effects on sediment flows and operations for various water resource projects. Pakistan cannot afford to ignore the threat of climate change to its economy and socio-political stability. To date, despite overwhelming evidence of this threat, Pakistan’s response

has been poor. For the planning & development of water related projects detailed analysis of climate & flows condition of upper catchments is ultimate need of time, as the UIB comprises 198,000 Km2, for simplicity present study has been conducted in the selected catchments of Upper Indus basin whereby, impact of the climate change on the temperature, precipitation, flows and sediments is analyzed by using distributed GIS based techniques

This study will address the effect of inflows and alterations in sediment flows regime associated with climate change for the selected catchments in Upper Indus Basin. Therefore, the ability to understand the hydrologic response of climate change will help policy makers to guide planning and form more resilient infrastructure in the future. It will be important to avoid the temptation to give into short-sighted solutions, which while addressing the energy deficit on the short term will hamper development of cheap green solutions. So it is necessary to minimize the risks arising from the expected increase in frequency and intensity of extreme weather events such as floods, droughts and tropical storms. To promote conservation of natural resources and long term sustainability.

1.4 OBJECTIVES OF RESEARCH

The objectives of the study are given below:

- Assessment of change in Climate parameters i.e. Precipitation, Temperature and their impact on land use changes.
- Modeling in climate change impact on runoff and sediment yield in upper Indus basin catchments.
- Projection of climate change scenarios for potential change inland use and sediment flows of selected area and management options under changed climate conditions.

To achieve the above mentioned objectives, start with a preliminary analysis (trend analysis) of the available historical gauge hydro-meteorological data and the land use change i.e. to estimate the variation in the snow cover in study area MODIS (MOD10A2) data has been used. The hydrological and climate data are treated and discussed for better understanding of the hydrological regime of the area. Modeling the impact of climate change on the sediment an appropriate model (SWAT model) has been selected which simulates the historical changes in sediments yields for Gilgit and Ghorband Rivers. Precipitation, temperature, topography (digital elevation model), land use / cover and soil data are used to simulate the discharge and sediment by SWAT model.

Statistical downscaling model (SDSM) model is used downscale climate variables (precipitation and temperature) to use as input of selected hydrological model climate change analysis (sediment flow). The climate and land-use change components are integrated into SWAT to develop an integrated framework for the prediction of changes in stream flow and sedimentation in the future. The scenarios have generated at the end of 21st century and different sediment management options are discussed for the water managers & planners for the planning and development of water sector projects.

1.5 LIMITATIONS OF RESEARCH

- Climate change can affect both quantity and quality of water but this study is limited to the quantitative analysis of meteorological and hydrological parameters of selected region. Qualitative analysis has not been done in this research.

- It is assumed that landuse and soil type to be same in all future time steps.

- Regional Scale model has been used for the projection of climate.

1.6 THESIS OUTLINE

This thesis consists of five chapters which are organized as follows:

- Chapter I Introduction
- Chapter II Review of Literature
- Chapter III Study Area, Data Base
- Chapter IV Methodology
- Chapter V Results and Discussion
- Chapter VI Summary, Conclusions and Recommendations

Chapter 2
LITERATURE REVIEW

2.1 GENERAL

This chapter includes the review of previous studies related the statistical tests for trend analysis, climate change, sediment modelling, Land use changes, down scaling the rainfall and temperature. Change in climate parameters i.e. temperature, precipitation and its impact on flows and sediment yield is also described. A brief outlines of the chapter is given below:

1. Global Climate Change Studies
2. Overview of Climate Change in Pakistan
3. Statistical Tests for trends analysis
4. Land Use / Cover Change
5. Climate change and Sedimentation in Catchments/basin
6. Description of Distributed SWAT model
7. Downscaling Techniques / Models

2.2 GLOBAL CLIMATE CHANGE STUDIES

Various studies are available on climate change and its impact on all around the world. The climate change is occurring globally and there is severe need to review its reasons and analyze its impacts. In recent years, public concern about the consequences of global climate change to natural and socio-economic systems has increased (IPCC AR4, 2008). The assessment of the impact of future climate change on climate affected systems (water resources, agricultural yields, and energy and transport systems) requires climate scenarios in a high spatial resolution. Being one of

the very sensitive parameter, climate change can cause significant impacts on water resources by resulting changes in the hydrological cycle (Bates et al., 2008; Archer and Fowler, 2004).

2.2.1 Global Change in Temperature, Precipitation and Flows

The changes on temperature and precipitation components of the cycle have a direct consequence on the quantity of evapotranspiration component and on both quality and quantity of the runoff component. Consequently, the spatial and temporal water resource availability or in general the water balance, can be significantly affected which clearly amplifies its impact on sectors like agriculture, industry and urban development. Changing climate will also have significant impacts on the availability of water as well as the quality & quantity of water that is available & accessible.

Gautam et al., (2010) used the non-parametric approach for the auto-correlation of Jhikhu Khola Watershed (JKW) in Nepal and the analysis showed that annual average, maximum, and minimum flows are increasing. This increase in stream flow coincides with the increasing rainfall trend of the yearly monsoon (June–September) and pre-monsoon (March–May) periods. The post-monsoon (October–February) period does not show any statistical trend. No consistent trend is observed in temperature changes for the whole watershed.

As per Intergovernmental Panel on Climate Change (IPCC) (IPCC, 2008), the global average surface temperature has increased by 0.074°C (± 0.018°C) and 0.13°C (± 0.03°C) per decade over the last 100 years (1906–2005) and 50 (1956-2005) years,

respectively. Since 1981, the rate of warming is faster, with a value of approximately 0.177 °C (±0.052°C) per decade.

Hannaford and Buys (2012) analyzed the impacts of climate change on seasonal river flows of 89 catchments around the UK and used approximately 39 (1969–2008) years data. He categorized the trends into four seasons for the analysis (March-May, June-August, September-November, December-February). Spatial patterns in observed trend magnitude for median, high and low flows were analyzed by using the trend analysis. Some findings resonate with observed rainfall changes and also with potential future climate changes e.g. increased runoff and high flows in winter and autumn, and decreased flows in spring.

Wing et al., (2008) carried a study on trend analysis of annual and seasonal rainfall in Ethiopia at national and watershed scales and found no significant changes/ trends in annual rainfall at the national or watershed level in Ethiopia between 1960 and 2002. Trends in Belg season (from March to May) rainfall did not display any significant changes over the study period, while in Kiremt (from June to September) rain was decreasing in some watershed.

Climate change is happening in China over the last century. The average temperature has increased by 1.1°C from 1951 to 2001 (Ding et al., 2007) and the warming trend has become significant since the 1980s (Edition broad of national assessment report for climate change in China, 2007). On the other hand, reduction in diurnal temperature range (DTR) has been observed widely. This trend indicates that the increase in temperature is greater at night than in the daytime.

Kumar et al., (2009) analyzed the high, medium, seasonal low and annual flows of Indian catchments by using four variations of the Mann-Kendall test. These variations includes:

(I) Mann–Kendall without autocorrelation

(ii) Mann-Kendall with lag-1 autocorrelation and trend-free pre-whitening

(iii) Mann–Kendall with complete autocorrelation structure

(iv) Mann–Kendall with long term persistence.

Mann- Kandal test was also applied on the precipitation to check the relationship between precipitation and discharge. It was conclude that there are increasing medium and low flows conditions.

Fischer et al (2010) precipitation and temperature data to identify the climate change in Zhujiang River Basin, South china and collected the daily data for 47 years (1961-2007) for 92 stations. For the analysis, categorized two temperature indicators i.e. monthly maximum mean & monthly mean and three precipitation indicators i.e. monthly total, monthly maximum consecutive 5-day precipitation and monthly dry days. Many stations show significant positive trends (above the 90% confidence level) for monthly mean temperatures and monthly maximum mean temperatures. It can be observed that temperature has increased significantly particularly in the coastal areas of the Zhujiang River Basin. Positive trends of precipitation extremes can be observed from January to March. Negative trends are detected from September to November. The number of dry days in October increased significantly at 40% of all meteorological stations. An aggregation of heat waves and droughts can be detected

which is accompanied by significant increases of temperature extremes and the negative tendencies in precipitation extremes.

Chang and Jung (2010) have estimated the potential changes in annual, seasonal, and high and low runoff and associated uncertainty in the 218 sub-basins of the Willamette River basin of Oregon for the 2040s and the 2080s. The US Geological Survey's Precipitation–Runoff Modeling System (PRMS) was calibrated and validated for representative river basins between 1973 and 2006. They used a combination of eight general circulation models (GCMs) and two emission scenarios downscaled to 1/160 resolution to estimate spatial and temporal changes in future runoff at a sub-basin scale. The seasonal variability of runoff is projected to increase consistently with increases in winter flow and decreases in summer flow. These trends are amplified under the A1B emission scenario by the end of the 21st century with increases in top 5% flow and decreases in 7-day low flow. Streams flowing from High Cascade basins that contain a large component of groundwater are projected to sustain summer flows, although the uncertainty associated with future projections is high. The main source of uncertainty stems from GCM structure rather than emission scenarios or hydrologic model parameters, but the hydrologic model parameter uncertainty for projecting summer runoff and 7-day low flow is relatively high for Western Cascade basins.

Tao et al., (2011) applied the non-parametric trend approach on the Tarim River Basin, China and collected the annual data of 39 weather stations and 29 hydrological stations for the period 1961–2008 and 1952–2008, respectively. Analysis shows an increasing trend of precipitation, vapour pressure, relative humidity, and the

aridity index since 1986. Surface temperature has started increasing in 1996. A decreasing trend in sunshine was started in 1990. The potential evapotranspiration (ET) was calculated by using the Penman–Monteith equation, and decreasing trend of potential evapotranspiration has been observed since 1985. This negative trend can also be detected for wind speed in both the same time scale and spatial extent. The stations with significant increasing trends in annual stream flow are mainly distributed at the southern slope of Tianshan Mountain, which can only be explained by climatic changes. The detected negative runoff trend of the main stream of the Tarim River can be explained by anthropogenic activities (such as irrigation and domestic water use) and climatic changes. A quantitative assessment reveals that local human activities since the 1970s led to a decrease of the water volume diverted into the main stream of the Tarim River Basin, which has been aggravated in the 2000s.

Lorenzo et al., (2012) analyzed stream flow trends in 187 sub-basins in the Iberian Peninsula for the period 1945–2005. A database of monthly river discharges for the entire Iberian Peninsula including natural and regulated river regimes enabled assessment of the magnitude and spatial patterns and mechanisms of the hydrological trends. Annual and seasonal trend analyses were conducted. The results showed a marked decrease in annual, winter, and spring stream flows in most of the Iberian sub-basins, especially those in the south. In addition, changes in the seasonality of river regimes have occurred, most of them as consequence of dam regulation and water management strategies. We showed how river regulation by dams does not affect the sign of the trends, but its magnitude, by decreasing the releases during winter to meet the demand of water in summer creating important seasonal differences. The decrease of stream flows during the second half of the Twentieth Century in the Iberian

Peninsula may accelerate in coming decades, as future climate projections show a generalized decrease in precipitation and more evapotranspiration induced by higher temperatures.

Sonali and Kumar (2013) performed the spatial and temporal trend analysis of annual, monthly and seasonal maximum and minimum temperatures in India. Recent trends in annual, monthly, winter, pre-monsoon, monsoon and post-monsoon extreme temperatures have been analyzed for three time slots viz. 1901–2003, 1948–2003 and 1970–2003. For this purpose, time series of extreme temperatures of India as a whole and seven homogeneous regions, viz. Western Himalaya (WH), Northwest (NW), Northeast (NE), North Central (NC), East coast (EC), West coast (WC) and Interior Peninsula (IP) are considered. Rigorous trend detection analysis has been exercised using variety of non-parametric methods which consider the effect of serial correlation during analysis. During the last three decades minimum temperature trend is present in all India as well as in all temperature homogeneous regions of India either at annual or at any seasonal level (winter, pre-monsoon, monsoon, post-monsoon). Sequential MK test reveals that most of the trend both in maximum and minimum temperature began after 1970 either in annual or seasonal levels.

Chen et al., (2014) tried to accessed the impact of human occupation and the intensity of human impacts changes on the hydrology of the Yangtze River in China, they analysed both the annual flows of the Yangtze River and annual temperature and precipitation for the Yangtze catchment for the period 1955– 2011 and for the three sections of the catchment, Upper, Middle and Lower as defined by the location of the gauging stations at Yichang, Hankou and Datong respectively. Mean annual

temperature increases downstream from 12.7 oC in the Upper to 16.0 oC in the Lower section. A significant increasing trend in mean annual temperature is detected over the period 1955–2011 in the whole catchment and all subsections. Mean annual precipitation for the whole catchment is 1045 mm ranging from 859 mm in the elevated Upper section to 1528 mm in the Lower section. Precipitation variability is low by world standards with an annual Cv of 0.066. Using the Mann–Kendal and Rank Sums tests they have not find any trend in precipitation in the catchment. Mean annual runoff for the whole catchment is 515 mm ranging from 421 mm in the Upper Catchment to 838 mm in the Lower Catchment. Runoff variability is also low by world standards with an annual runoff Cv of 0.129. For the Middle Catchment we find a small but statistically significant increase in runoff and the runoff ratio over the period 1955–2011, possibly caused by change in the nature of the surface due to accelerated urbanization post 1980 and increased area of water storage. Overall, annual runoff in the Yangtze River shows little response to the major changes occurring in the basin. In a multiple correlation analysis of discharge, precipitation, dam volume, population and GDP, only precipitation is significantly correlated with discharge, explaining 80% of the variance.

Sun et al., (2016) assessed the annual and decadal trends in 12 extreme temperature and 10 extreme precipitation indices in terms of intensity, frequency, and duration over the Loess Plateau of China during 1960–2013. The results of study indicated that the regionally averaged trends in temperature extremes were consistent with global warming. The occurrence of warm extremes, including summer days (SU), tropical nights (TR), warm days (TX90), and nights (TN90) and a warm spell duration indicator (WSDI), increased by 2.76 (P b 0.01), 1.24 (P b 0.01), 2.60

(P=0.0003), 3.41 (P b 0.01), and 0.68 (P=0.0041) days/decade during the period of 1960–2013, particularly, sharp increases in these indices occurred in 1985–2000. Over the same period, the occurrence of cold extremes, including frost days (FD), ice days (ID), cold days (TX10) and nights (TN10), and a cold spell duration indicator (CSDI) exhibited decreases of −3.22 (P b 0.01), −2.21 (P = 0.0028), −2.71 (P = 0.0028), −4.31 (P b 0.01), and −0.69 (P = 0.0951) days/decade, respectively. Moreover, extreme warm events in most regions tended to increase while cold indices tended to decrease in the Loess Plateau, but the trend magnitudes of cold extremes were greater than those of warm extremes. The growing season (GSL) in the Loess Plateau was lengthened at a rate of 3.16 days/decade (P b 0.01). Diurnal temperature range (DTR) declined at a rate of−0.06 °C /decade (P=0.0931). Regarding the precipitation indices, the annual total precipitation (PRCPTOT) showed no obvious trends (P=0.7828). The regionally averaged daily rainfall intensity (SDII) exhibited significant decreases (−0.14 mm/day/decade, P= 0.0158), whereas consecutive dry days (CDD) significantly increased (1.96 days/decade, P=0.0001) during 1960–2013.Most of stations with significant changes in SDII and CDD occurred in central and southeastern Loess Plateau. However, the changes in days of erosive rainfall, heavy rain, rainstorm, maximum 5-day precipitation, and very-wet-day and extremely wet-day precipitation were not significant. Large-scale atmospheric circulation indices, such as the Western Pacific Subtropical High Intensity Index (WPSHII) and Arctic Oscillation (AO), strongly influences warm/cold extremes and contributes significantly to climate changes in the Loess Plateau. The enhanced geo-potential height over the Eurasian continent and increase in water vapor divergence in the rainy season have contributed to the changes of the rapid warming and consecutive drying in the Loess Plateau.

Addis et al., (2016) has applied SWAT model on high lands of Ethopia and estimated the stream flow and sediment yield. Further, they applied SWAT-Cup for auto-calibration of results. The resulting Nash-Sutcliffe efficiency (NSE) for daily streamflow simulation was 0.56 for the calibration and 0.48 for the validation period, suggesting satisfactory model performance.

The main goal of this study was to present a basic methodology to calibrate sub-hourly SWAT models using SWAT-Cup. SWAT model was tested using data from Blunn Creek watershed in Australia, Texas. The mode; was calibrated and evaualted using two separate resprestnataive periods bricking hydrologic conditions experienced in watershed. Results showed that the sub-daily SWAT provides reasonable estimates of stream flow for multiple storm events.

2.3 OVERVIEW OF CLIMATE CHANGES IN PAKISTAN

As per Fourth Assessment Report of the Intergovernmental Panel on Climate Change (IPCC 2007) has concluded that any delayed action could lead to severe/irreversible consequences for the developing countries like Pakistan and the country will be affected most. The IPCC (FAR, 2007) had also predicted that feeding Glaciers of Pakistan Himalaya karkoram Hindu Kush are rapidly melting and as a result reduction in the net flow of feeding rivers of Pakistan is will occurs. Other dire predictions included disruption and unpredictability of monsoon rains (too little or too much; too early or too late) which replenish rivers, lakes and wetlands as well as underground aquifers.

2.3.1 Local Studies Change in Temperature, Precipitation and Flows

Ahmad et al., (2014) collected the monthly 40 years (1971-2010) climatic data of 12 gauging stations in the Indus Basin and applied non parametric seasonal kandal test to analyze the long term meteorological trends in the middle and lower parts of Indus basin of Pakistan. The analyzed meteorological parameters are rainfall, mean minimum temperature and maximum temperature. Analysis was performed for four seasons (spring — March to May, summer — June to August, fall—September to November and winter—December to February). The results showed that maximum temperature has an average increasing trend of magnitude +0.16, +0.03, 0.0 and +0.04 °C/decade during all the four seasons, respectively. The average trend of min. temperature during the four seasons also increases with magnitude of +0.29, +0.12, +0.36 and +0.36 °C/decade, respectively. Persistence of the increasing trend is more pronounced in the min. temperature as compared to the max. temperature on annual basis. Analysis of rainfall data has not shown any noteworthy trend during winter, fall and on annual basis. However during spring and summer season, the rainfall trends vary from −1.15 to +0.93 and −3.86 to +2.46 mm/decade, respectively. It is further revealed that rainfall trends during all seasons are statistically non-significant. Overall the study area is under a significant warming trend with no changes in rainfall.

Mahmood et al., (2015) investigated the future spatial and temporal changes in maximum temperature, minimum temperature, and precipitation in two sub-basins of the Jhelum River basin—the Two Peak Precipitation basin (TPPB) and the One Peak Precipitation basin (OPPB). An advanced interpolation method, kriging, was used to explore the spatial variations in the study area. Average R2 value for the precipitation 0.22-0.62 and for temperature R2 was 0.92-0.97.

Mean annual temperature was projected to raise significantly in the entire basin under two emission scenarios of HadCM3 (A2andB2). However, these changes in mean annual temperature were predicted to be higher in the TPPB than the OPPB. On the other hand, mean annual precipitation showed a distinct increase in the TPPB and a decrease in the OPPB under both scenarios. In the case of seasonal changes, spring in the TPPB and autumn in the OPPB were projected to be the most affected seasons, with an average increase in temperature of 0.43–1.7 °C in both seasons relative to baseline period. Summer in the TPPB and autumn in the OPPB were projected to receive more precipitation, with an average increase of 4–9% in both seasons, and winter in the TPPB and spring in the OPPB were predicted to receive 2–11% less rainfall under both future scenarios, relative to the baseline period. In the case of spatial changes, some patches of the basin showed a decrease in temperature but most areas of the basin showed an increase. During the 2020s (2011–2040), about half of the basin showed a decrease in precipitation. However, in the 2080s (2071–2099), most parts of the basin were projected to have decreased precipitation under both scenarios.

Ahmad et al., (2012) studied the hydrology of the northern mountainous areas of Pakistan and estimate flow pattern, long-term trend in river flows, characteristics of the watersheds, and variability in flow and water resource due to impact of climate change. They analyses the 45 (1960-2005) years data of eight watersheds Chitral, Shyok, Gilgit, Swat, Hunza, Jehlum, Astore and Shigar and monitor hydrological changes in relation to the trend of snow melt runoff, temperature and mean monthly flows, water yield and runoff relationship, variability in precipitation, analysis of daily hydrographs, and flow duration curves. Winter and summer rainfalls are not

uniformly distributed in the northern areas. For the temperature categorized the Upper Indus Basin into three hydrological regimes i.e. middle-altitude catchments south of Karakoram, high-altitude catchments with large glacierized parts and foothill catchments. Analysis of daily runoff data (1960–2005) of eight watersheds indicated nearly a uniform pattern with much of the runoff in summer (June–August). Impact of climate change on long-term recorded annual runoff of eight watersheds showed fair water flows at the Hunza and Jhelum Rivers while rest of the rivers indicated increased trends in runoff volumes. The study of the water yield availability indicated a minimum trend in Shyok River at Yogo and a maximum trend in Swat River at Kalam. Long-term recorded data used to estimate flow duration curves have shown a uniform trend and very important for hydropower generation for Pakistan which is seriously facing power crisis in last 5 years.

Fowler and Archer (2006) show that mean temperature has increased over the last century but long-term trends (>100 years) could not be detected. The same study showed statistically significant ($p < 0.05$) increases in winter maximum temperature of 0.27, 0.55, and 0.51°C decade-1 at Gilgit, Skardu, and Dir in the UIB. Akhtar et al. (2008) found that the annual mean temperature rise by the end of the century ranges from 0.3 to 4.8 ˚C in Hindukush-Karakoram-Himalaya (HKH). The warming is more pronounced in the Hunza (4.5˚C) 14 and Gilgit (4.8˚C) river basins compared to the Astore (0.3˚C) river basin where in the summer season the temperature even decrease by 0.2˚C. The precipitation changes in the Hunza (+19%) and Gilgit (+21%) river basins are somewhat similar, while precipitation changes in the Astore (113%) river basin are comparatively large.

Khattak et al., (2010) found that summer (June–August) precipitation in upper region of UIB has increased statistically significantly at the rate of 23.9 mm per 39 year (1965-2005). The middle region showed a decreasing trend, with p = 0.33 (52.1 mm per 39 yr), while the lower region showed an increasing trend, but the trends were not statistically significant. Annual precipitation has increased non-significantly in the upper and lower regions of the UIB with the rate 72 mm and 86 mm per 39 year and a decreasing trend was observed in the middle region with the rate of 11 mm per 39 year.

2.4 STATISTICAL TESTS FOR TRENDS ANALYSIS

2.4.1 Basic Concepts

2.4.1.1 Hypothesis

The starting point of a statistical test is to define a null hypothesis (H0) and an alternative hypothesis (H1). For example, to test for trend in a time series, H0 would be that there is no trend in the data, and H1 would be that there is an increasing or decreasing trend.

2.4.1.2 Test Statistic

The test statistic is a means of comparing H0 and H1. It is a numerical value calculated from the data series that is being tested.

2.4.1.3 Power and Errors

There are two possible types of errors.

Type I error is when H0 is incorrectly rejected.

Type II error is when H0 is accepted when H1 is true. A test with low Type II error is said to be powerful.

2.4.1.4 Significance Level

The significance level (α) is a means of measuring whether the test statistic is very different from values that would typically occur under H0. Specifically, the significance level is the probability of a test statistic value as extreme as, or more extreme than the observed value assuming no trend/change (H0). For example, for $\alpha = 0.05$, the critical test statistic value is the value that would be exceeded by 5% of test statistic values obtained from randomly generated data. If the test statistic value is greater than the critical test statistic value, H0 is rejected.

The significance level is therefore the probability that a test detects a trend/change (reject H0) when none is present (Type I error).

A possible interpretation of the significance level might be:

$\alpha > 0.1$ little evidence against H0

$0.05 < \alpha < 0.1$ possible evidence against H0

$0.01 < \alpha < 0.05$ strong evidence against H0

$\alpha < 0.01$ very strong evidence against H0.

For most traditional statistical methods, critical test statistic values for various significance levels can be looked up in statistical tables or calculated from simple formulas, provided that the test assumptions are satisfied. Where test assumptions are violated, resampling methods can be used to estimate the significance level of a test

statistic. For detecting trend/change of any direction, the critical test statistic value at $\alpha/2$ is used (two-sided tail). For detecting trend/change in a pre-specified direction (e.g., an increasing trend), the critical test statistic value at α is used (one-sided tail).

2.4.2 Parametric Tests

Parametric tests assume that the time series data and the errors (deviations from the trend) follow a particular distribution (usually normal distribution). Parametric tests are useful as they also quantify the change in the data (e.g., magnitude of change in the mean or gradient of the trend). Parametric tests are generally more powerful that non-parametric tests. Following parametric statistical tests that can be used to test for trend, change and randomness in hydrological and other time series data:

1. Linear Regression (parametric test for trend)
2. Worsley Likelihood Ratio (parametric test for step jump in mean)
3. Cumulative Deviation (parametric test for step jump in mean)
4. Student's t (parametric test for difference in mean from two data periods)
5. Autocorrelation (parametric test for randomness).

2.4.3 Non-Parametric Tests

Non-parametric tests are generally distribution-free. They detect trend/change, but do not quantify the size of the trend/change. They are very useful because most hydrologic time series data are not normally distributed. Following non-parametric statistical tests that can be used to test for trend, change and randomness in hydrological and other time series data:

1. Mann-Kendall (non-parametric test for trend)
2. Spearman's Rho (non-parametric test for trend)
3. Distribution-Free CUSUM (non-parametric test for step jump in mean)
4. Rank-Sum (non-parametric test for difference in median from two data periods)
5. Median Crossing (non-parametric test for randomness)
6. Turning Points (non-parametric test for randomness)
7. Rank Difference (non-parametric test for randomness)

2.5 LAND USE / COVER CHANGE

A water and energy budget-based distributed hydrological model with improved snow physics (WEBDHM-S) was applied to show the impact of climate change on mountain snow hydrology in the Shubuto River basin, Hokkaido, Japan. The spatial distribution of snow was analysed by using Moderate Resolution Imaging Spectroradiometer (MODIS). They used four Atmosphere Ocean General Circulation Models (AOGCMs) and SRESA1B emission scenario of the Intergovernmental Panel on Climate Change was used to describe climate predictions in the basin. All AOGCMs predict a future decrease in snowmelt contribution to total discharge 11–22% (bhati A m., et al (2016).

Schober (2014) access the assess the spatial variability of snow at the end of the accumulation season (April–May) in a glacierized catchment (167 km2) in Tyrol, Austria by using the multi-temporal Lidar (Light detection and ranging) data. Snow cover characteristics in the Tyrolean Alps have been analysed using regular snow measurements and snow course data the results of this study are further used for

conversion of basin-wide Lidar snow depth into snow water equivalent (SWE). The study focuses especially on the simulation of snow accumulation and the corresponding variability of snow Results at the watershed scale are in agreement with respect to the total water volume of the snow cover with deviations lower than 5% between SWE from Lidar or from the hydrological model.

Tahir et al., (2011) has used the snowmelt runoff model (SRM) integrated with MODIS remote-sensing snow cover products was selected to simulate the daily discharges and to study the climate change impact on these discharges in the Hunza River basin (the snow- and glacier-fed sub-catchment of the Indus River). The results obtained suggest that the SRM can be used efficiently in the snow- and glacier-fed sub-catchments of the Upper Indus River Basin (UIB). The application of the SRM under future climate (mean temperature, precipitation and snow cover) change scenarios indicates a doubling of summer runoff until the middle of this century.

Iida et al., (2012) analyzed the impact of seasonal snow on the suspended sediment in the mountainous catchment. They concluded that during the snow melt season sediments increases in the streams.

Bavay et al., (2013) has conducted model study on the impact of climate change on snow cover and runoff for the Swiss Canton of Graubünden. They used 35 years automatic weather stations data to investigate the snow and runoff under the current climates. The data set has then been modified to reflect climate change as predicted for the 2021–2050 and 2070–2095 periods from an ensemble of regional climate models. The predicted changes in snow cover will be moderate for 2021–2050

and become drastic in the second half of the century. Towards the end of the century the snow cover changes will roughly be equivalent to an elevation shift of 800 m. Seasonal snow water equivalents will decrease by one to two thirds and snow seasons will be shortened by five to nine weeks in 2095. Small, higher elevation catchments will show more winter runoff, earlier spring melt peaks and reduced summer runoff. Whereas glacierized areas exist, the transitional increase in glacier melt will initially offset losses from snow melt. Larger catchments, which reach lower elevations, will show much smaller changes since they are already dominated by summer precipitation.

Khadka et al., (2014) predicted the future changes in climatic parameters of the Tamakoshi basin of Nepal, estimating changes in snow covered area for changed climate, and subsequently quantifying temporal change in the runoff from the basin. Future climate of the basin is predicted by statistical downscaling outputs from two GCMs (HADCM3 for SRES A2 and B2 and CGCM3 for SRES A2 and A1B scenarios). Results show that temperature and precipitation will both increase in future under these scenarios. The relationship between the snow covered area with temperature and precipitation is developed from the observed data, and is used to predict snow covered area for future where it was found that spring and winter snow covers are more vulnerable to climate change. A temperature index based snowmelt runoff model is used to simulate basin runoff from the year 2000 to 2059. The analysis during observed period (2000–2009) shows that about 18% of the annual runoff in the basin is contributed by snow and ice melting. Snowmelt is largest during summer with an average melt of about 230 mm, which is about 17% of total water produced for runoff during this season. In terms of percentage contribution, snowmelt

is found more significant during spring season where the average snowmelt is about 44 mm, which is about 25% of total water produced for runoff during the season. Along with snowmelt, basin runoff is also expected to increase in future at the rate of 5.6 mm/year. Findings of this study will serve as a reference for further studies and planning of future water management strategies in the Tamakoshi basin.

2.6 CLIMATE CHANGE AND SEDIMENTATION IN CATCHMENTS/ BASIN

Climate change can change the time and magnitude of flow and the sediments. Warming temperature trends and rainfall intensity increasing has significant effect on the flow and sediment s. some of previous studies on the impact of climate change on the flows and sediment is described in this section.

2.6.1 Local and Global Studies

Nerantzaki et al., (2015) modeled the suspended sediment transport and access the impact of climate change on karstic Mediterranean watershed. The Soil and Water Assessment Tool (SWAT) model was coupled with a karstic flow and suspended sediment model in order to simulate the hydrology and sediment yield of the karstic springs and the whole watershed. Both daily flow data (2005–2014) and monthly sediment concentration data (2011–2014) were used for model calibration. The results showed good agreement between observed and modeled values for both flowand sediment concentrations. Flash flood events account for 63–70% of the annual sediment export depending on a wet or dry year. Simulation results for a set of IPCC "A1B" climate change scenarios suggested that major decreases in surface flow (69.6%) and in the flow of the springs (76.5%) take place between the 2010–2049 and

2050–2090 time periods. An assessment of the future ecological flows revealed that the frequency of minimum flow events increases over the years. The trend of surface sediment export during these periods is also decreasing (54.5%) but the difference is not statistically significant due to the variability of the sediment. On the other hand, sediment originating from the springs is not affected significantly by climate change.

Serpa et al., (2015) has evaluated the the impacts of climate and land use changes on stream flow and sediment export for a humid (São Lourenço) and a dry (Guadalupe) Mediterranean catchment, using the SWAT model. SWAT was able to produce viable stream flow and sediment export simulations for both catchments, which provided a baseline for investigating climate and land use changes under the A1B and B1 emission scenarios for 2071–2100. Compared to the baseline scenario (1971–2000), climate change scenarios showed a decrease in annual rainfall for both catchments (humid:−12%; dry:−8%), together with strong increases in rainfall during winter. Land use changes were derived from a socio-economic storyline in which traditional agriculture is replaced by more profitable land uses (i.e. corn and commercial forestry at the humid site; sunflower at the dry site). Climate change projections showed a decrease in stream flow for both catchments, whereas sediment export decreased only for the São Lourenço catchment. Land use changes resulted in an increase in stream flow, but the erosive response differed between catchments. The combination of climate and land use change scenarios led to a reduction in stream flow for both catchments, suggesting a domain of the climatic response. As for sediments, contrasting results were observed for the humid (A1B:−29%; B1:−22%) and dry catchment (A1B:+222%; B1:+5%), which is mainly due to differences in the present-day and forecasted vegetation types. The results highlight the importance of climate-induced land-use change impacts, which could be similar to or more severe than the direct impacts of climate change alone.

Giang et al., (2014) described that the Changes in stream sediment yield impact material fluxes, water quality, aquatic geochemistry, stream morphology, and aquatic habitats. Quantifying sediment yield is important for predicting watershed erosion and understanding sediment transport processes. In the context of a changing climate, this is important for the management and conservation of soil and water to cope with the effects of increasingly severe climate conditions that are likely to occur in the near future. This study aims to predict seasonal trends in sediment yield under climate change impacts in the Laos-Vietnam transnational Upper Ca River Watershed. The SWAT model was used for hydrological simulation, coupled with future climate projections under three IPCC emission scenarios, B1, B2, and A2. We found an increase in the seasonality of sediment yield due to increases in the seasonality of both rainfall and runoff. However, the increase of sediment yield in the wet season appeared more significant than its decrease in the dry season, due to more significant increases in rainfall as well as runoff in that season compared to decreases in these factors in the dry season. Consequently, annual sediment yield is predicted to increase, with a rate ranging from 12.1% to 16.5% by the end of this century, depending on emission scenario. The seasonal sensitivity of sediment yield to climate change found in this study is expected to be useful in collaborative management initiatives related to soil and water resources in the watershed.

Cousino (2015) has used the Soil and Water Assessment Tool (SWAT) model analyses the effects of climate change on water, sediment, and nutrient yields Maumee River watershed. Considering the Moderate climate change scenarios reduced annual flow up to −24% and sediment up to −26% yields, whereas more extreme scenario showed smaller flow reductions up to −10% and an increase in

sediment up to +11%. No-till practices had a negligible effect on flow but produced 16% lower average sediment loads than scenarios using current watershed conditions. Mukundan et al (2013) has applied Soil and Water Assessment Tool-Water Balance (SWAT-WB), a physically based semi-distributed model to identify suspended sediment generating source areas under current conditions and to simulate potential climate change impacts on soil erosion and suspended sediment yield in the study watershed for a set of future climate scenarios representative of the period 2081–2100.

Rehman (2012) used the Soil and Water Assessment Tool (SWAT) for simulating stream flow in the upper Rhone watershed located in the south western part of Switzerland. The catchment area is 5220 km2, where mostly land cover is dominated by forest and approximately 14 % is glacier. Stream flows were calibrated for the period 2001-2005 and validated for the period 2006-2010.Two different approaches were used for simulating snow and glacier melt process, namely the temperature index approach with and without elevation bands. The hydropower network was implemented based on the intake points that form part of the inter-reservoir network. Sub-basins were grouped into two major categories.

Future scenarios has been developed using nine global climate model (GCM) simulations indicated a sharp increase in the annual rates of soil erosion although a similar result in sediment yield at the watershed outlet was not evident. Future climate related changes in soil erosion and sediment yield appeared more significant in the winter due to a shift in the timing of snowmelt and also due to a decrease in the proportion of precipitation received as snow. Although an increase in future summer

precipitation was predicted, soil erosion and sediment yield appeared to decrease owing to an increase in soil moisture deficit and a decrease in water yield due to increased evapotranspiration.

2.7 DESCRIPTION OF DISTRIBUTED SWAT MODEL

The SWAT (Soil and Water Assessment Tool) model is semi-distributed physically based simulation model. SWAT is a river basin, or watershed, scale model developed to predict the impact of land management practices on water, sediment, and agricultural chemical yields in large, complex watersheds with varying soils, land use, and management conditions over long periods of time. The model is physically based and computationally efficient, uses readily available inputs and enables users to study long-term impacts. SWAT can be used to simulate a single watershed or a system of multiple hydro-logically connected watersheds. Each watershed is first divided into sub-basins and then in hydrologic response units (HRUs) based on the land use and soil distributions. Key procedures to run the SWAT model are

1. Load or select the ArcSWAT extension in ArcGIS
2. Delineate the watershed and define the HRUs
3. (Optional) Edit SWAT databases
4. Define the weather data
5. Apply the default input files writer
6. (Optional) Edit the default input files
7. Set up (requires specification of simulation period, PET calculation method, etc.) and run SWAT
8. (Optional) Apply a calibration tool
9. (Optional) Analyze, plot and graph SWAT output

Table 2.1 Description of SWAT

Description	SWAT Model
Model type	Distributed, Physically-based
Model objective	Predict the impact of land management practices on water and sediment
Temporal scale	Day, Monthly, Yearly
Spatial scale	Medium
Process modeled	Continuous

2.7.1 Hydrological Component of SWAT

The simulation of a basin's hydrology can be separated into two components (a) the land phase which controls the amount of soil moisture and nutrient concentration at HRUs and sub-basin level (b) the routing phase, which deals with the movement of water, sediments, etc., through the channel network of the basin towards the outlet.

Major components of the hydrological balance are surface runoff, lateral flow in the soil profile, groundwater flow, evapotranspiration, channel routing, and pond and reservoir storage. The water balance equation that represents the hydrologic cycle simulated in SWAT Figure 2.1) can be expressed mathematically as:

$$\llbracket SW_t = SW_0 + \sum_{i=1}^{t}(P - Q_f - ET_a - W - Q_g) \qquad (2.1)$$

Where:

SWt = Soil water content at time t (mm)

SW0 = Initial soil water content on day i (mm)

t = Time (days)

P = The amount of rainfall on day i (mm)

Qf = Surface runoff on day i (mm)

ETa = Evapotranspiration on day i (mm)

W = Water entering the vadose zone from the soil profile on day i (mm)

Qg = Return flow on day i (mm)

2.7.2 Precipitation / Rainfall

Hydrologic cycle of land phase is driven by the amount of precipitation that fall in the watershed. Precipitation is the general term which covers the all types of moisture coming to earth from atmosphere like rain, hail and snow fall. Precipitation is a basic and important input to model the hydrology of a basin. SWAT has the capability to estimate the missing data values using the historic data observations. In this model, sub-daily or daily data for precipitation can be used.

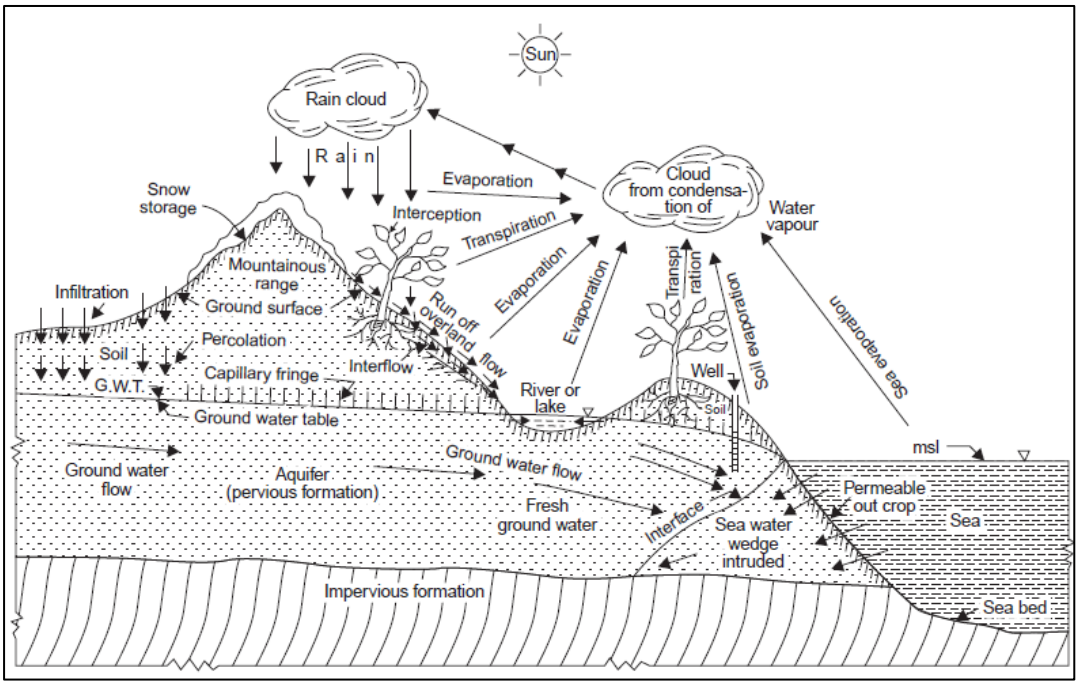

Fig. 2.1 Description of Hydrologic Cycle

2.7.2.1 Discharge / Surface Runoff

Modeling of surface runoff with SWAT model, it uses two methods (i) SCS curve number method (SCS, 1972) and (ii) Green & Ampt Infiltration method (1911). SCS curve number is an empirical method used in model which shows relationship between runoff and rainfall that gives a solid basis for estimating the amount of runoff under different land cover and soil types. The mathematical equation of SCS curve number shown as:

$$Q_f = \frac{(R_{d-} I_i)^2}{(R_d - I_i + S)} \quad (2.2)$$

Retention parameter S varies spatially and depends upon soil type, land cover and management practices (Neitsch et al., 2005). Mathematically it is expressed as:

$$S = 25.4(\frac{1000}{CN} - 10) \quad (2.3)$$

Where:

Qf = Runoff or rainfall excess (mm)

Rd = Rainfall on a given day (mm)

Ii = Abstraction from surface storage, interception and infiltration (mm)

S = Retention parameter (mm

CN = Curve number

2.7.2.2 Evapotranspiration

Evapotranspiration is a combined term used to express the removal of water from the earth. It includes all the processes that are used to convert water from liquid to vapors. It involves evaporation from soil and transpiration from canopy. It is the

primary mechanism by which water is removed in the hydrologic cycle during basin level modeling. An accurate estimation of evapotranspiration is crucial in the management of water resources.

Potential evapotranspiration (PET) is the rate at which evapotranspiration can take place under the given climatic condition when excessive amount of water is available to plants. PET is climatic data dependent and has many methods to calculate. SWAT provides Hargreaves method (Hargreaves et al., 1985), Priestly-Taylor method (Priestly and Taylor, 1972) and the Penman-Monteith method for the estimation of PET (Monteith, 1965; Allen et al., 1989).

2.7.2.3 Soil Water

When the water infiltrates into the soil, it may be removed from soil through evapotranspiration by plants or may percolate pass the bottom of the soil strata and finally becomes the ground water recharge, or may move horizontally in the soil profile and contribute to stream flow.

Percolation is the downward movement of water within soil profile up to the saturation zone. In SWAT model percolation is calculated for each layer of soil profile. Percolation starts when water content of soil layer exceeds the field-capacity of that layer, and if the layer below is not saturated. Storage routing methodology is used in SWAT to calculate the amount of water that moves from one layer to the next underlying layer. Equation used to calculate the amount of water that percolates to the next layer is as:

$$W = SW_{ly}\left\{1 - e^{\left(\frac{-\Delta t}{TTper}\right)}\right\} \quad (2.4)$$

TTper is calculated as:

Where

W = Water that percolate to the next underlying soil layer (mm of water)

SW_{ly} = Volume of drainable water in the soil layer on a given day (mm of water)

Δt = Time duration (hrs)

TT_{per} = Travel time for percolation (hrs)

S_{ly} = Water in the soil layer when completely saturated (mm)

FC_{ly} = Water content of the soil at field capacity (mm)

K_s = Saturated hydraulic conductivity for the layer (mmh-1)

For the subsurface flow in two-dimensional cross section along a flow direction down to a steep hill slope, kinematic storage model is used in SWAT.

2.7.2.4 Groundwater

Two types of groundwater aquifers are simulated in each sub-basin in the SWAT model. One is unconfined aquifer that can contribute to flow in the main channel if channel is not an irrigation channel, and the other is confined aquifer that is assumed to contribute to stream flow outside of the basin. Unconfined aquifer is called shallow aquifer and confined aquifer is called deep aquifer in SWAT.

In a groundwater storage system, water enters mainly by infiltration and percolation and possibly by seepage from water bodies. Water leaves the groundwater storage system by discharge into rivers or lakes and possibly by capillary rise.

Recharge to the unconfined aquifers occurs by percolation of excessive water that pass the root zone after fulfilling the crop water requirement. Recharge to confined aquifers occurs due to the percolation from the surface occurs only at the upstream end of the confined aquifer, where geologic formation containing aquifer is exposed at the surface of earth.

The water balance equation for aquifer as written as:

$$Aq_i = Aq_{i-1} + W_{rch} - Q_g - W_{rev} - W_{pum} \quad (2.5)$$

Where:

Aqi = Water stored in the aquifer on day i (mm)

Aqi-1 = Water stored in aquifer on day i-1 (mm)

Wrch = Recharge entering aquifer on day i (mm)

Qg = Groundwater flow into main channel on day i (mm)

Wres = Water moving into the soil zone on day i (mm)

Wpum = Water removed from aquifer by pumping on day (mm)

2.8 DOWNSCALING TECHNIQUES / MODELS

Hulme et al., (2001) developed a set of climate scenarios for the African continent using change fields from 7 different models. They used pattern scaling to generate climate scenarios with a range of climate sensitivities and greenhouse gas concentrations. Change fields for the 30-year time period centered on the 2080s were used to scale to two additional time slices about the 2020s and 2050s. Four traces from one model (HadCM2) were explored for significance in temperature and precipitation change fields by using 1400 years of the model control run to estimate natural temperature and precipitation variability. In all scenarios, continent wide

temperature increases exceeded the estimates of natural variability and were considered significant. The scenarios project temperature increases over Africa of 2° to 6° C within 100 years. Precipitation scenarios were less conclusive. Under the low to moderate forcing scenarios, few areas indicated 'significant' changes in precipitation. Even under the more extreme forcing scenarios, with considerable areas of 'significant' precipitation changes, median model response is often less than the intermodal range of responses. The seasonal and spatial patterns of changes vary considerably. In equatorial Africa, Dec-Feb precipitation is estimated to increase, while near the Horn of Africa Jun-Aug precipitation experiences significant decreases.

Wake (1989) suggests the possibility that a higher proportion of annual precipitation occurs during the monsoon season at higher elevations. Climate change is a change in the statistical distribution of weather over periods of time that range from decades to millions of years. It can be a change in the average weather or a change in the distribution of weather events around an average (for example, greater or fewer extreme weather events). Climate change may be limited to a specific region, or may occur across the whole Earth. In recent usage, especially in the context of environmental policy, climate change usually refers to changes in modern climate. It may be qualified as anthropogenic climate change, more generally known as "global warming" or "anthropogenic global warming" (AGW).

Compared to other downscaling methods (e.g. dynamical downscaling), the statistical method is relatively easy to use and provides station-scale climate information from GCM-scale outputs (Wilby et al., 2002). Thus, statistical

downscaling methods are the most widely used in anticipated hydrologic impact studies under climate-change scenarios.

2.9 SUMMARY

1. Over all temperature increase in Pakistan, as a whole, would be higher than the global average temperature increase.

2. Water resources already severely constrained by population growth and inefficient use would face additional stress due to variability in water flows in the Indus River System (IRS) resulting from reduced glacial melt in Himalayan ranges. Furthermore, climate change will enhance variability in monsoon and winter rains leading to more frequent and intense floods or droughts in the country.

3. Saline water intrusion, due to ongoing sea level rise in Pakistan, would damage the coastal zones and marine ecosystems in particular Indus delta with enhanced possibility of increased storm events. The current sea level rise in Pakistan is reported to be about 1.1 milli meter per year.

4. Increased heat, water scarcity and increased intensity and duration as well as frequency of droughts would seriously threaten our agriculture and food security.

5. Health care would face an additional challenge from outbreak of heat related and insect-transmitted diseases, from malnutrition as well as growing food and water insecurity.

2.9.1 Research Gaps Identified from Previous Studies

The research gaps identified from the previous studies are primarily related to the conditions of Pakistan which are given below:

- Impact of climate change on the sediment is needed to be investigated thoroughly.

- A research on integrated watershed management techniques is required to mitigate the sediment flow into the rivers under the intense rainfall events as a result of climate change.

Chapter 3
STUDY AREA

3.1 DESCRIPTION OF UPPER INDUS BASIN

This study has been carried out in the selected catchments of Upper Indus Basin (UIB). The catchment of said basin falls in the range of 33º, 40′ to 37º, 12′ N latitude and 70º, 30′ to 77º, 30′ E, longitude. The catchment area of upper Indus basin lies in Afghanistan, China and India as shown in Figures 3.1 and 3.2. Due to unavailability of data from China and India, the study area was confined to the catchment falling within Pakistan boundary. The Upper Indus watershed boundary was derived from Digital Elevation Model (DEM) just upstream of Massan (Gauging station) as shown in Fig. 3.2. The elevation varies from 254 m (833 ft) to 8,570 m (28,117 ft) above Mean Sea Level. There are many rivers which contribute water to the main Indus River. The main sub basins are Chitral, Swat, Kabul, Hunza, Gilgit, Astore, Shigar, Shyok, Kunhar, Neelum, Ghorband, Kanshi, Poonch, Soan, Siran, Sil, Haro etc. Indus River originates from the north side of the Himalayas at Kaillas Parbat in Tibet having altitude of 5,787 m (18000 ft). Traversing about 500 miles in North West direction, it is joined by Shyok River near Skardu (elevation 9000 feet).

After traveling for about 100 miles in the same direction, it reaches Nanga Parbat and join Gilgit River at an elevation of 1,524 m (5000 ft). Moving towards Tarbella dam, Ghorband river merges into the Indus near Bisham Qila at an elevation 581 m (1906 ft). Flowing further for about 200 miles in SW (South West) direction, the river enters into the plains of the Punjab province at Kalabagh, 244 m (800 ft). The Kabul River, a major western flank tributary, joins with Indus near Attock. The

Kunar, which is also called Chitral River joins Indus downstream the Warsak. About five miles below Attock, another stream Haro river drains into the Indus River. About seven miles upstream of Jinnah Barrage, another stream called Soan river joins the Indus. The tributaries of Indus Rivers are detailed in Fig. 3.3. One of the important Eastern river draining into the Indus River System is River Jhelum which originates from Pir Panjal and flows parallel to the Indus at an elevation of (1,677 m) 5,500 ft. The basin is located on the southern slope of the Himalayas with an elevation ranging from 300 m (984 ft) to 6,282 m (20,610 ft) above the mean sea level (a.m.s.l.) band has basin area of around 33,425 km^2 at Mangla dam.

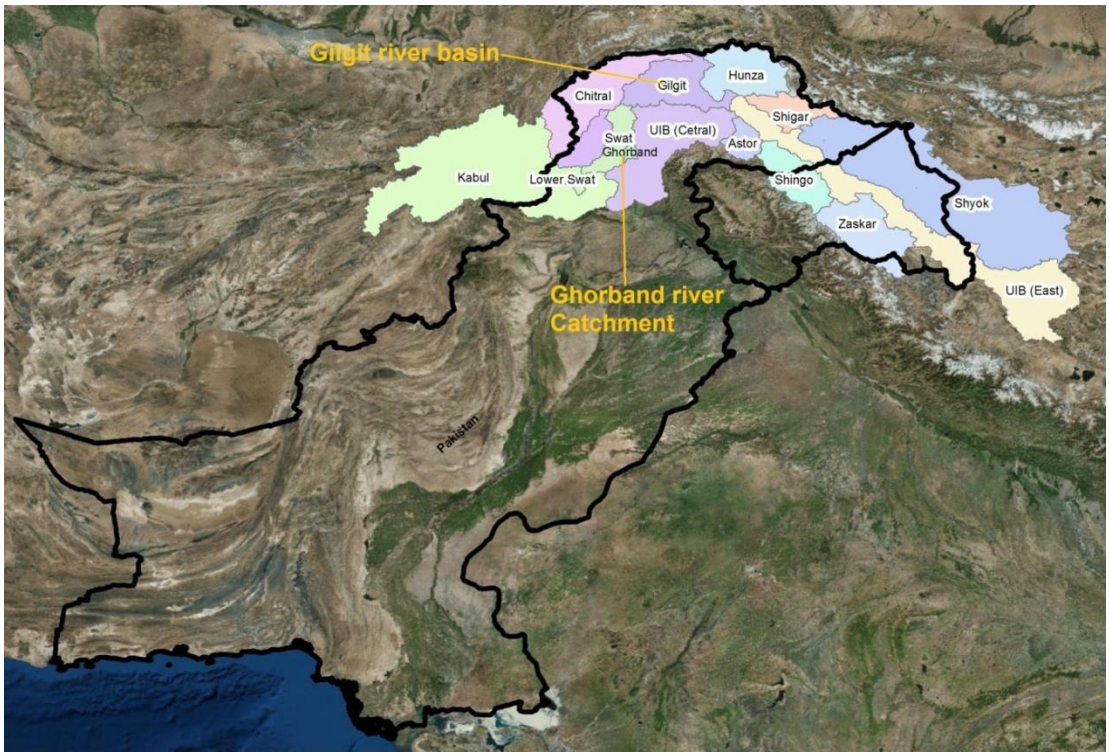

Fig. 3.1 Location Map Pakistan Boundary and Upper Indus Basin

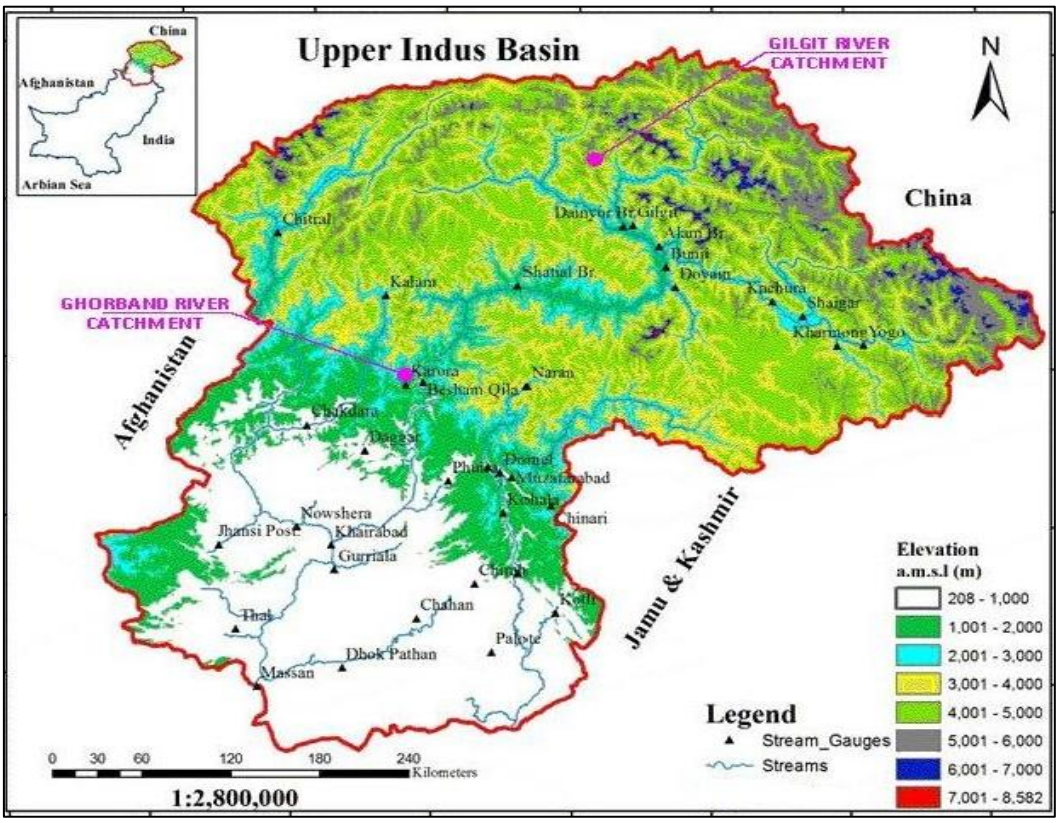

Fig. 3.2 Upper Indus Basin confined in Pakistan boundary showing stream gauges, rivers, and elevation

This dam serves hydropower generation and regulates the flow from Mangla reservoir. About 55% of the area lies in Indian held Kashmir and 45% lies in Pakistan including Azad Kashmir. There are five sub-catchments i.e. Jhelum, Poonch, Kanshi, Neelum/ Kishan Ganga and Kunhar which drain water to Mangla reservoir Fig. 3.3. The largest tributary of the Jhelum, Neelum River joins at Domel Muzaffarabad, as does the next largest, the Kunhar River of the Kaghan valley joins on Kohala Bridge. The flow of Jhelum River enters into the Mangla Dam reservoir in the district of Mirpur. The flows of Poonch and Kanshi Rivers also enter into Mangla reservoir.

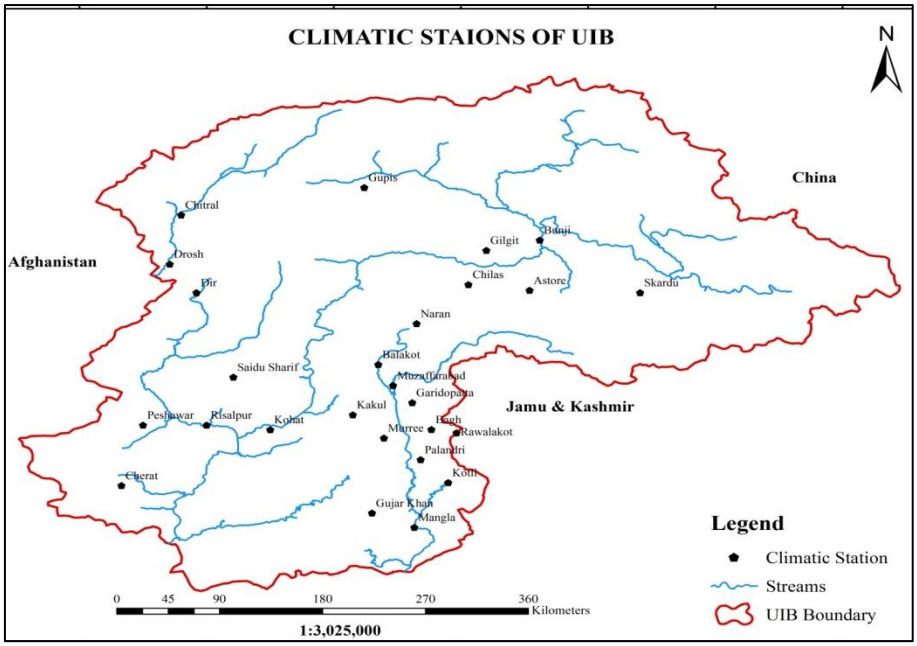

Fig. 3.3 Upper Indus Basin showing climatic stations, rivers and catchment area laying in Pakistan

Table 3.1 List of stream gauges used in the present study and their characteristics

Sr. No.	Station	Lat (dd)	Long (dd)	River	Basin	Area (Km^2)	Period	No of Years	Mean Annual Stream flows (cumec)
1	Naran	34.9	73.7	Kunhar	Jhelum	1036	1961-2012	52	47
2	G. Habibullah	34.4	73.4	Kunhar	Jhelum	2355	1961-2012	52	103
3	Muzaffarabad	34.4	73.5	Neelum	Jhelum	7275	1963-2012	50	332
4	Chinari	34.2	73.8	Jhelum	Jhelum	13598	1970-2012	43	293
5	Domel	34.4	73.5	Jhelum	Jhelum	14504	1975-2012	38	322
6	Kohala	34.1	73.5	Jhelum	Jhelum	24890	1965-2012	48	778
7	Azad Pattan	33.7	73.6	Jhelum	Jhelum	26485	1970-2012	43	1207
8	Kotli	33.5	73.9	Poonch	Jhelum	3238	1961-2012	52	126
9	Palote	33.2	73.4	Kanshi	Jhelum	1111	1961-2012	52	6
10	Kharmong	35.2	75.9	Indus	Indus	67858	1983-2012	30	447
11	Yogo	35.2	76.1	Shyok	Indus	33670	1973-2012	40	358
12	Shigar	35.4	75.7	Shigar	Indus	6610	1982-2002	20	209

Sr. No.	Station	Lat (dd)	Long (dd)	River	Basin	Area (Km^2)	Period	No of Years	Mean Annual Stream flows (cumec)
13	Kachura	35.5	75.4	Indus	Indus	112665	1970-2012	43	1081
14	Gilgit	35.9	74.3	Gilgit	Indus	12095	1961-2014	45	309
15	Dainyor Br.	35.9	74.4	Hunza	Indus	13157	1966-2012	47	325
16	Alam Br.	35.8	74.6	Gilgit	Indus	26159	1966-2012	47	638
17	Bunji	35.7	74.6	Indus	Indus	142709	1963-2012	50	1792
18	Doyain	35.5	74.7	Astore	Indus	4040	1974-2012	39	139
19	Shatial Br.	35.5	73.6	Indus	Indus	150220	1984-2012	29	2076
20	Karora	34.9	72.8	Gorband	Indus	635	1975-2010	36	18
21	Besham Qila	34.9	72.9	Indus	Indus	162393	1969-2012	44	2401
22	Daggar	34.5	72.5	Brandu	Indus	598	1970-2012	43	6
23	Phulra	34.3	73.1	Siran	Indus	1057	1969-2012	44	20
24	Kalam	35.5	72.6	Swat	Kabul	2020	1961-2012	52	86
25	Chakdara	34.6	72.0	Swat	Kabul	5776	1961-2012	52	188
26	Chitral	35.9	71.8	Chitral	Kabul	11396	1965-2012	48	276
27	Jhansi Post	33.9	71.4	Bara	Kabul	1847	1962-2012	51	6
28	Nowshera	34.0	72.0	Kabul	Kabul	88578	1961-2012	52	837
29	Gurriala	33.7	72.3	Haro	Indus	3056	1969-2012	44	26
30	Khairabad	33.9	72.2	Indus	Indus	252525	1988-2012	25	2834
31	Thal	33.4	71.5	Kurram	Indus	5543	1968-2012	45	25
32	Chirah	33.7	73.3	Soan	Indus	326	1961-2012	52	5
33	Chahan	33.4	72.9	Sil	Indus	241	1963-2012	50	2
34	Dhok Pathan	33.1	72.3	Soan	Indus	6475	1964-2012	49	41
35	Massan	33.0	71.7	Indus	Indus	286000	1972-2012	41	3703

3.2 DESCRIPTION OF STUDY AREA

A major part of the glaciated ice and snow of the Pakistan is concentrated in the Indus basin watershed. These watersheds can be divided into different river basins, namely Indus, Jhelum, Shingo, Shyok, Shigar, Astor, Swat, Ghorband, Chitral, Gilgit and Hunza River. Gilgit and Ghoband River catchments are selected for the study. Both rivers catchments lies in the Pakistanis' territory. The climate and stream flow data of these catchments is available from the Government of Pakistan. The description of selected catchments is given below.

3.2.1 Description of Gilgit Basin

The Gilgit River starts from Shandur lake. It lies in the northern area of Pakistan and catchment area of the river is 12,095 Km^2. It is the tributary of Indus river passing through town Gilgit and meets the Indus River near village Parri. It is also the confluence point of three world biggest mountains i.e. Hamayala, Karkoram and Hindukush. The river basin in the north is bordered with Afghanistan and China. The Gilgit River network comprises of the Ghizar, Yasin, Ishkuman and Hunza River and joins the Indus River near Jaglot. The upper reaches of the basin are mostly glaciated and covered with permanent snow. Mean annul flow of Gilgit river is 309 m^3/s. Gilgit River basin in upper part of the Upper Indus Basin is shown in Fig. 3.1.

3.2.1.1 Topography

Topographically, the area is very rough with high peaks and steep slopes. Maximum and minimum elevation of basin is 7667 and 1248 meter (25,154 and 4095 ft) respectively as shown in Fig. 3.4.

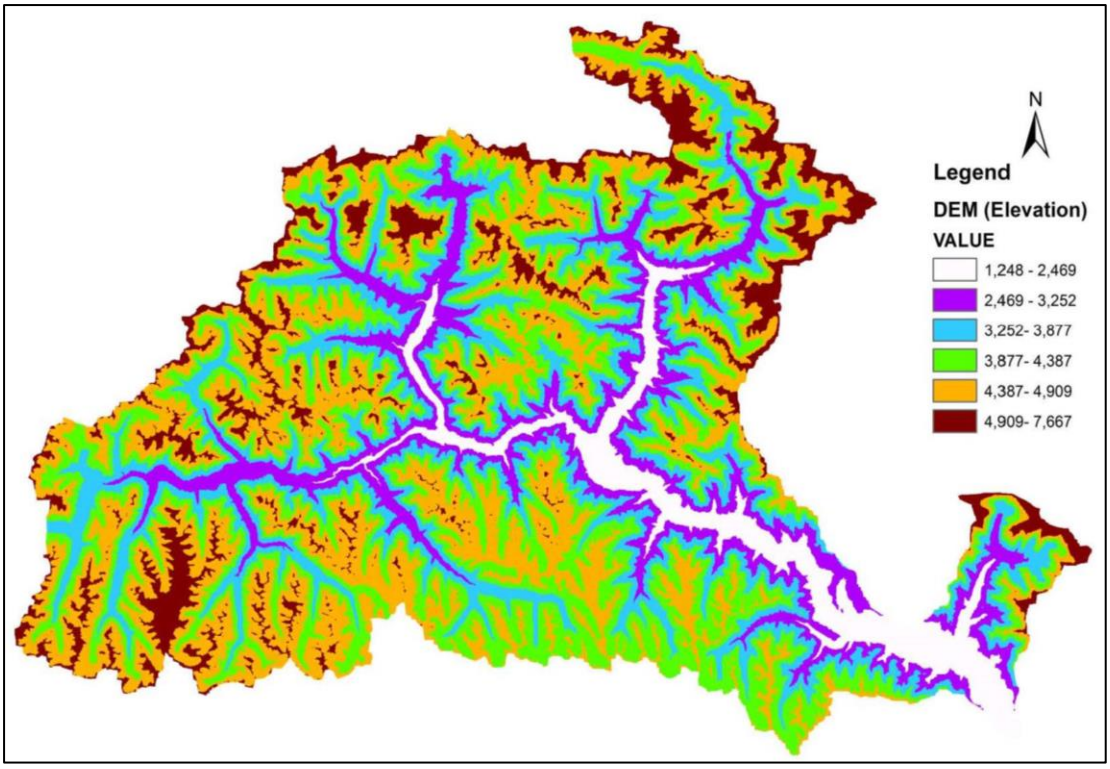

Fig. 3.4 Elevation Range of Giligt River Catchment

3.2.1.2 Soil Type

Soil classes' data[1] is downloaded from the International Soil Reference and Information Centre (ISRIC) and found that Gilgit basin falls in the soil class with highly active clay (HAC), elaborated as 80 % area soil type is slightly moderate to weather soil type, dominated 2:1 clay type material and remaining 20% area is glaciers /land Ice.

3.2.1.3 Land Use

Natural vegetation is largely confined to the lower part in the valley. The soil cover of Gilgit basin has been investigated through European Space Agency Global Cover[2] soil maps, satellite imagery. The land use of basin is categorized into

[1] IPCC soil classes derived from derived from Harmonized World Soil Data Base (ver 1.1) November 2010. http://www.isric.org/content/download-form?dataset=CBP_Global_IPCC_soil_classes_2010Nov04.zip

[2] Source: European Space Agency Global Cover http://due.esrin.esa.int

permanent glaciers, snow and ice cover area, irrigated and rain fed croplands, water bodies, barren area, shrubs, vegetation and grass lands. The land use map is shown in Fig. 3.5. Popular is a common tree and is mostly used in the construction of houses. The fruit trees grown in the area include apple, apricot, walnut, almond, mulberry, grape, peach and cherry. Wheat, barley and maize are the main crops.

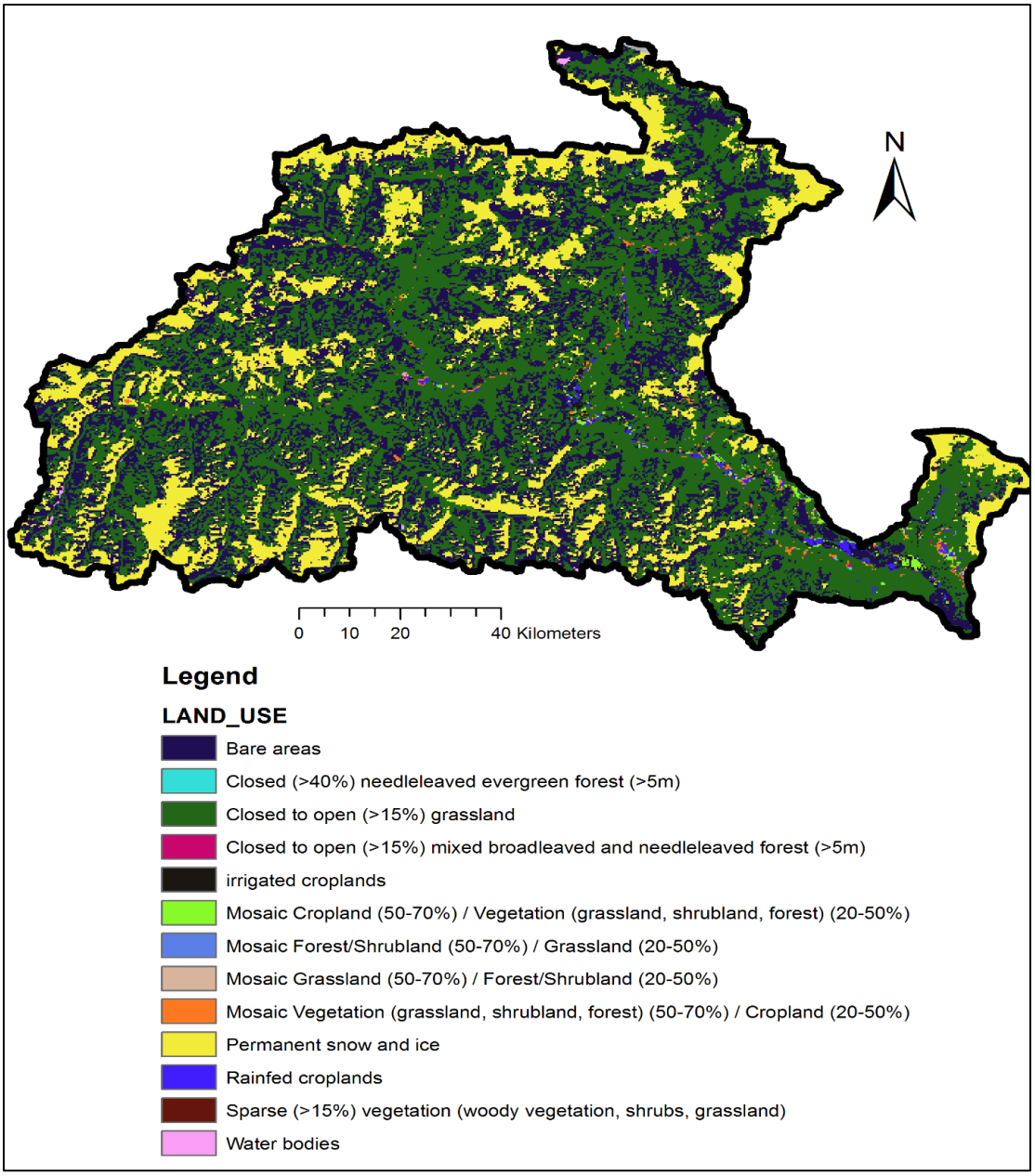

Fig. 3.5 Land Use of Gilgit Basin

3.2.2 Description of Ghorband Catchment

The catchment of Ghorband river is not a permanent snow glacier. Snow falls on the top hills during the winter season and melts in the summer season. The catchment area of the river 635 Km^2. It is the tributary of Indus river and joins near Bisham Qila in district Shangla, Khyber Pakhtunkhwa. Mean annul flow of Ghorband river is 18 m^3/s and lies in the lower reaches of Central Upper Indus Basin as shown in Fig. 3.1.

3.2.2.1 Topography

Maximum and minimum elevation of basin is 4,419 and 818 meter (14,498 and 2,684 ft) respectively as shown in Fig. 3.6.

3.2.2.2 Soil Type

Soil classes data[3] is downloaded from the International Soil Reference and Information Centre (ISRIC) and found that Ghorband Catchment falls in the soil class highly active clay (HAC), elaborate as slightly moderate to weather soil type dominated 2:1 clay type material The Project area is situated in the Indian Plate rock mass a few km south of Main Mantle Thrust (MMT), which marks the regional boundary of the sub-ducting Indian mass under the Kohistan Island Arc (KIA). The tectonics and the mountain building forces have resulted into the formation of large tectonic blocks in the Indian rock mass. One of these blocks is the Besham nappe which is separated in the East and West by other nappes through N-S trending shears. The Project area is situated in the Besham nappe.

[3] IPCC soil classes derived from derived from Harmonized World Soil Data Base (ver 1.1) November 2010. http://www.isric.org/content/download-form?dataset=CBP_Global_IPCC_soil_classes_2010Nov04.zip

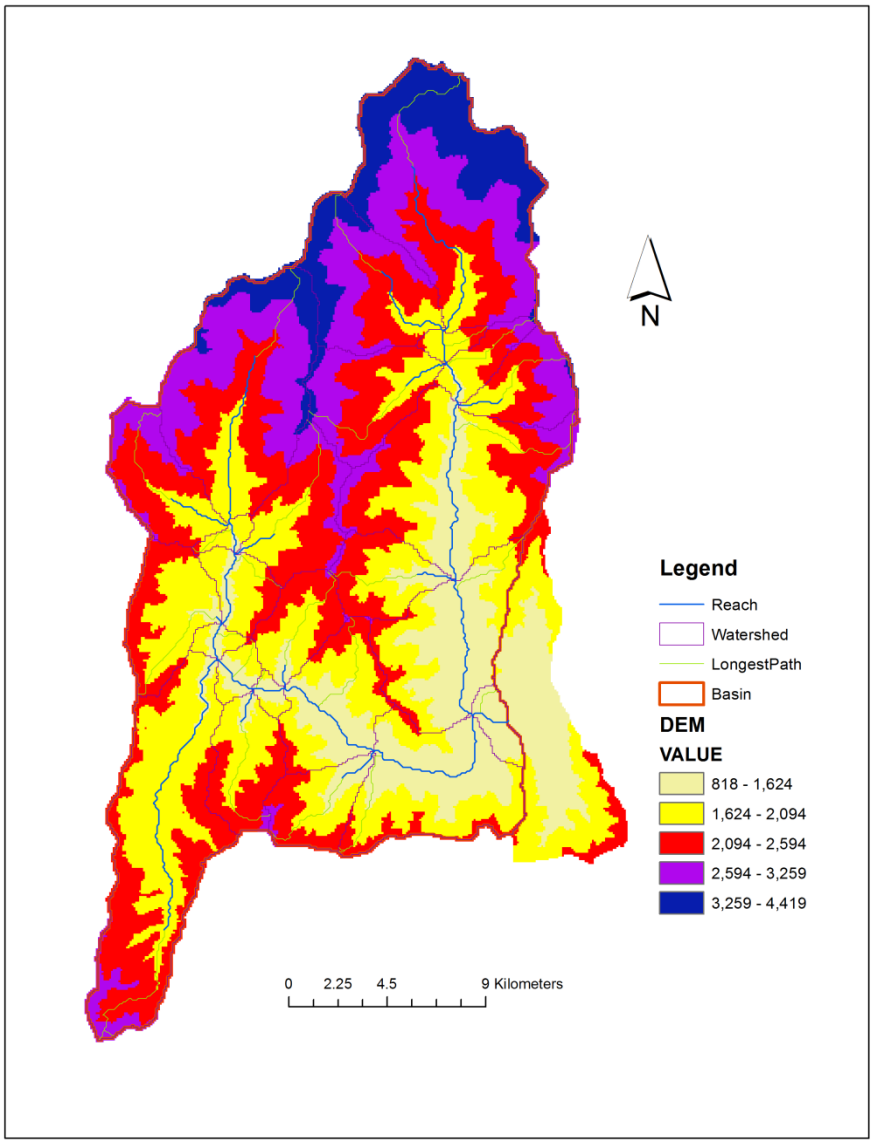

Fig. 3.6 Elevation Range of Ghorband River Catchment

3.2.2.3 Land Use

The soil cover of Ghorband Catchments has been investigated through European Space Agency Global Cover[4] soil maps, satellite imagery. The land use of basin is categorized into permanent glaciers, snow and ice cover area, irrigated and rain fed croplands, water bodies, Forest, barren area, shrubs, vegetation and grass lands. The land use map is shown in Fig. 3.7.

[4] Source: European Space Agency Global Cover http://due.esrin.esa.int

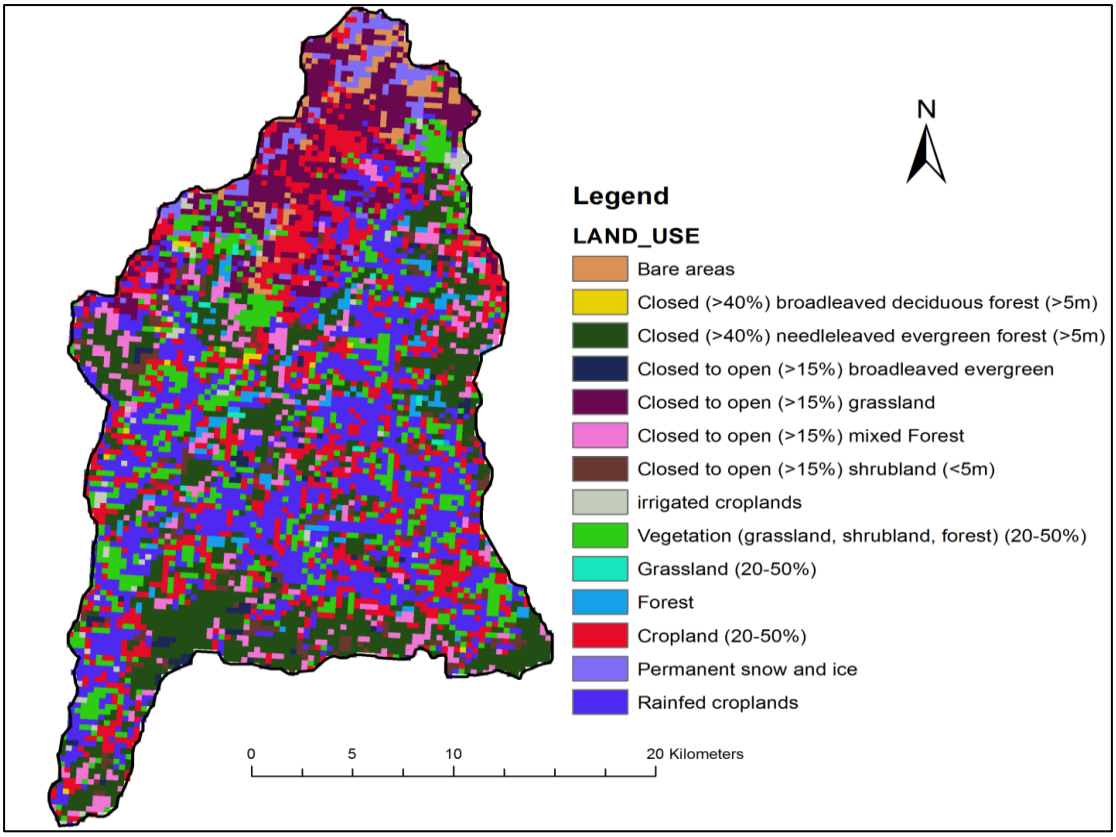

Fig. 3.7 Land Use map of Ghorband Catchment

3.2.3 Reasons for Selection of Study Area

The followings are the reasons for the selection of the Gilgit and Ghorband river catchment

- Snow and Glaciers are major source of water in Indus river and Tarbela dam as well as for Pakistan, as the snow and glacier area is effected or likely to be effected by climate change, the detailed analysis of selected area using different technologies could provide us knowledge in depth about change in snow cover and impact on water scarcity.
- Similar analysis can be applied on rest of Indus basin for assessment, planning and management of water resources in the future.

- Finer scale remote sensing data is required, due to large area of upper Indus basin (UIB), it is very expensive to have a finer scale data for whole basin therefore, detailed analysis of selected basins could be helpful for present and future conditions of changing trends in snow and glacier cover area.
- In this region, most of studies have been carried out in correlation with climate and flows, as the sediment is also problem in Indus Basin, no study has been under taken for the detailed analysis of climate, snow & glacier, runoff and sediment yield due to climate change perspective.
- The boundaries of upper Indus basin lies beyond the Pakistan and tributaries from China, Afghanistan and India contribute into the Indus river. The Gilgit and Ghorband river catchments are selected for the study because both lies in Pakistan, s territory.
- The climate and stream flow data availability also a reason for the selection of both catchments, The data of selected catchments is available from the Government of Pakistan.
- The Upper part of Gilgit basin is permanently covered with glaciers & snow whereas, Ghorband river catchment is not covered with permanently with snow. In this regard the impact of climate change and analysis can be done in the catchments having different characteristics like land use, soil type, snow cover, rainfall, etc.
- The Maximum and minimum elevation of Gilgit river catchment is 7,667 and 1,248 meters (25,154 and 4095 ft) respectively whereas, maximum and minimum elevation of Ghorband river catchment is 4,419 and 818 meters (14,498 and 2,684 ft) respectively.

- Gilgit basin is on upper part of the Upper Indus Basin whereas, Ghorband river lies in lower reaches of Central Upper Indus Basin as shown in Fig. 3.1. High altitude is difficult to access and not commonly monitored, less data is available as 60% of upper Indus basin have similar conditions so, technique validated on selected catchment shell be applied on rest of the UIB.

Chapter 4
METHODLOGY

This chapter includes the data required, stepwise/ detailed methodology and procedure to achieve the objectives. The Major steps involved are as follows:

1. Data Collection and Digitization
2. Trend Analysis of Gilgit and Ghorband river catchments by using Mann-Kandal test.
3. Land use Analysis e.g. Snow Covers and Glacier melts.
4. Hydrological modeling of Gilgit and Ghorband River Catchments by using SWAT model and estimation of sediment yield.
5. Model calibration and Validation
6. Downscaling the GCM out for the Gilgit and Ghorband River Catchments/Basin
7. Run the SWAT Model for future scenario of rainfall and temperatures
8. Result Compilation and Analysis

The detailed Methodology flow chart is given in Figure 4.1.

4.1 DATA COLLECTION AND DIGITIZATION

Different type of data is required for the analysis e.g Climatic data, Topographic, Land Use/ Cover and Soil type data.

4.1.1 Climatic Data

Historic data for the Giligit and Ghorband river catchments is collected from Government and Non-Government organizations like WAPDA, Pakistan

Meteorological Department, Irrigation and Power Department, NESPAK and digitized. The collected parameters are daily Precipitation (rainfall), daily stream flow and Sediments data, daily temperature (Min & Max), daily Solar Radiation, and daily Evaporation. The stations alongwith period of record within and near the Gilgit & Ghorband river catchments is given in Tables 4.1 and 4.2:

Table 4.1 Data Collected from PMD

Sr. No	Name of Station	Parameters	Daily	Monthly
1	Skardu	Daily Precipitation, Solar Radiation, Daily Temperatures (Min & Max), Wind Speed Data, Daily Evaporation, Humidity Data	1975-2014	1954-2014
2	Gilgit			
3	Astore			
4	Chilas			
5	Gupis			

Table 4.2 Data collected from SWHP[5], WAPDA

Sr. No	Stations	Parameters	Period
1	Gilgit River at Gilgit	Daily Discharge & Sediment data	1963-2013
2	Gilgit River at Alam Bridge		1974-2013
3	Ghorband River at Karora[6]		1974-2010
4	Shahpur	Daily Precipitation, Solar Radiation, Daily Temperatures (Min & Max), Wind Speed Data, Daily Evaporation, Humidity Data	1974-2010
5	Bisham Qila		1974-2010

[5] Surface Water hydrology Project, WAPDA

[6] Stream flow gauge is removed during the 2010 flood and still not maintained by SWHP, WAPDA

4.1.2 Topographic Data

The topographic data (Digital Elevation Model, DEM, ASTER) has been obtained from NASA Shutter Topography Radar Thematic Mapping (STRM) data sets with a spatial resolution of 90 m. The website link is http://srtm.csi.cgiar.org/. Advanced Space-borne Thermal Emission and Reflection Radiometer (ASTER) was down loaded. DEM and ASTER were further used for the watershed delineation to determine the Gilgit and Ghorband watershed parameters e.g. slope, channel length etc. The generated DEM is used in SWAT model for the estimation of sediment yield.

4.1.3 Historical Satellite Images

For the historical land use (snow cover and ice) changes/ analysis in Gilgit and Ghorband river catchment month-wise satellite image was downloaded from the MODIS (Moderate Resolution Spectrometer Imaging Spectrometer) website. A satellite image of pixel size 500 m × 500 m has been used. These products have been generated using the MODIS calibrated radiance data products (MOD02HKM and MYD02HKM), the geo-location products (MOD03 and MYD03), and the cloud mask products (MOD35_L2 and MYD35_L2) as inputs. The MODIS snow algorithm output (MOD10_L2 and MYD10_L2) contains scientific data sets (SDS) of snow cover, quality assurance (QA) SDSs, latitude and longitude SDSs, local attributes and global attributes. The snow cover algorithm identifies snow-covered land, it also identifies snow-covered ice on inland water. Satellite image has been down loaded for the first calendar day of every month, Month wise data for the Sixteen years (2001 to 2016) have been downloaded from the link. https://modis.gsfc.nasa.gov/data/dataprod/mod10.php

4.1.4 Land use/ Cover Data

Land cover data is downloaded from the European Space Agency Glob Cover Portal. The web link to download land cover data is given below.

http://due.esrin.esa.int/page_globcover.php.

4.1.5 Soil Type/ Classes Data

Soil Classes data has been downloaded from the International Soil Reference and Information Centre (ISRIC). The web link to download soil classes data is given below

(http://www.isric.org/content/downloadform?dataset=CBP_Global_IPCC_soil_classes_2010Nov04.zip

ISRIC - World Soil Information is an autonomous, science-based establishment. The establishment was established in 1966 after a proposal of the International Soil Science Society (ISSS) and a determination of the United Nations Educational, Scientific and Cultural Organization (UNESCO). ISRIC has a mission to serve the universal group with data about the world's soil assets to help tending to major worldwide issues.

4.2 TREND ANALYSIS

The trend analysis has been done by using the non-parametric statistical test on the monthly, seasonal and annual data series of selected stations for Gilgit and Ghorband river catchments. For this study Mann Kendal test has been used.

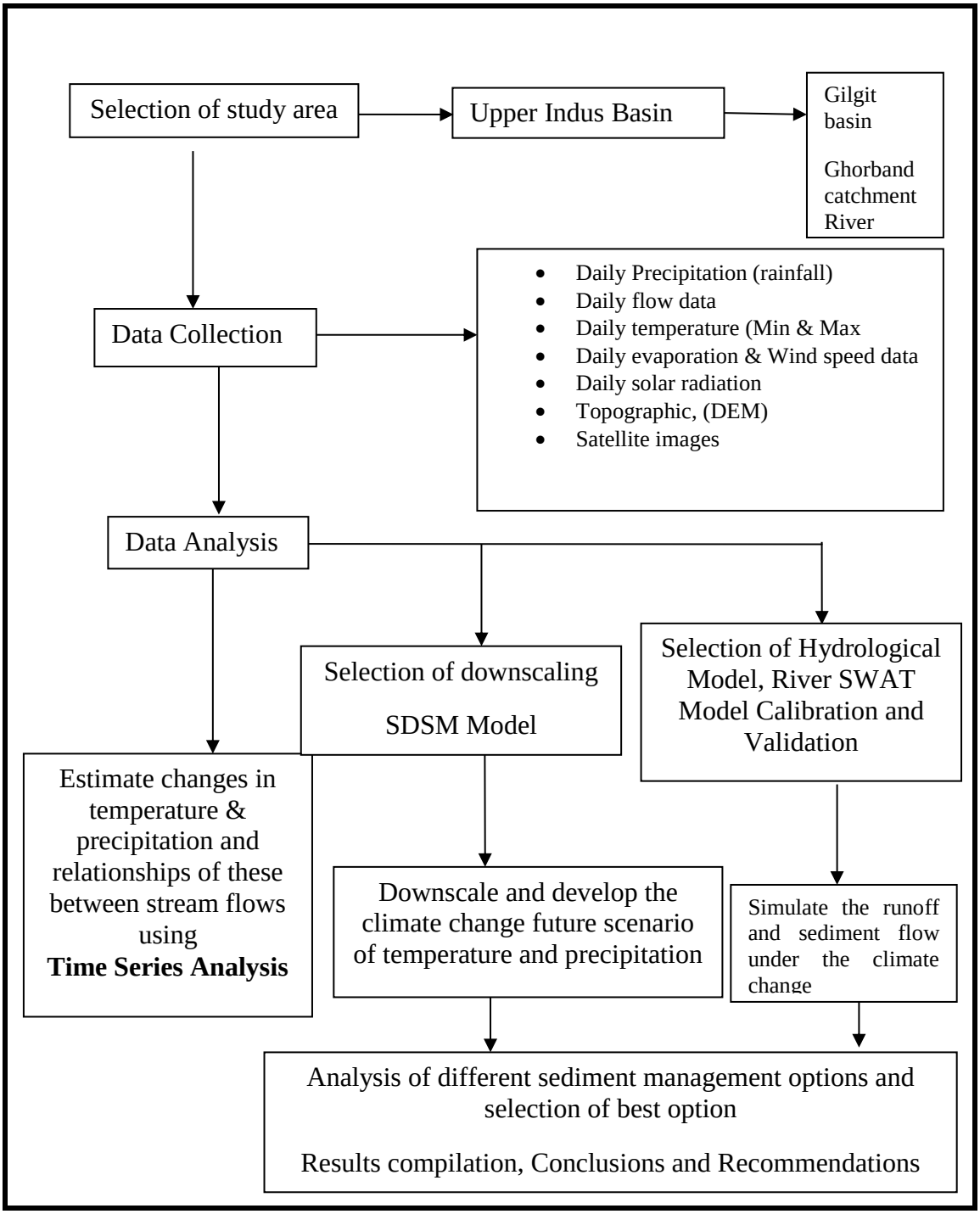

Fig. 4.1 Flow Chart of Methodology

4.2.1 Mann Kendall Test

Mann Kendall test is a statistical test widely used for the analysis of trend in climatologic (Tabari et al. 2012, Caloiero et al. 2011, Mavromatis and Stathis, 2011, Bhutiyani, 2007, Rio del et al. 2005,) and in hydrologic time series (Yue and Wang, 2004). There are two advantages of using this test. First, it is a non-parametric test and does not require the data to be normally distributed. Second, the test has low sensitivity to abrupt breaks due to inhomogeneous time series [Tabari et al. 2011]. This test was found to be an excellent tool for trend detection.

The number of annual values of the data series is denoted by *n*. The differences of annual values *x* were determined to compute the Mann-Kendall statistics. The Mann-Kendall statistic, S was computed using equation 4.1:

$$S = \sum_{k=1}^{n-1} \sum_{j=k+1}^{n} \operatorname{sgn}(x_j - x_k) \qquad (4.1)$$

Where *sgn* $(x_j - x_k)$ is an indicator function that takes on the values 1, 0 or -1 according to sign of difference $(x_j - x_k)$, where $j > k$:

$$\operatorname{sgn}(x_j - x_k) = \begin{cases} 1 & \text{if } x_j - x_k > 0 \\ 0 & \text{if } x_j - x_k = 0 \\ -1 & \text{if } x_j - x_k < 0 \end{cases} \qquad (4.2)$$

The values x_j and x_k are the annual values in the year j and k respectively.

The variance *S* was computed by the following equation:

$$VAR(S) = \frac{1}{18}\left[n(n-1)(2n+5) - \sum_{p=1}^{q} t_p(t_p-1)(2t_p+5)\right] \qquad (4.3)$$

Where q is the number of tied groups and t_p is the number of data in the p group. Before computing *VAR(S)* the data was checked to find all the tied groups and number of data in each tied group.

S and *VAR(S*) were used to compute the test statistic Z as follows:

$$Z = \begin{cases} \frac{S-1}{[VAR(S)]^{1/2}} & \text{if } S > 0 \\ 0 & \text{if } S = 0 \\ \frac{S+1}{[VAR(S)]^{1/2}} & \text{if } S < 0 \end{cases} \qquad (4.4)$$

The trend was evaluated using *Z* values. A positive value of *Z* indicates an upward (warming) trend while negative value shows downward trend (cooling trend). The statistics *Z* has a normal distribution. The null hypothesis, Ho is true if there is no trend and thus uses the standard normal table to decide whether to reject H_o. To test for either upward or downward trend (a two-tailed test) at a level of significance H_o is rejected if the absolute value of *Z* is greater than $Z_{1-a/2}$, where $Z_{1-a/2}$, was obtained from standard normal tables.

In this study the existence and significance of trend was evaluated by using four different α values that is α = 0.1, α = 0.05, α = 0.01 and α = 0.001.

Steps to perform Trend Analysis by Mann Kendal Test

1. Pre-whiten the time series to eliminate effect of serial correlation of observations
2. Apply Mann–Kendall trend analysis to identify if trends are significant
3. Estimate the trend value by applying Sen's estimator

4.3 LAND USE/ COVER CHANGES / ANALYSIS

The Moderate Resolution Imaging Spectroradiometer (MODIS) snow products were selected to calculate the snow cover on the study area. MODIS/Terra Snow Cover 8-Day L3 Global 500 m Grid (MOD10A2) used for this study contains data fields for maximum snow cover extent over 8-day compositing period and a

chronology of snow occurrence observations in HDF-EOS (Earth Observation System) format, along with corresponding metadata. MOD10A2 consists of 1200x1200-km tiles of 500-m resolution data gridded in a sinusoidal map projection (Hall et al., 2000, updated weekly).

The MODIS/Terra V005 data set available from March 2000 to December 2016 has been downloaded. MODIS cryosphere data is based on a snow mapping algorithm that employs a Normalized Difference Snow Index (NDSI) and other criterion tests (Hall et al., 2000, updated weekly; Hall et al., 2002). The snow mapping algorithm differentiates pixels as snow, ice lakes, cloud, water, land or other. Snow extent was the primary variable of interest in this data set. Version 5 (V005) of the MOD10A2 snow products is the latest version and provided the best quality of data used in this study. Our present database used in this study consists of 453 processed MOD10A2 images for each of the Gilgit and Ghorband River basin.

4.3.1 MODUS Data Analysis

The step-wise procedure carried out for the snow cover analysis is given below:

1. Downloaded the MODIS data from the following link
   https://modis.gsfc.nasa.gov/data/dataprod/mod10.php

2. Downloaded the Terra Prod ID/DAAC Link data of 0.05Deg CMG as shown in Figure.

Product Name	Terra Prod ID/ DAAC Link	Aqua Prod ID/ DAAC Link
MODIS Snow Cover 5-Min L2 Swath 500m	MOD10_L2	MYD10_L2
MODIS Snow Cover Daily L3 Global 500m Grid	MOD10A1	MYD10A1
MODIS Snow Cover Daily L3 Global 0.05Deg CMG	MOD10C1	MYD10C1
MODIS Snow Cover 8-Day L3 Global 500m Grid	MOD10A2	MYD10A2
MODIS Snow Cover Daily L3 Global 0.05Deg CMG	MOD10C2	MYD10C2
MODIS Snow Cover Monthly L3 Global 0.05Deg CMG	MOD10CM	MYD10CM

3. Imported the data into ArcGIS and selected the Day_CMG_Snow_Cover from the sub dataset present in the MODIS data as shown in figure.

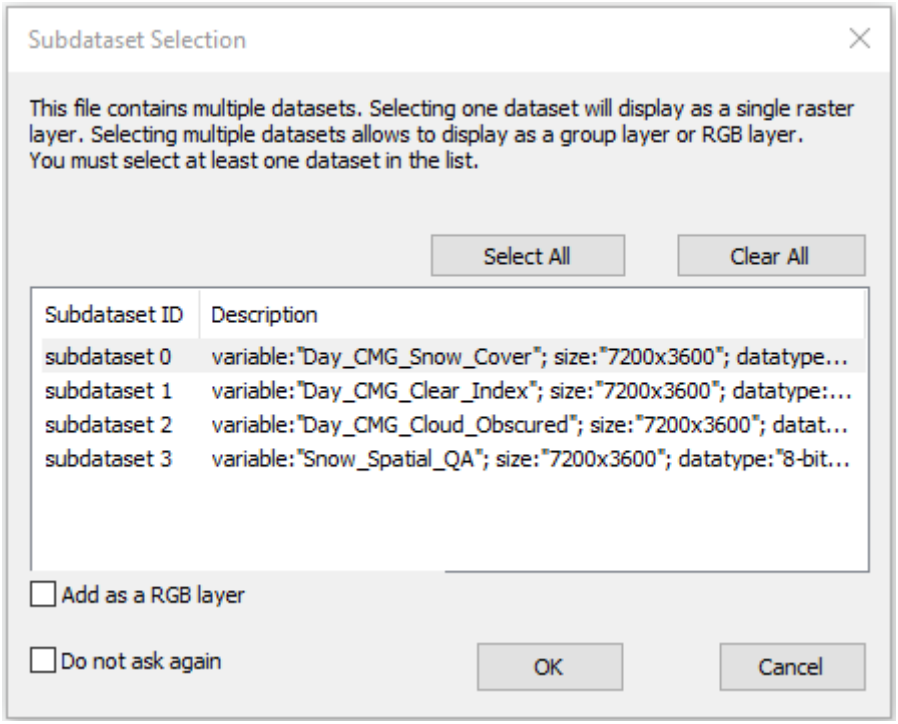

4. Projected the imported raster into GCS_WGS_1984 coordinate system as it has no coordinate system.
5. Imported the Shapefile of required area (Gilgit basin and Ghorband catchment) into GIS and extract the required region.
6. Extracted the values ranging from 1 to 100 which displayed the snow cover.
7. If result showed only 0 value which was extra so deleted this as selected in Figure.

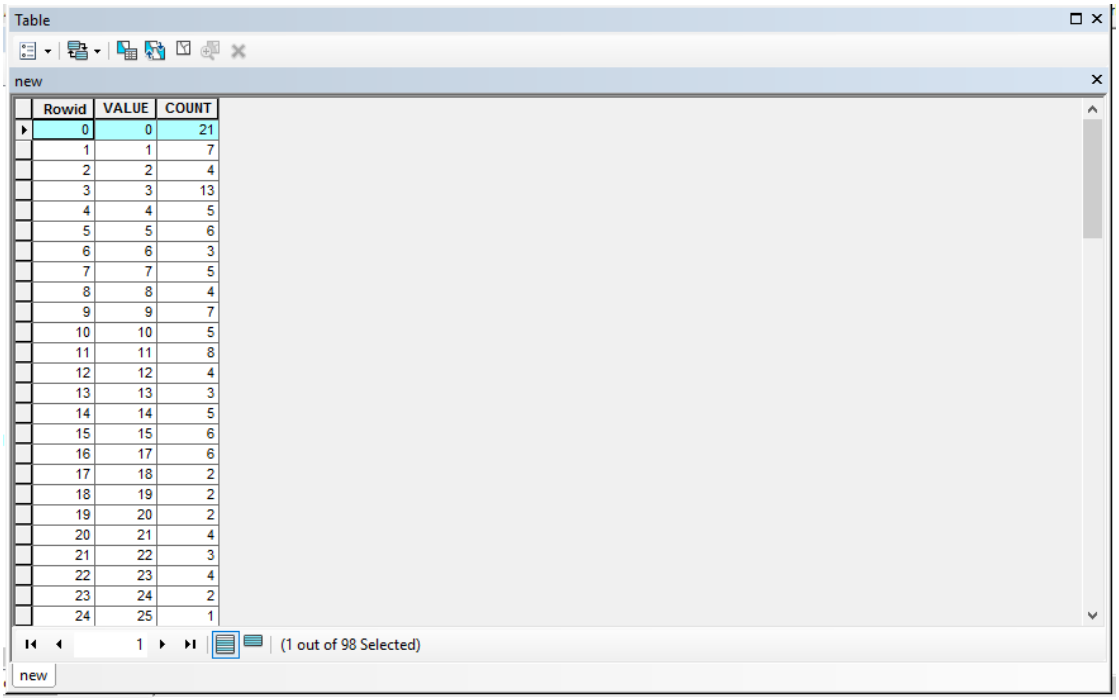

8. Opened the Set Null tool to make the 0 value raster to null value as shown in Figure.

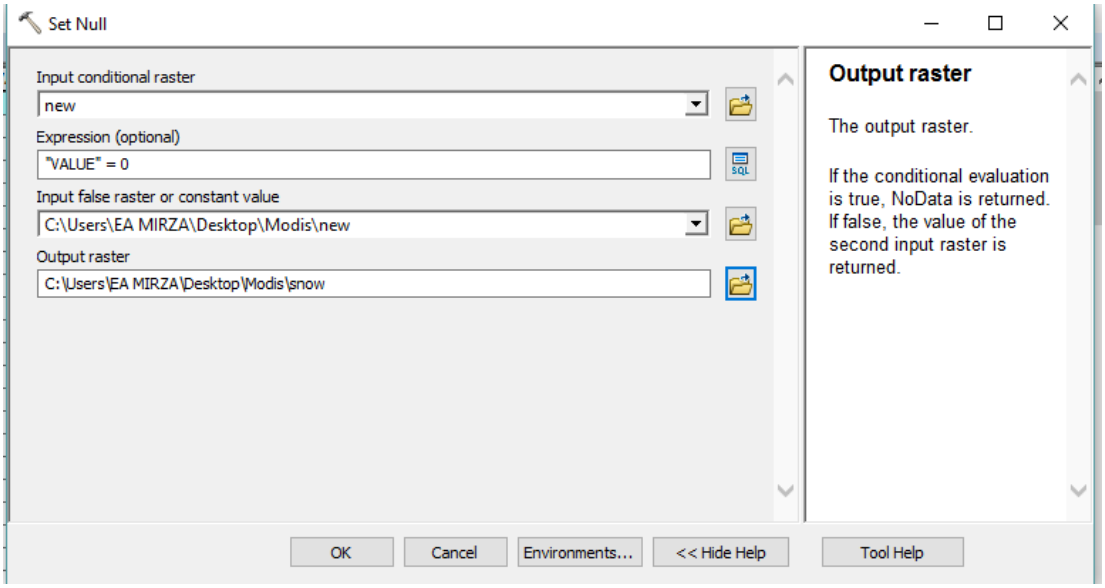

9. Clicked on SQL query builder and make the query of “VALUE”=0 as shown in Figure.

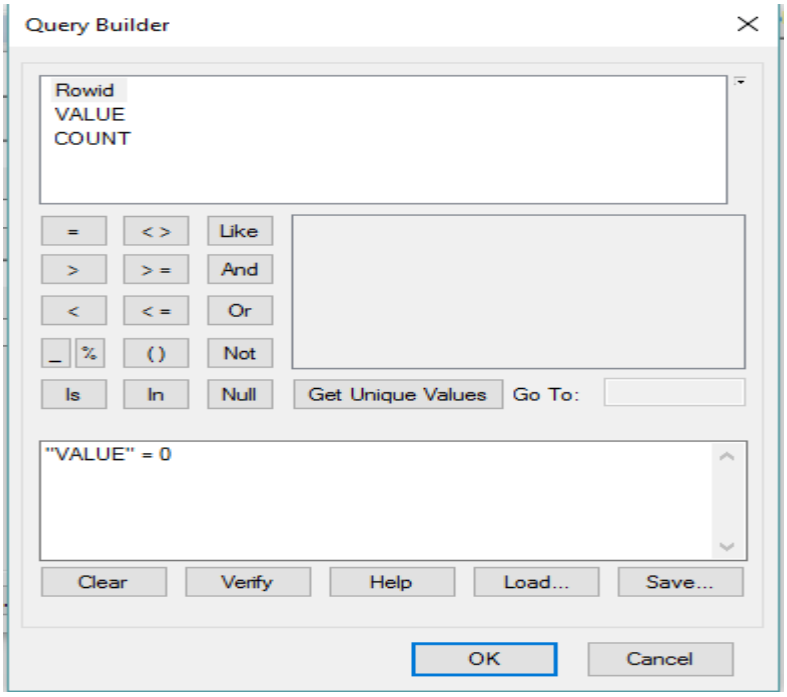

10. This tool has made the 0 VALUE attribute equal to null and deleted it.

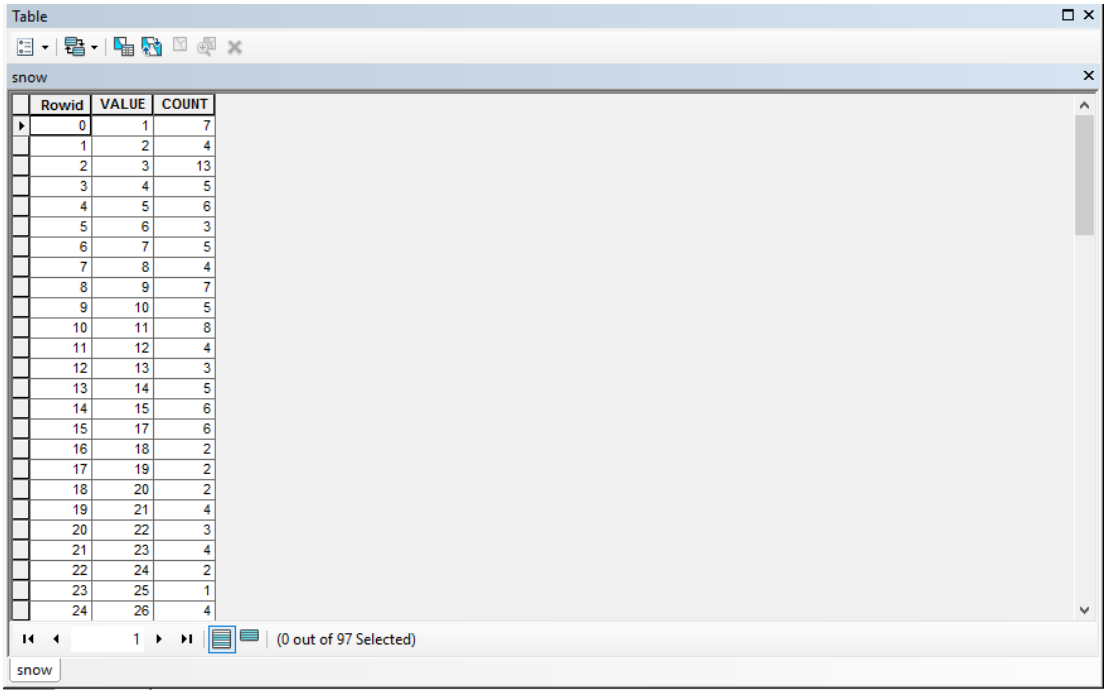

11. VALUE ranging from 1 to 100 has been shown in Figure.

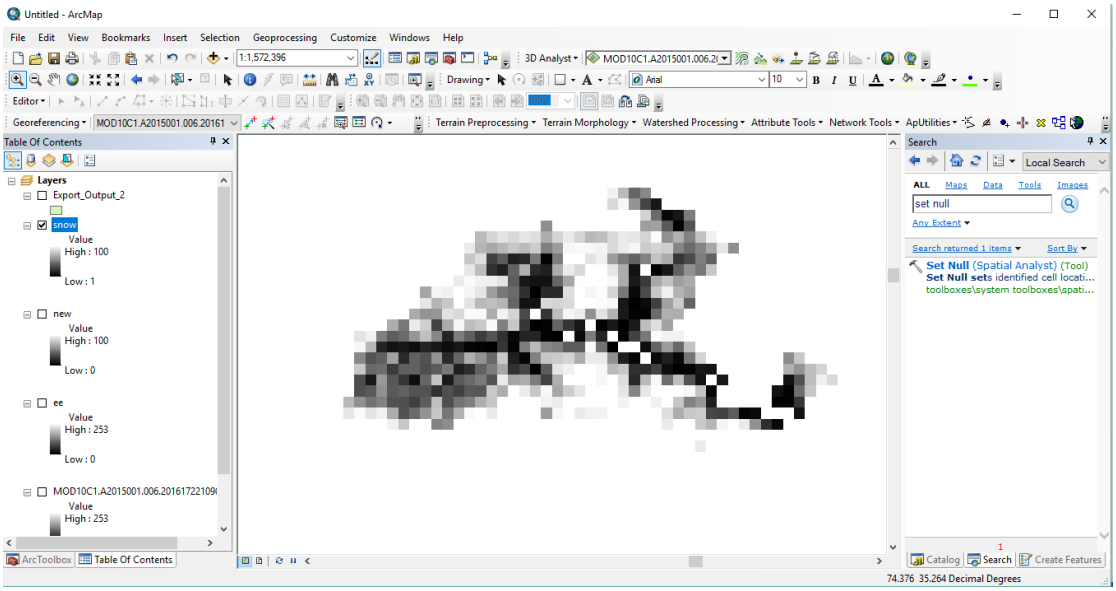

12. Made the polygon of this raster by Raster to Polygon tool.

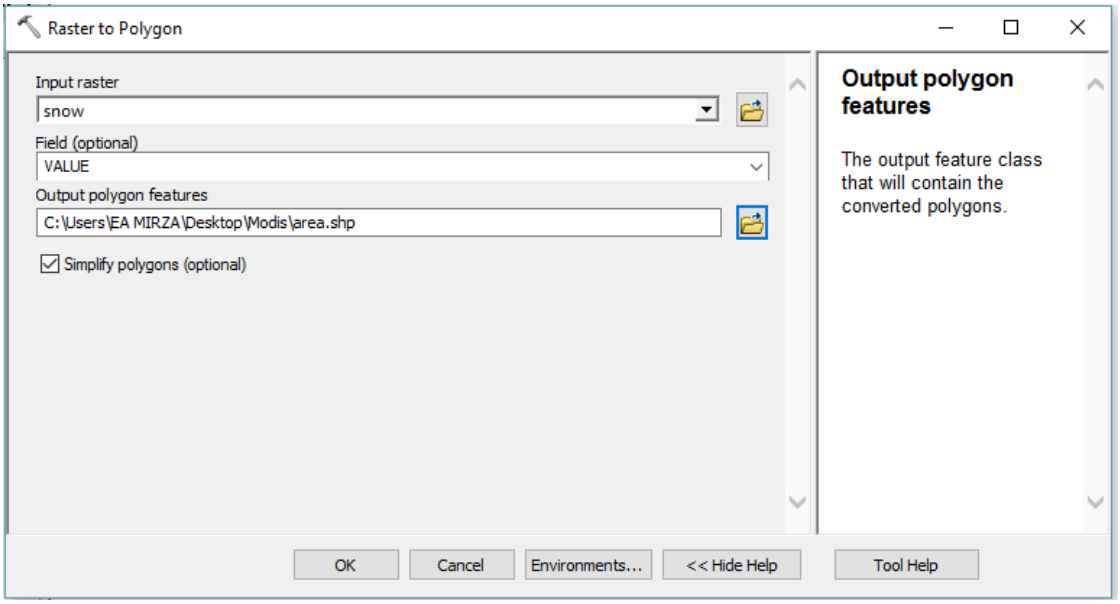

13. Calculated the area of this polygon. This was the area of snow that present on the mountains of that downloaded image date.

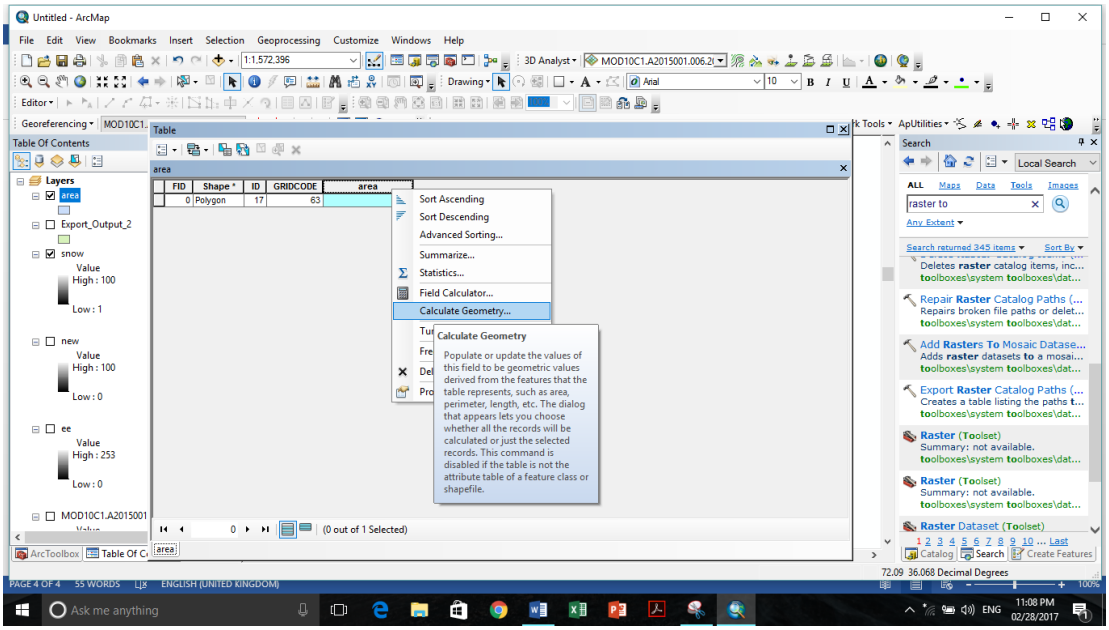

14. To calculate the changes of snow in a month, downloaded the first and last day image and calculated the difference of snow level.

4.4 STATISTICAL DOWNSCALING MODEL (SDSM)

The SDSM software reduced the task of statistically downscaling daily weather series into seven discrete steps:

a) Quality control and data transformation

Few meteorological stations had complete or accurate data sets. Handling of missing and imperfect data was necessary for most practical situations. Simple quality control checks in SDSM enabled the identification of gross data errors, specification of missing data codes and outliers prior to model calibration. In many instances it was appropriate to transform predictors or the predict and prior to model calibration. The transform facility takes chosen data files and applied selected transformations (e.g., logarithm, power, inverse, lag, binomial, etc).

b) Screening of variables

Identifying empirical relationships between predictors e.g. Mean Sea Level pressure and single site predict and i.e. station precipitation and temperature were the necessary data required for statistical downscaling methods. The main purpose of the screen variables operation was to assist the user in the selection of appropriate downscaling predictor variables. This is one of the most challenging stages in the development of any statistical downscaling model since the choice of predictors largely determines the character of the downscaled climate scenario. The decision process is also complicated by the fact that the explanatory power of individual predictor variables varies both spatially and temporally e.g. Mean Sea Level pressure may have strong correlation with temperature and rainfall in coastal areas but it has to be ignored in regions away from sea even if it has strong correlation with rainfall and temperature. Screen Variables facilitated the examination of seasonal variations in predictor skill.

c) Model calibration

The Calibrate Model operation took a user specified predict and along with a set of predictor variables and computed the parameters of multiple regression equations via optimization algorithm (either dual simplex of ordinary least squares). The user specified model structure, either monthly, seasonal or annual models are required, the process is unconditional or conditional. In unconditional models a direct link has been assumed between the predictors and predict and (e.g., local wind speeds may be a function of regional airflow indices). In conditional models, there was an intermediate process between regional forcing and local weather (e.g., local

precipitation amounts depend on the occurrence of wet–days, which in turn depend on regional–scale predictors such as humidity and atmospheric pressure).

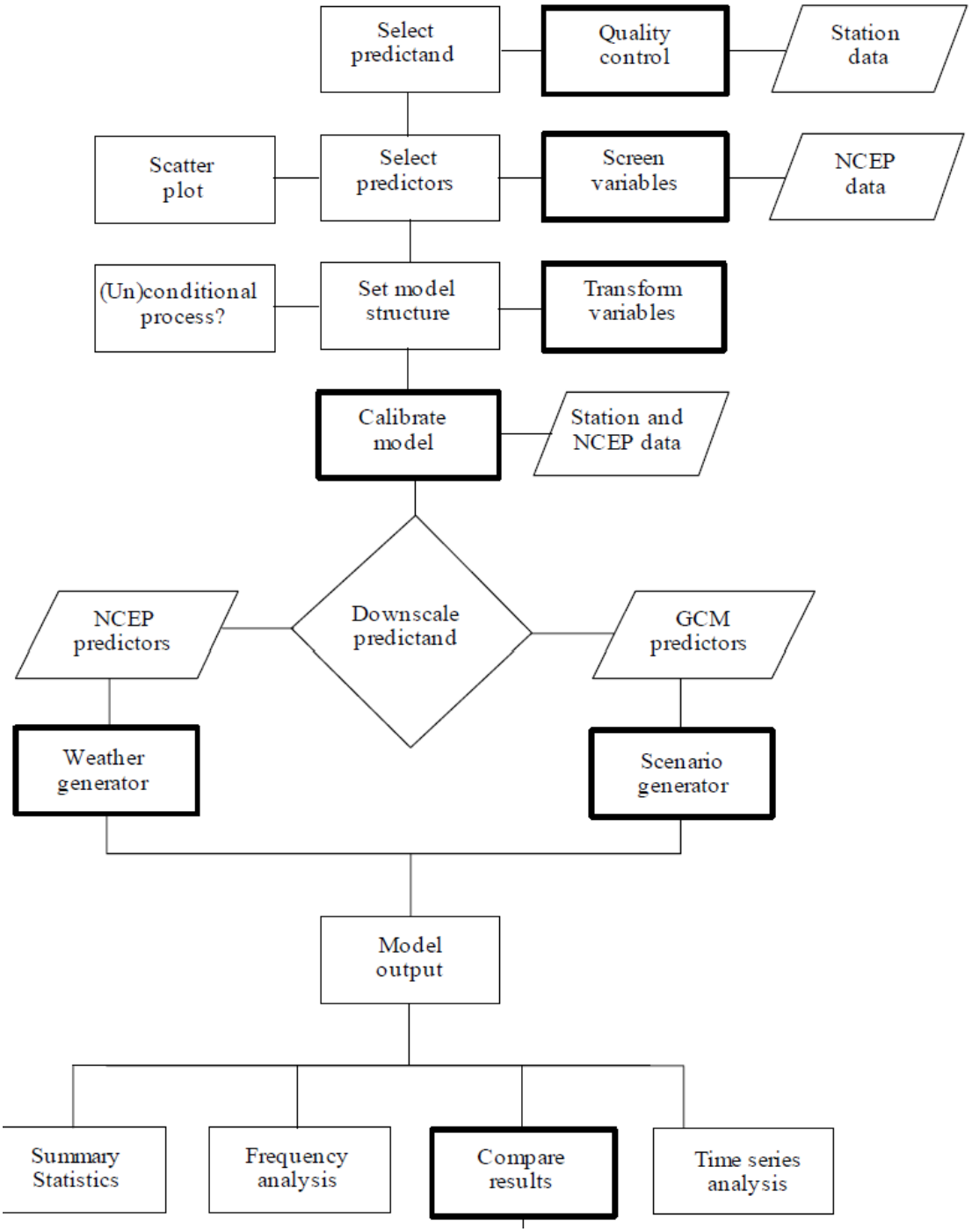

Fig. 4.2 Flow Chart of SDSM
(Source: SDSM User Manual, page 13)

d) Weather generator

The Weather Generator operation generated ensembles of synthetic daily weather series given observed atmospheric predictor variables. The procedure enabled the verification of calibrated models (using independent data) and the synthesis of artificial time series i.e. when model was calibrated using observed data of period 1960-2000, a new time series of data was generated for same number of years i.e. 1960-2000 or less with in the same period to check if model is calibrated correctly, for present climate conditions. Then I have selected a calibrated model and SDSM automatically links all necessary predictors to model weights. I have specified the period of record to be synthesized as well as the desired number of ensemble members. Synthetic time series have been written to specific output files for later statistical analysis, graphing and/or impacts modelling.

e) Data analysis

SDSM provided means of interrogating both downscaled scenarios and observed climate data with the Summary Statistics and Frequency Analysis tools in the model. In both cases, I have specified the sub–period, output file name and chosen statistics. For model output, the ensemble member or mean, must also be specified. In return, SDSM displayed a suite of diagnostics including monthly/ seasonal/ annual means, measures of dispersion, serial correlation and extremes.

f) Graphical analysis

Three options for graphical analysis were provided by SDSM through the Frequency Analysis, Compared results and the Time Series Analysis screens. The Frequency Analysis screen allowed to plot extreme value statistics of the chosen data files. Analyses included Empirical, Gumbel, Stretched Exponential and Generalized

Extreme Value distributions. The Compared results screen enabled me to plot monthly statistics, produced by the Summary Statistics screen. Having specified the necessary input file, either bar or line charts may be chosen for display purposes. The graphing option allowed simultaneous comparison of two data sets and hence rapid assessment of downscaled versus observed or present versus future climate scenarios. The Time Series Analysis tool allowed to produce time series plots up to a maximum of five variables. The data could be analyzed as monthly, seasonal, annual or water year periods for statistics such as Sum, Mean, Maximum, Winter/Summer ratios, Partial Duration Series, Percentiles and Standardized Precipitation Index.

g) Scenario generation

Finally, the Scenario Generator operation produced ensembles of synthetic daily weather series given atmospheric predictor variables supplied by a climate mode (either for present or future climate experiments), rather than observed predictors. This function was identical to that of the Weather Generator operation in all respects except that it might be necessary to specify a different convention for model dates and source directory for predictor variables. The input files for both the Weather Generator and Scenario Generator options need not be the same length as those used to obtain the model weights during the calibration phase.

4.5 SWAT MODEL SETUP

Geographic information systems data for the SWAT model were preprocessed by two distinct functions such as, watershed delineation and determination of hydrologic response units (HRUs) Step-wise procedure is described under:

Geographic data frameworks information for the SWAT model was preprocessed by two different functions which are, watershed delineation and determination of hydrologic response units (HRUs). For the flow and sediment modeling the Step-wise procedure is described under:

1. Watershed Delineation
2. Hydrologic Response Unit (HRU) Analysis
3. Input Tables data (Weather station data files)
4. SWAT Simulations
5. Model Calibration and Validation

4.5.1 Watershed Delineation

Watershed analysis is the first step to run the SWAT model. Watershed delineation for the Gilgit and Ghorband river catchments was performed using ArcSWAT2012. A 90 m by 90 m resolution DEM was incorporated to Arc SWAT model for the watershed delineation of study area.

Primarily defined the unit system to project and also defined the projection to the DEM. The process flow directions and accumulations, stream network and create streams were completed and defined manually outlets at the point of interest. The watershed was divided into sub-catchments. Watershed delineation for the Gilgit and Ghorband river catchments are shown in Figure 4.3 and 4.4 respectively.

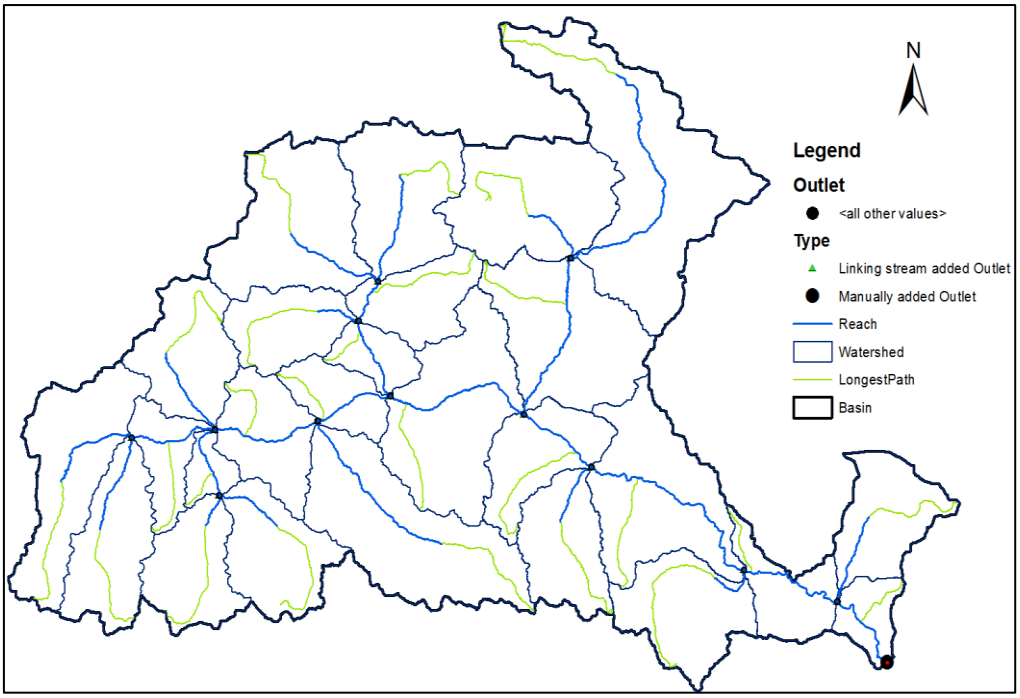

Fig. 4.3 Watershed Delineation of Gilgit River Catchment

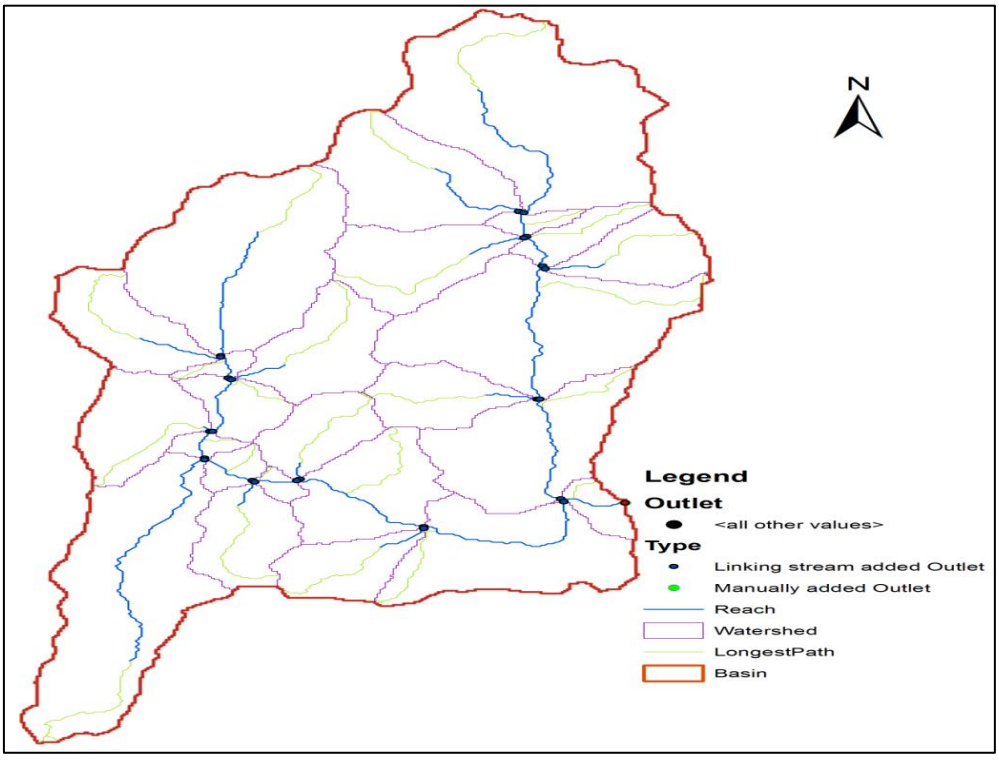

Fig. 4.4 Watershed Delineation of Ghorband River Catchment

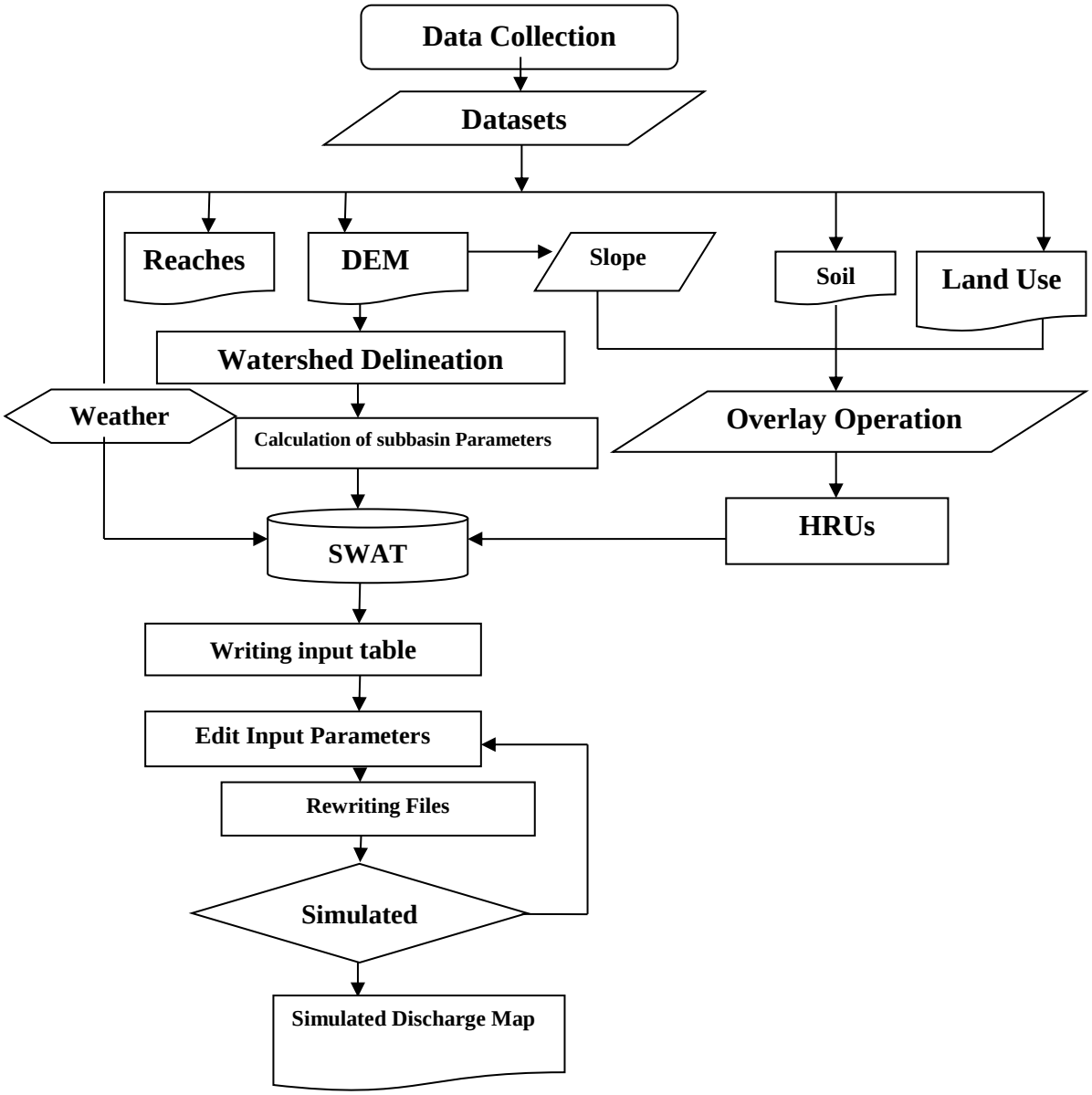

Fig. 4.5 Flow Chart of modelling with SWAT Model

4.5.2 Hydrologic Response Unit (HRU) Analysis

SWAT a watershed was subdivided into sub basins based on the number of tributaries. The sizes of watersheds and number sub basins in the watershed vary from place to place. The sizes of sub basins also vary based on the nature of the topographic and the stream network system of an area. The HRU in SWAT are spatially implicit, their exact position on the surface cannot be identified and the same

HRU may cover different locations in a sub basin (Neitsch et al., 2002). The water balance of each HRU in the watershed was represented by four storage volumes: snow, soil profile (0-2 meters), shallow aquifer (typically 2-20 meters) and deep aquifer (more than 20 meters). Each HRU in a sub watershed is liable for flow sediment, nutrient, and pesticide loadings that are routed through channels, ponds or reservoirs to the watershed outlet. Detailed descriptions of the model and model components can be found in (Arnold et al., 1998) and (Neitsch et al., 2000). Hydrologic response units (HRUs) are the lumped areas within the sub-basin which have been made up of distinctive area soil, land use, slope and different managing combinations. HRUs make it possible for the model to reflect differences in evapo-transpiration and other hydrological conditions for various soil and land use. The runoff can be approximated individually for each and every HRU and routed to get the entire runoff for the watershed. This increased the accuracy within the runoff prediction and provided an improved physical description of the water balance. HRU analysis includes the land use, soil type, slope definition and HRU definition.

4.5.2.1 Land Use / Cover Data

The first step in HRU analysis was to load projected coordinate system data of land use into the Arc SWAT interface. Land use classes of the project area were defined. A look up table was used to define the land use classes. Thirteen (13) different types of land use were obtained for the Gilgit basin and Fourteen (14) different land use classes were obtained for Gorband Catchment as shown in Tables 4.3 and 4.4 respectively. Land use categories for Gilgit and Gorband river Catchments are shown in Tables 4.3 and 4.4.

Table 4.3 Land use categorization of Gigit Basin

Sr. No.	Land Use Category
1	Irrigated Croplands
2	Rain fed Croplands
3	Closed (>40%) needle leaved evergreen forest (>5m)
4	Mosaic Cropland (50-70%) / Vegetation (grassland, shrubland, forest) (20-50%)
5	Mosaic Vegetation (grassland, shrubland, forest) (50-70%) / Cropland (20-50%)
6	Closed to open (>15%) mixed broadleaved and needleleaved forest (>5m)
7	Mosaic Forest/Shrubland (50-70%) / Grassland (20-50%)
8	Mosaic Forest/Shrubland (50-70%) / Grassland (20-50%)
9	Mosaic Grassland (50-70%) / Forest/Shrubland (20-50%)
10	Sparse (>15%) vegetation (woody vegetation, shrubs, grassland)
11	Barren
12	Water bodies
13	Permanent Snow and Ice

Table 4.4 Land use categorization of Ghorband Catchment

Sr. No.	Land Use Category
1	Irrigated Croplands
2	Rain fed Croplands
3	Closed (>40%) needle leaved evergreen forest (>5m)
4	Mosaic Cropland (50-70%) / Vegetation (grassland, shrubland, forest) (20-50%)
5	Mosaic Vegetation (grassland, shrubland, forest) (50-70%) / Cropland (20-50%)
6	Closed to open (>15%) mixed broadleaved and needle leaved forest (>5m)
7	Mosaic Forest/Shrubland (50-70%) / Grassland (20-50%)
8	Mosaic Forest/Shrubland (50-70%) / Grassland (20-50%)
9	Mosaic Grassland (50-70%) / Forest/Shrubland (20-50%)
10	Sparse (>15%) vegetation (woody vegetation, shrubs, grassland)
11	Barren
12	Water bodies
13	Permanent Snow and Ice
14	Forest

4.5.2.2 HRU Definition

HRU definition was the last step in HRU analysis. In this study HRU dissemination was determined by assigning multiple HRUs to each sub catchment. In multiple HRUs definition, a threshold value was used to exclude minor land uses, soils or slope classes which were not contributing enough flow in each sub-basin. Land use, soils or slope classes which cover less than the threshold value were excluded. As per defined SWAT user guide it was suggested that it is better to use a larger number of sub-basins than larger number of HRUs in a sub-basin, a maximum of 10 HRUs in a sub-basin was recommended (Winchell et al 2013). Hence, taking the recommendations into consideration, 2%, 4%, and 6% threshold values for the land use, soil and slope classes were used.

4.5.3 Weather Data Definition

The climate of a watershed gives the moisture and energies inputs that control the water balance and focus the relative significance of the diverse parts of the water cycle. The climatic variables needed by SWAT are maximum and minimum temperature, daily precipitation, relative humidity, solar radiation and wind speed were arranged in the proper database format. Because of data accessibility and quality daily precipitation, and maximum and minimum temperature in text format were the climatic data variables imported together with their weather location.

4.5.4 SWAT Simulation

In the next task, the database files containing the information needed to generate default input for SWAT model were built. In SWAT, once the default input database files are built, the necessary parameters values can be entered later and edited manually. The HRU distribution was also modified whenever it was needed.

The soil parameters values of each type of soil were entered. The land use/cover parameters were edited where it was necessary. Since the Penman-Monteith equation requires detailed climatological data which are not easily available especially in developing nations, the Hargreaves (Hargreaves et al, 2003) method was chosen to calculate evapotranspiration (ETo). Hargreaves equation can be used in the lack of sufficient or reliable data to solve the Penman Monteith equation (Allen, et al.1998). The equation can estimate the ETo using only daily mean, maximum and minimum air temperature, usually available at most weather stations worldwide and extraterrestrial radiation. The curve number for runoff and the variable storage for channel routing were chosen. Percolation component was modeled with a layered storage routing technique combined with a crack flow model. A skewed normal distribution was assumed for rainfall distribution.

SWAT simulation run was carried out for three periods 1991-1992, 2000-2001 and 2009-10. The run output data imported to database and the simulation results were saved in different files of SWAT output. The file named basins.rch contains stream-flow and water quality parameters in streams and rivers. It is used for SWAT model calibration since most of the observations of the watershed's behavior are obtained by measuring these parameters.

4.6 MODEL CALIBRATION AND VALIDATION

Model calibration was done to obtain optimal values of sensitive parameters. SWAT 2012 provides manual calibration method for model calibration. For this study, manual calibration was done first to modify the parameters little bit. First, some model parameters were adjusted by manual calibration. In this technique, parameters values were balanced by changing maybe a couple parameters at once within the

permissible ranges either by replacement the initial value or addition or by multiplication of the initial value. Then, auto calibration tool SWAT-CUP was used. In SWAT 2012 the auto-calibration tool has been excluded which was included in SWAT 2009. Auto-calibration is now included in SWAT-CUP. The calibration was done on monthly time steps using the average measured stream flow data of the Simly Dam watershed covering three time spans 1991-92, 2000-01, 2009-2010. Auto calibration was performed for sensitivity parameters that formed medium, high and very high mean sensitivity values. Arc SWAT includes a multi objective, automated calibration procedure that was developed by (Van Griensven, 2006). The calibration procedure is based on a Shuffled Complex Evolution Algorithm (SCE-UA) and a single objective function. For this study, SUFI-2 option was selected (Van Griensven et al., 2006). This method was chosen for its applicability to both simple and complex hydrological models. In this procedure, by entering the Arc SWAT interface Auto-Calibration window, first the SWAT simulation was specified for performing the auto-calibration and the location of the sub basin where observed data could be compared against simulated output. Then, the desired parameters for optimization, observed data file, and methods of calibration were selected. Hence, 10 flow parameters were considered in the calibration process. After the auto calibration runs completed, the model was run using the best parameter output values.

4.7 MODEL EVALUATION

The performance of SWAT was evaluated using statistical measures to determine the quality and reliability of predictions when compared to observed values. Coefficient of determination (R2) and Nash-Sutcliffe simulation efficiency (ENS) were the goodness of fit measures used to evaluate model prediction. The R2

value is an indicator of strength of relationship between the observed and simulated values. The Nash-Sutcliffe simulation efficiency (ENS) indicates how well the plot of observed versus simulated value fits the 1:1 line. If the measured value is the same as all predictions, ENS is 1. If the ENS is between 0 and 1, it indicates deviations between measured and predicted values. If ENS is negative, predictions are very poor, and the average value of output is a better estimate than the model prediction (Nash, Sutcliffe, 1970). The R2 and ENS values are explained in equations below.

$$R^2 = \frac{[\sum(Q_{m,i}-\bar{Q}_m)(Q_{s,j}-\bar{Q}_s)]^2}{\sum(Q_{m,j}-\bar{Q}_m)^2 \sum(Q_{s,i}-\bar{Q}_s)^2} \quad (4.5)$$

$$NSE = 1 - \frac{\sum_i(Q_m-Q_s)^2}{\sum_i(Q_{m,i}-\bar{Q}_m)^2} \quad (4.6)$$

Where Q_m, Q_s,$\bar{Q}_m$ $\bar{Q}_s$ are the measured, simulated, average measured discharge and average simulated Discharge respectively.

Table 4.5 General performance ratings for recommended statistics for a monthly time

Performance Rating	**For Stream Flow**	
	RSR	**NSE**
Very good	0.0<=RSR<=0.5	0.75<NSE<=1
Good	0.5<RSR<=0.6	0.65<NSE<=0.75
Satisfactory	0.6<RSR<=0.7	0.5<NSE<=0.65
Unsatisfactory	RSR>=0.7	NSE<=0.5

4.8 SWAT-CUP

SWAT-CUP is a public domain program, and as such may be used and copied freely. SWAT-CUP uses 5 different algorithms for the calibration, validation and sensitivity analysis, i.e. The Sequential Uncertainty Fitting ver. 2 (SUFI-2), Generalized Likelihood Uncertainty Estimation (GLUE), Parameter Solution (PARASOL). SUFI-2 was used in this study. SWAT-CUP has following advantages:

1. Various calibration/uncertainty analysis procedures are integrated for SWAT in one user interface.
2. Makes the calibrating procedure easy to use for students and professional users,
3. Provides a faster way to do the time consuming calibration operations and standardize calibration steps.
4. Extra functionalities for calibration operations are added such as creating graphs of calibrated results, data comparison, etc.

A step by step operation of SWAT-CUP is given below.

1. First click on New and then New Project and then locate the "TxtInOut" directory which is created when SWAT model is run.
2. Then click next button and select the SWAT version you have used and the processor type either it is 32bit or 64bit.
3. Then Select a program from the list provided (SUFI2, GLUE, ParaSol, MCMC, PSO). In this study SUFI-2 was used.
4. Now choose from the menu for which you have the measured data for calibration and sensitivity analysis the appropriate button. These are from

SWAT output file output.rch, output.hru, and output.sub. Output.rch was selected for this study.

5. Under the Calibration Inputs edit the following files:

4.8.1 Par_inf.txt

This file contains model input parameters to be optimized. New parameters can also be added in this file. Parameters range is also set in this file.

4.8.2 SUFI2_swEdit.def

This file contains the beginning and ending of simulation. Beginning and ending year of simulation can also be checked from OUTPUT.rch file.

4.8.3 File.cio

This file is put here for our convenience. Here we can set simulation years and warm up period for the model.

4.8.4 Absolute_SWAT_Values.txt

All parameters are given in this file plus the range of different parameters is also given in this file. Most of the parameters are included in this file. Parameter are also added from this file.

1. Under “Observation” three observed variables are given Rch, HRU, and Sub. As described earlier we select that variable for which we have the observed data. In this study “Rch” was selected. In “Observed.rch” we put the observed for our outlet.

2. Under “Extraction” number of variables, total no of reaches in a watershed, the beginning and ending year of simulation and time step for which calibration is done are edited.
3. After we edit all files then calibration command is executed. A batch file runs the preprocessing procedures, which include Latin hypercube sampling program. This batch file usually does not need to be edited. After that it runs the post-processing procedures, which runs the programs for objective function calculation, new parameter calculation, 95ppu calculation and 95ppu for behavioral simulations.
4. After pre and post-processing a summary file is achieved. This file has the statistics comparing observed data with the simulation band through p-factor and r-factor and the best simulation of the current iteration by using R^2, NS, bR^2, MSE, and SSQR.

4.9 SENSITIVITY ANALYSIS

4.9.1 One-At-A-Time Sensitivity Analysis

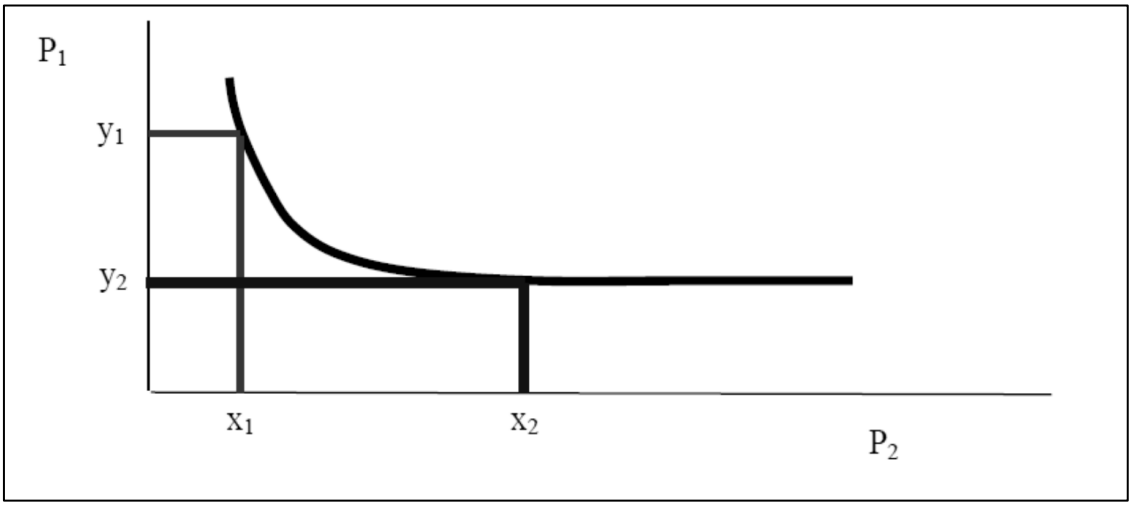

Fig. 4.6 One-At-A-Time Sensitivity Analysis

One-at-a-time sensitivity demonstrates the sensitivity of a variable to the adjustments in a parameter if every other parameter are kept constant at some value. The issue here is that we never recognize what the estimation of those other consistent parameters ought to be. This is a critical thought as the sensitivity of one parameter relies on upon the estimation of different parameters. One-at-a-time sensitivity analysis was performed in ArcGIS interface. 3-4 simulations were performed and in each simulation different value of parameter was taken and results of that changed value was checked in the SWAT output file. If the minor change in value results in 15% increase or decrease in the output results, the parameter was called the sensitive parameter.

The above graph shows this point. In the event estimation of parameter P1 is kept steady at y1, then little changes in parameter P2 roll out critical changes in the output and shows that P2 is truly a sensitive parameter. While if the estimations of parameter P1 is kept steady at y2, then changes in parameters P2 around x2 will give the feeling that P2 is not a sensitive parameter. Consequently, the value of the fixed parameter make a difference to the sensitivity of parameter. Following is the description of the parameters which were used in one-at-a-time sensitivity analysis.

4.9.2 Maximum Canopy Storage

The plant canopy can altogether influence evapotranspiration, surface runoff and infiltration. With the start of rainfall, canopy interception decreases the erosive vitality of drops and traps a segment of the precipitation inside of the canopy. The impact the canopy applied on these processes is a functions is a function of the density of plant cover and the morphology of the plant species.

4.9.3 Base Flow Alpha Factor

The baseflow recession constant is an immediate index of groundwater flow reaction to changes in recharge. Values ranges from 0.1-0.3 for area with moderate reaction to recharge to 0.9-1.0 for area with a fast reaction. Despite the fact that the baseflow recession constant can be calculated, the best estimation are obtained by breaking down measured streamflow during times of no recharge in the basin. It is basic to discover the baseflow days reported for a stream gage or watershed.

4.9.4 Threshold Depth Shallow Aquifer

Threshold depth of water in the shallow aquifer is needed for return flow to happen (mm H20). Groundwater flow to the reach is permitted just if the depth of water in the shallow aquifer is equivalent to or more than GWQMN.

4.9.4.1 Soil Evaporation Compensation Factor

This coefficient has been incorporated to permit the user to adjust the depth distribution used to meet of the soil evaporation demand to record for the impact of crusting, cracks and capillary action. ESCO must be somewhere around 0.01 and 1.0. As the ESCO value is decreased, the model has the capacity to extract a greater amount of the evaporation demand from lower soils.

4.9.4.2 Plant Uptake Compensation Factor

The measure of water uptake that happens on a given day is function of the amount of water needed by the plant for transpiration, and the amount of water accessible in the soil zone, SW. if upper layers in the soil profile don't contain enough water to meet the potential water uptake, user may permit lower layers to adjust. The

plant uptake compensation factor can extend from 0.01 to 1.00. As EPCO of 1.0, the model permits a greater amount of the water uptake to be met by soil lower layers. As EPCO of 0.0, the model permits less variation.

4.9.4.3 Surface Runoff Lag Coefficient

In vast sub-basins with a time of concentration more than 1 day, just a bit of the surface overflow will reach the channel on the day it is created. SWAT has a surface runoff storage feature to lag a part of the surface flow discharge to the channel. SURLAG controls the part of the water that will be permitted to enter the channel on any one day.

4.9.4.4 Groundwater Delay Time

Water that moves down the lower soil profile by percolation enters and flow through the vadose zone before getting into shallow aquifer. The lag time between the water leaves the soil profile and enters the shallow aquifer will rely on upon the depth of water table and hydraulic properties of the geologic formations.

4.9.4.5 Available Water Capacity of the Soil Layer

The plant accessible water, additionally mentioned to as the available water capacity, is ascertained by subtracting the water present at permanent wilting point from that present at capacity, AWC = FC —WP where AWC is the plant accessible water content, FC is the water content at field capacity, and WP is the water content at permanent wilting point. Accessible water limit is evaluated by deciding the measure of water discharged between in situ field capacity and the permanent wilting point.

4.9.4.6 Effective Channel Hydraulic Conductivity

Effective hydraulic conductivity is in river channel alluvium (mm/hr). The parameter controls transmission losses from surface flow as it flows to the main channel in the sub-basin.

4.9.4.7 Manning's "n" Value

The Manning's equation is an empirical equation that applies to uniform flow in open channels and is a function of the channel velocity, flow area and channel slope.

Table 4.6 Manning's n for Open Channels

Characteristics of Channel	Median	Range
Excavated or dredged		
Earth, straight and uniform	0.025	0.016-0.033
Earth, winding and sluggish	0.035	0.023-0.050
Not maintained, weeds and brush	0.075	0.040-0.140
Natural streams		
Few trees, stones or brush	0.050	0.025-0.065
Heavy timber and brush	0.100	0.050-0.150

4.9.5 Global Sensitivity Analysis

Parameter sensitivities are dependent on calculating the several regression system which relapses the Latin hypercube generated parameters contrary to the objective function.

$$g = \alpha + \sum_{i=1}^{m} \beta_i b_i \qquad (4.7)$$

A t-test is then utilized to know the relative value of each parameter bi. The sensitivity given above is estimates of the normal variations in the objective function as a result of adjustments to each parameter, while all other parameters are varying. This offers

relative sensitivity determined by linear estimates and, hence, only offers partial data of the sensitivity of the objective function to model parameter.

Parameter Name	t-Stat	P-Value
v__GW_DELAY.gw	-3.337574158	0.015658773
v__ALPHA_BF.gw	-2.433339763	0.050930647
v__GWQMN.gw	-2.073586080	0.083472224
r__SOL_AWC(1).sol	-1.770079408	0.127110027
r__SOL_K(1).sol	-1.518643093	0.179654451
r__SOL_BD(1).sol	-0.538486165	0.609622018
v__GW_REVAP.gw	-0.287790123	0.783189355
v__SFTMP.bsn	0.050625906	0.961266915
v__CH_K2.rte	0.524989407	0.618415467

Fig. 4.7 Sensitivity Analysis

T-stat gives a way of measuring sensitivity (larger values are more sensitive) while p-values indicate the importance in the sensitivity. A parameter. In the preceding example, one of the most sensitive parameters are CN2 as well as ESCO and also GW_DELAY.

4.10 SCENARIOS DEVELOPMENT

Scenarios have come about helpful tools to check out unsure futures conditions throughout ecological and anthropogenic system. Scenarios alter from forecast, projection, and prediction for the reason that they illustrate alternative futures presented our recent perception of the ways involving landuse and land-cover (LULC) changes to have an impact on ecosystems. Simply because landuse changes have substantial impacts on ecological system, partially explicit modeling enables researchers, analysts and ecological modelers to analyze the actual impacts of landuse changes on hydrology, nearby and regional temperature and climatology, biochemical

fluxes, and biodiversity. In order to develop management practices for protecting the catchment and to assess the impacts of landuse changes specifically on runoff generation and water yield three scenarios were developed. Landuse maps were developed for different scenarios and model simulation. To develop landuse scenarios first changed landuse maps for the future were prepared on the basis of the past landuse changes. Percentage change per annum for every landuse classification was calculated and then on the basis of these per annum changes in landuse changes, future landuse maps were formed and then model simulation was performed using the changed landuse maps and results were obtained. Forest area decreased 0.5% per year, vegetation class decreased 0.2%, Build up areas increased 0.14%, rangeland increased 0.13% and Barren land increased 0.31% per year during the last 18 years. On the basis of these calculations the predicted landuse map for the next 20 years was prepared. Three landuse scenarios were performed, Scenario A: expansion of urban areas from 5% to 10% on the basis of past landuse changes, Scenario B: expansion of forests areas from 46% to 66% on the basis of past landuse changes, Scenario C: deforestation of the catchment from 46% to 36% on the basis of past landuse changes. Scenarios were developed keeping the rainfall pattern same for all the scenarios of base year (2010) to assess the landuse impacts on runoff generation in Simly Dam watershed.

4.11 OPTIONS TO REDUCE SEDIMENT YIELD IN THE BASIN

The determination of the threshold which characterizes the risk in any area depends on the basin, the amount of sediment that it is generating and the purpose of the determination. Tamene et al (2005) regarded more than 50t/ha/year as very high sediment yield. Tim et al., (1992) on the other and, defined only 9 t/ ha/ year as the

critical erosion tolerance for the Nomini Creek watershed. Singh et al, in 1992 defined the critical erosion rates in India to be 0-5, 5-10, 10-20, 20-40, 4080 and >80 t/ha/year as slight, moderate, high, very high, severe and very severe. Based on the reviews stated above, the sediment yield in this study is categorized in 6 classes and the values for the threshold are shown in the Table 4.7.

Table 4.7 Threshold values for critical areas for sediment generation

Sr. No.	Sediment Yield Range (t/ha/year)	Zone
1	0-4	Slight
2	4-8	Moderate
3	8-16	High
4	16-32	Very High
5	32-64	Severe
6	>64	Very Severe

The sub basin generating severe and very severe amount of sediment yield under present conditions have been selected in this study to apply adaptation options to reduce soil erosion and manage the sediment. Preventing soil erosion and sedimentation requires political, economic and technical actions (Okalp, 2005). It is very important to examine all the adaptation possibilities according to the best available information. Based on the results of this study, structural or non-structural adaptation measures may be recommended to reduce the erosion and the resulting sediment yield in the critical areas in Gilgit and Ghorband river basin.

In order to adapt to the increasing sediment yield and erosion in the basin, steps can be taken to either manage the sediment in the basin or decrease the loss of soil from the ground, i.e, to reduce the erosion. Details of both alternatives are given below.

4.11.1 Sediment Management Options

Two options for the sediment managements have been analyzed for the selected study area, the details area given below:

4.11.1.1 Check Dams

These are small dams temporarily built across small streams and channels. Check dams reduce erosion by reducing the velocity of the concentrated flow in a channel. In SWAT, check dams can be simulated as they are impoundments located in the subbasin area Input in SWAT model for check dam is given below

- Fraction of sub basin area that drains into pond = FR = 1
- Surface area of the ponds when filled to principle spillway (ha) = PSA = 10
- Volume of water stored in ponds when filled to principle spillway (104 m^3 of H_2O) = P_VOL = 50
- Surface area of the ponds when filled to emergency spillway (ha)= ESA = 1
- Volume of the water stored in ponds when filled to the emergency spillway = E_VOL= 62
- Initial volume of water in ponds (104 m^3 of H_2O) = VOL = 50
- Initial sediment concentration in pond water (mg/L) = SED = 2000
- Equilibrium sediment concentration in pond water (mg/L) = 2000

4.11.1.2 Sediment Basin

Sediment trap basin or sediment basin is constructed to collect debris. They are constructed to preserve the capacity of reservoirs, wetlands, canals, ditched and streams. Sediment basin traps the sediment which originates from construction sites and other disturbed lands. It can be simulated as a pond in SWAT. Input in SWAT model for sediment basin is given below

- Fraction of sub basin area that drains into pond = FR = 1
- Surface area of the ponds when filled to principle spillway (ha) = PSA = 5
- Volume of the water stored in ponds when filled to principle spillway (104 m^3 H_2O) = P_VOL = 25
- Hydraulic conductivity through bottom of ponds = K = 0.2

4.11.2 Sediment Reduction Options

Two options for the sediment managements has been analyzed for the selected study area, the details area given below:

4.11.2.1 Filter Strip

Filter strips are vegetative areas between grazing land, cropland, disturbed land or forest land and surface water bodies (i.e, streams or lakes). They are provided in the location where runoff leaves the land with the purpose that the sediment and nutrients are filtered from going into the water body.

Input in SWAT model for filter strip is given below

- Fraction of the total runoff from the entire field entering the most concentrated 10% of the VFS = VFSCON =0.25
- Field area to VFS area ratio = FS RATIO =50

- Fraction of stream flow through the most concentrated 10% of the VFS that is fully channelized = VFSCH = 0
- VFSI=1

4.11.2.2 Grassed Waterway

Grassed waterways are channels that are either manmade or natural which regulate the velocity of a concentrated flow to a safe level using suitable vegetation. The vegetation decreases the velocity and the soil erosion from the surface of the channel is therefore reduced

Input in SWAT model for Grass waterway is given below

- Flag to turn on the grassed waterway = GWATI = 1
- Manning's n value for the main channel = GWATn = 0.04
- Length of the grassed waterway (km) = L = 1000
- Average width of grassed waterway (m) = W = 10
- Depth of grassed waterway (m) = D = 4,
- Slope of waterway (%) = S = .005
- Linear parameter for calculating sediment in waterway = SPCON =0.005

Chapter 5
RESULTS AND DISCUSSIONS

The first objective is assessment of change in Climate parameters i.e. Precipitation, temperature and their impact on land use changes. The said objective is discussed in two sections primarily, assessment of climate parameters and secondly land use changes i.e. snow and glaciers changes.

5.1 ASSESSMENT OF CHANGE IN CLIMATE PARAMETERS

In this section trend analysis and variability in precipitation, temperature and stream flow of twenty-five climatic and thirty-five stream flow station were performed in Upper Indus Basin (UIB) over the period 1961-2014.The analysis has been carried out on annual, seasonal (winter (Dec-Feb), spring (Mar-May), summer (Jun-Aug), autumn (Sep-Nov) time series. The spatial distribution of trends and changes in precipitation, temperature and stream flow are discussed in preceding sections.

5.2 TEMPERATURE TRENDS UPPER INDUS BASIN

Temperature analysis has been performed on annual and seasonal data on the maximum, minimum and mean temperature data at the climate stations in upper Indus Basin.

5.2.1 Annual Trends in Upper Indus Basin

Analysis of the Annual maximum temperature has indicated the overall trend of the region is shifting towards warming trends for the period of 1961 to 2014, which is the signal of climate change. Among the twenty-five climate stations, Cherat and Bunji show

decreasing (negative) tends in annual maximum temperature. At the Skerdu station, the highest warming trend has been observed i.e. with the rate of 0.49 ^{0}C per decade at 99.9% significant level which is alarming for this very important zone of UIB. The warming trend is observed in the stations Gilgit, Gupis, Drosh, Chitral, Astore and Dir per decade temperature is increasing 0.3, 0.22, 0.23, 0.28 and 0.21 ^{0}C respectively with the maximum significant level of 99.9%. Parachinar and Kohat stations are shifting towards warming trend with rate of 0.18 and 0.27 ^{0}C per decade with 99% significant level. Annual maximum temperature of Peshawar and Saidu Sharif is also moving towards the warming trend with the rate of 0.14 and 0.3 ^{0}C per decade at 95% significant level. Bisham Qila, Risalpur and Chilas showed warming trend but statistically not significant. The annual maximum temperature decreased with the rate of 0.03, 0.38 and 0.18 ^{0}C per decade at Bunji, Cherat, and Kakul respectively as shown in Figure 5.1. The overall analysis of these twenty-five meteorological stations applying Mann-Kendall test and Sen‟s showed an increase of annual mean maximum temperature (20 out of 25) for the period 1961 to 2014. The analysis of the maximum, minimum and mean temperature for the selected stations is shown in Figures 5.1 and 5.2 respectively. The upward and downward arrows show per decade increasing and deceasing trends.

5.2.2 Seasonal Variability in Trends Upper Indus Basin

Figure 5.1 shows the variability of maximum temperature in Winter, Spring, Autumn and summer seasons, upward and downward arrow shows the per decade increase in temperature and bold arrow shows significant trend. Overall maximum temperature is increasing in the upper Indus basin, at the 75% stations maximum warming trend is observed in the winter season (Dec-Feb) during the spring season at the18% stations warming trends was observed and no stations shows the decreasing

trend of maximum temperature during the spring and winter seasons. Whereas during the autumn season 12% stations shows very strong increasing trends of maximum temperature.

Figure 5.2 demonstrates the spatial distribution of seasonal trends in minimum temperature for the period 1961-2014. The study reveals that most of stations have increasing trends in winter and autumn seasons whereas have cooling trends in spring and summer seasons. About 54%, 46%, 38% and 69% of the stations have warming trend in winter, spring, summer and autumn seasons respectively whereas 23%, 15%, 23% and 15% of stations have significant trends respectively.

5.3 PRECIPITATION TRENDS UPPER INDUS BASIN

Precipitation trend analysis has been performed on annual and seasonal data at climate stations in upper Indus Basin (UIB).

5.3.1 Annual Variability Upper Indus Basin

The results of analysis by applying Mann-Kendall besides Sen slope estimation methods; annual rainfall was summarized in Figure 5.4. At ten (15) stations out of sixteen (25) stations, the annual precipitation has been increased for the period 1961 to 2014.At the stations Risalpur, Bunji, Chilas, and Peshawar and Risalpur annual precipitation with highest significance level (99.9%) was observed with the rate of 40.24 (6%), 16.41 (9%), 40.33 (9%) and 9.41 (6%) mm per decade respectively. At the stations Skardu, Gilgit and Gupis increasing trend of annual precipitation has been observed with 99%% significance level and per decade increase in annual rainfall is 16.81(8%), 5. 8 (5%), and 12.2 (7%) respectively. Chitral station showed 95% significance level with rate of 22.65 (5%) mm

per decade. There are also some stations where annul maximum rainfall is decreased for period 1960-2013.At the stations Parachinar, Drosh, Cherat, Dir, Kohat and Astore 1.84 (1%) 9 (1%), 30 (5%), 41 (3%), 12.49 (2%) and 7.27 (1%), mm per decade respectively but all these were statistically inconsequential. The spatial distribution of the annual rainfall trends is shown in Figure 5.3. The upward and downward arrows show per decade increasing and deceasing trends.

5.3.2 Seasonal Variability Upper Indus Basin

Figure 5.4 shows the variability of precipitation in winter, spring, autumn and summer seasons, upward and downward arrow shows the per decade increase in precipitation and bold arrow shows significant trend. Majority (81%) of stations has the increasing trends during the winter precipitation, during the spring season 50% of stations have the increasing trends, during the summer season at the 83% of stations precipitation trends are increasing significantly and during the autumn season at the higher elevated areas precipitation is increasing significantly.

5.4 TEMPERATURE TRENDS IN GILGIT AND GHORBAND CATCHMENTS

5.4.1 Variability of Mean Maximum Temperature

The highest warming trend was observed in Gilgit station at the rate of 0.3 ^{o}C per decade which is highly statistically significant (at 99.9% significance). At Gupis station 0.2 ^{o}C per decade warming trend was observed in the maximum temperature at 99 % significance level. At Saidu Sharif station 0.5 ^{o}C per decade warming trend was observed during the winter season in the maximum temperature at 95 % significance level. Bunji showed decrease in 0.03 ^{o}C and Bisham Qila shown increase in 0.2 ^{o}C per decade temperature but statistically insignificant.

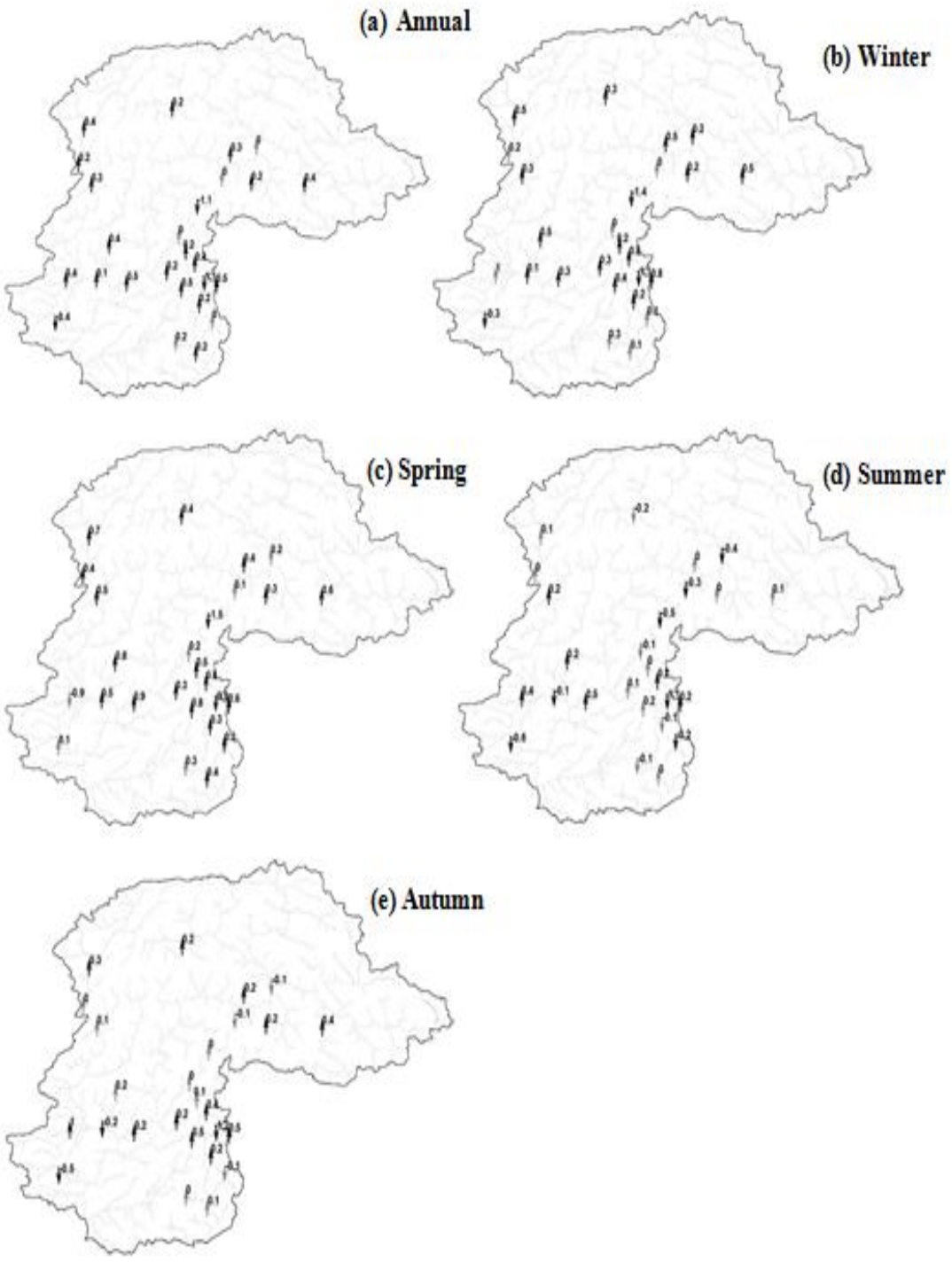

Fig. 5.1 Spatial distribution of trends detected by Mann-Kendal and trend values estimated by Sen's method showing change in % decade-1 of maximum temperature in: (a) annual, (b) winter, (c) spring, (d) summer, (e) autumn. (Upward and downward arrow shows positive and negative trends respectively; bold arrow shows significant trends at α=0.1)

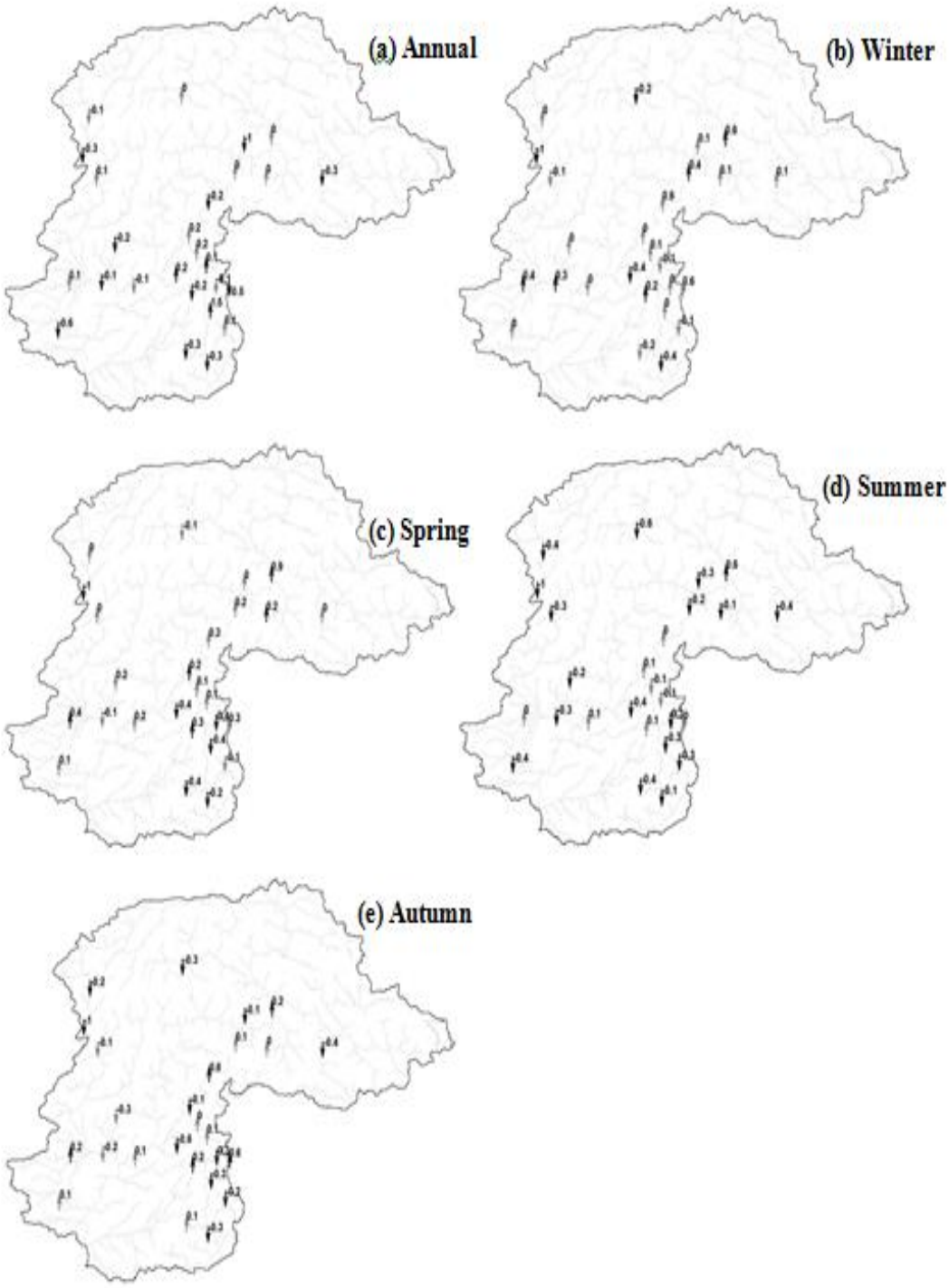

Fig. 5.2 Spatial distribution of trends detected by Mann-Kendal and trend values estimated by Sen's method showing change in ^{o}C decade-1 of minimum temperature in: (a) annual (Jan-Dec), (b) winter (Dec-Feb), (c) spring (Mar-May), (d) summer (Jun-Aug), (e) autumn (Sep-Nov), and. (Upward and downward arrow shows positive and negative trends respectively, bold arrow shows significant trends at $\alpha = 0.1$)

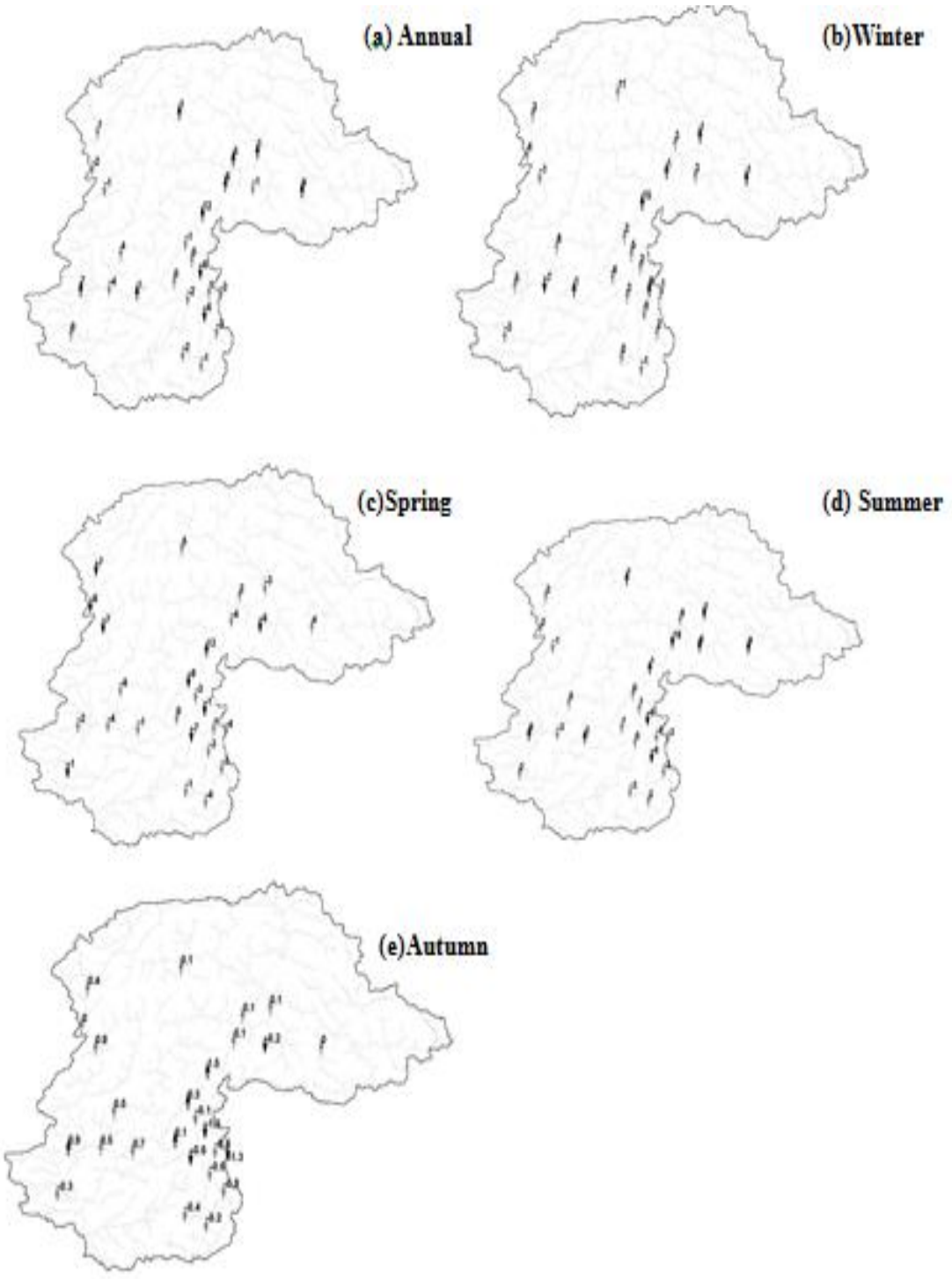

Fig. 5.3 Spatial distribution of trends detected by Mann-Kendal and trend values estimated by Sen's method showing change in % decade-1 of precipitation in: (a) annual (Jan-Dec), (b) winter (Dec-Feb), (c) spring (Mar-May), (d) summer (Jun-Aug), (e) autumn (Sep-Nov), (Upward and downward arrow shows positive and negative trends respectively; bold arrow shows significant trends at α=0.1)

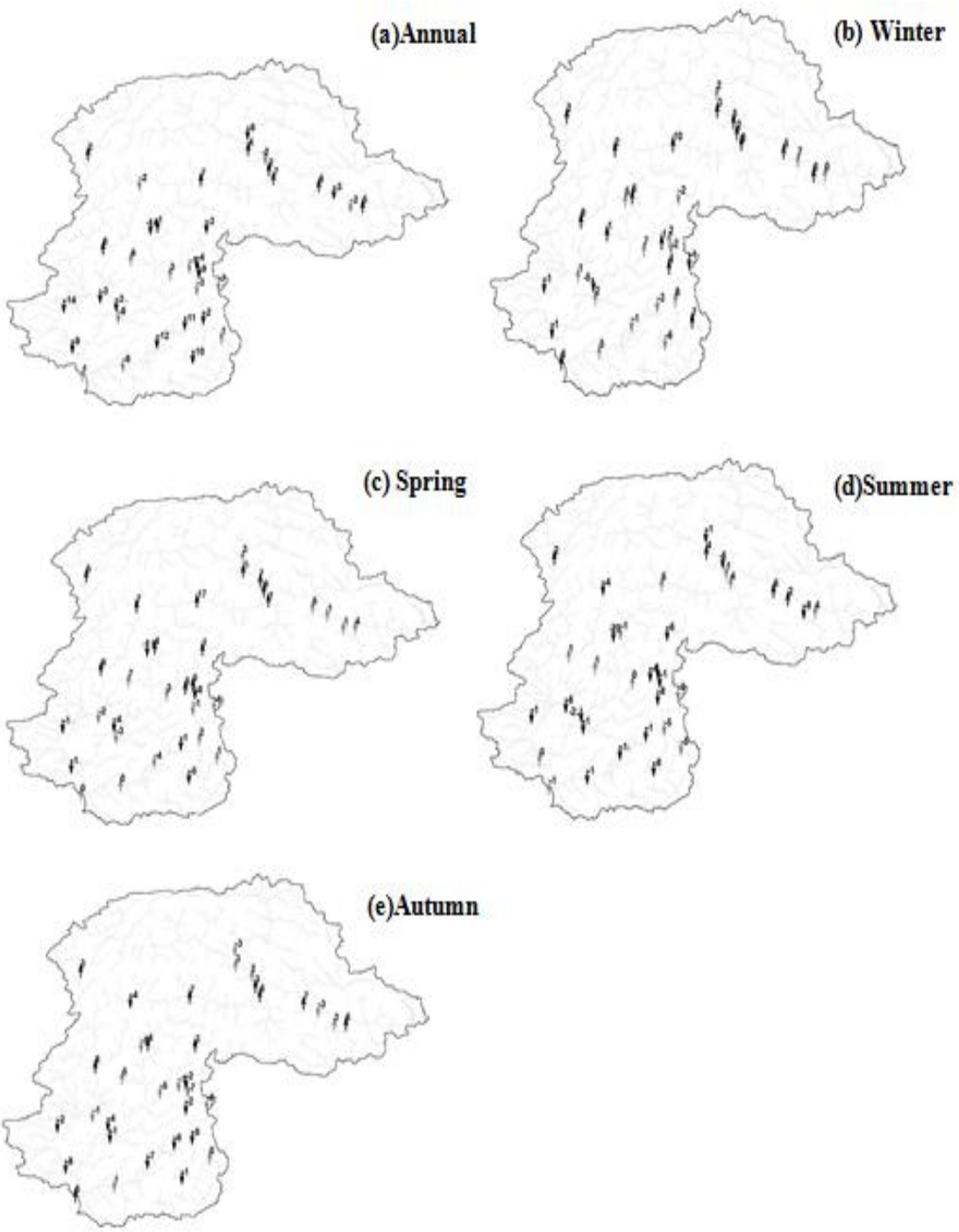

Fig. 5.4 Spatial distribution of trends detected by Mann-Kendal and trend values estimated by Sen's method showing change in % decade-1 of stream flows in: (a) annual (Jan-Dec), (b) winter (Dec-Feb), (c) spring (Mar-May), (d) summer (Jun-Aug), (e) autumn (Sep-Nov), and (f) % all and significant trends. (Upward and downward arrow shows positive and negative trends respectively; bold arrow shows significant trends at α = 0.1)

The overall analysis of three stations (Gupis, Gilgit and Bunji) indicate mean annual maximum temperature has significantly increased in the Gilgit basin. Whereas mean annual maximum temperature in Ghoband catchment is also increasing. As per studies Shrestha (2000) indicated that annual maximum temperature in mostly party of Himalaya is increasing at 0.6 ^{o}C per decade. Annual analysis of mean annual maximum temperature of selected climate station in and vicinity of Gilgit and Ghorband river catchmnts are given in Figure 5.5.

1.1.1 5.4.2 Seasonal Variability of Mean Maximum Temperature

During the winter season highest warming trend was observed at Gupis and Gilgit station at the rate of 0.3 and 0.3 ^{o}C per decade which is highly statistically significant (at 99.9% significance). At Bunji and Bisham Qila station 0.2 and 0.5 ^{o}C per decade warming trend was observed during the winter season in the maximum temperature at 95 % significance level. Saidu sharif showed decrease in 0.5 ^{o}C per decade temperature but statistically insignificant. The overall analysis of climate stations in Gilgit and Ghorband basin indicates that during the winter season mean maximum temperature is increasing. During the spring season highest warming trend was observed at Gilgit station at the rate of 0.4 per decade which is highly statistically significant (at 99.9% significance). At Gupis station 0.4 ^{o}C per decade warming trend was observed in the maximum temperature at 99 % significance level. At Bunji and Saidu Sharif station 0.2 and 0.6 ^{o}C per decade warming trend was observed during the spring season in the maximum temperature at 95 % significance level. Bisham Qila showed increase in 0.3 ^{o}C per decade temperature but statistically insignificant. The overall analysis of climate stations in Gilgit and Ghorband basin indicates that during the spring season mean maximum temperature is increasing.

During summer season mean annual temperature at Gupis and bunji is decreasing, and on the other at Bisham qila and Gilgit it is increasing. The analysis of climate stations in Gilgit basin summer temperature is decreasing and in Ghorband basin it is increasing. At some stations mean annual temperature during the autumn season increasing and decreasing at in study area. Seasonal analysis of mean annual maximum temperature of selected climate station in and vicinity of Gilgit and Ghorband river catchments are given in Figure 5.6.

5.4.3 Variability of Mean Minimum Temperature

It is clear from the Table 5.1 that annual minimum temperature Gupis, Gilgit and Bunji is decreasing at the rate of -0.3, -02, and -0.3 ^{o}C per decade which is highly statistically significant (at 99.9% significance). At Saidu Sharif showed increase in 0.01 ^{o}C and Bisham Qila shown decrease in 0.2 ^{o}C per decade temperature but statistically insignificant. Analysis indicates that mean annual minimum temperature in Gilgit basin is decreasing and in Ghorband catchment it consistent.

During the summer season annual minimum temperature Gupis, Gilgit and Bunji is decreasing at the rate of -0.5, -0.3, and -0.5 ^{o}C per decade which is highly statistically significant (at 99.9% significance). At Bisham Qila station -0.31 ^{o}C per decade cooling trend was observed in the maximum temperature at 95 % significance level. Saidu Sharif showed decrease in -0.2 ^{o}C per decade temperature but statistically insignificant. The overall analysis of climate stations in Gilgit and Ghorband basin indicates that mean minimum temperature is decreasing.

During the autumn season annual minimum temperature Gupis, Gilgit and Bunji is decreasing at the rate of -0.4, -0.4, and -0.5 ^{o}C per decade which is highly

statistically significant (at 99.9% significance). At Saidu Sharif showed decrease in -0.2 and at Bisham Qila shows increasing trend 0.04 ^{o}C per decade but statistically insignificant. Seasonal analysis of mean annual minimum temperature of selected climate station in and vicinity of Gilgit and Ghorband river catchments are given in Figure 5.6.

5.5 PRECIPITATIONS TRENDS IN GILGIT AND GHORBAND CATCHMENTS

At the stations Gilgit and Gupis increasing trend of annual precipitation has been observed with 99%% significance level and per decade increase in annual rainfall is 5. 8 (5%), and 12.2 (7%) respectively. Mean annual precipitation also increased at Bunji, Saidu Sharif and Bisham Qila but statistically not significant. It is concluded that mean annual rainfall is increasing in Gilgit basin.

During the winter season increasing trend was observed at Gupis and Gilgit station at the rate of 0.2 and 0.1mm per decade which is highly statistically significant (at 99.9% significance). At Bunji and Saidu Sharif 0.5 and 21.1 mm per decade increasing trend was observed at 95 % significance level respectively. Bisham Qila showed increase in 5 mm per decade but statistically insignificant. The overall analysis of climate stations in Gilgit and Ghorband basin indicates that during the winter season mean annual precipitation is increasing. During the summer and autumn season precipitation is increasing in Gilgit basin where as in Ghorband catchment it is decreasing. Annual and seasonal analysis of precipitation of selected climate station in and vicinity of Gilgit and Ghorband river catchments are given in Table 5.1.

5.6 ALTITUDINAL IMPACT ON CLIMATE CHANGE VARIATION IN CLIMATE CHANGE WITH ELEVATION

Analysis of the maximum, minimum, mean temperature and the annual rainfall has been made with the elevation, which is shown in Figure 5.5. Percent per decade in maximum temperature increase with an increase in elevation whereas minimum temperature decreases with an increase in elevation. Mean Temperature is also increasing with elevation. Analysis on relation between elevation and maximum and mean temperature indicate increasing trends with higher temperatures whereas decreasing trend for the minimum temperature. The maximum and mean temperature has higher trends in high mountainous region. The low elevated region (<1300 m) of UIB has the positive trends ranging from 2% to 9% in annual precipitation whereas the high mountainous region (>1300 m) has the cooling trends. The most of sub-basins of UIB have the increasing trends.

5.7 VARIABILITY IN STREAM FLOWS

As per Table 5.1 mean annual flow Gilgit river at Gilgit is increasing insignificantly and Ghorband river at karora is decreasing significantly. During the Spring, summer and autumn season mean annual flow Ghorband at Karora is decreeing whereas during the winter season increasing. Mean annual flow Gilgit river at Gilgit increasing during winter, spring, summer and autumn season.

Maximum annual flow, summer, spring and autumn flow is decreasing in Ghorband river at Karora and increasing during the winter season. minim annual and season flow in Ghorband river is also decreasing. Minimum annual and seasonal in flow Gilgt river is increasing. Annual maximum summer flow in Gilgit river is decreasing due to the decreasing temperature in the summer season. Annual and

seasonal analysis of stream flow of Gilgit river at Gilgit and Ghorband river at Karora are given in Figure 5.5.

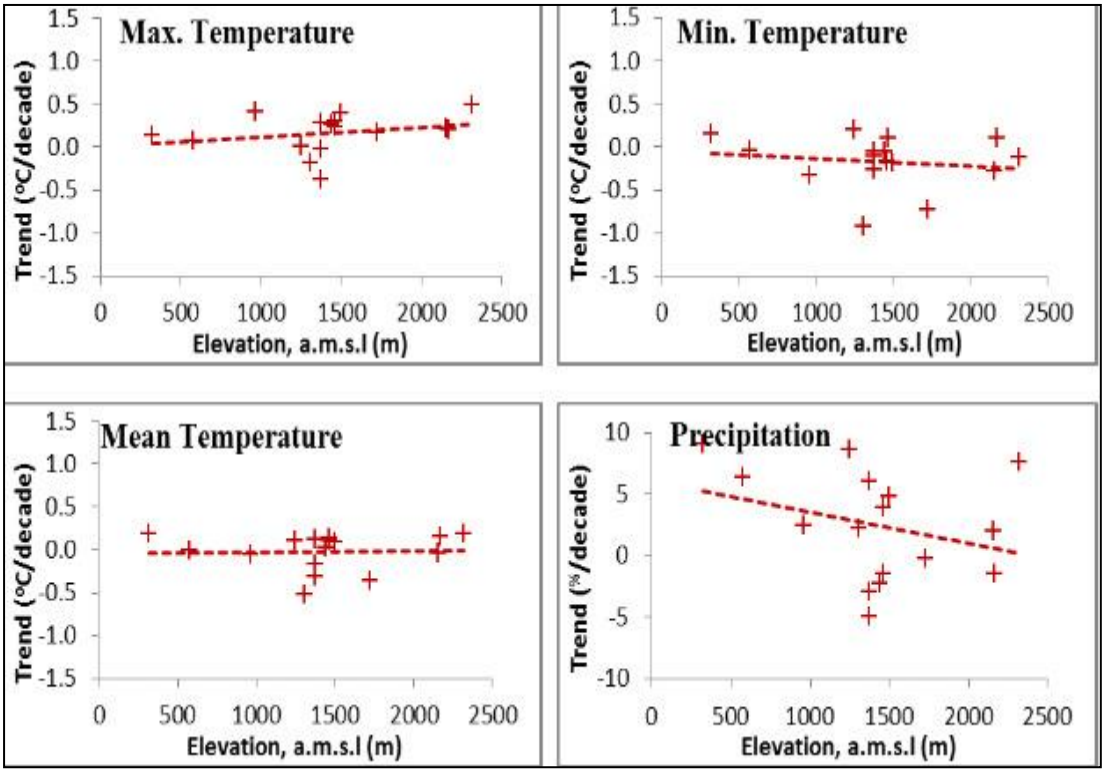

Fig. 5.5 Distribution of trends of precipitation, mean, maximum and minimum temperature with elevation.

Table 5.1 Trends detected by Mann-Kendal and trend values estimated by Sen's method in annual and seasonal (maximum & minimum temperature (oc decade-1), precipitation (mm per decade-1), mean, maximum & minimum flow) in Gilgit and Ghorband river catchments/ basins

Station	Basin / catchment	Annual	Bi-Annual (Oct to Mar)	Bi-Annual (Apr to Sep)	Winter (DJF)	Spring (MAM)	Summer (JJA)	Autumn (SON)
Mean Maximum Temperature ^{0}C								
Gupis	Gilgit	0.2**	0.3***	0.1	0.3***	0.4**	-0.1	0.1*
Gilgit	Gilgit	0.3***	0.3***	0.2*	0.3***	0.4***	0.1	0.2*
Bunji	Gilgit	-0.03	0.1+	-0.2*	0.2*	0.2*	-0.3**	-0.2*
Saidu Sharif	Ghorband	0.3*	0.3*	0.2	0.3+	0.6*	0.2	0.1

Station	Basin / catchment	Annual	Bi-Annual (Oct to Mar)	Bi-Annual (Apr to Sep)	Winter (DJF)	Spring (MAM)	Summer (JJA)	Autumn (SON)
Bisham Qila	Ghorband	0.2	0.2	0.1	0.5*	0.3	0.0	-0.1
Mean Minimum Temperature ^{0}C								
Gupis	Gilgit	-0.3***	-0.2**	-0.4***	-0.2*	-0.1	-0.5***	-0.4***
Gilgit	Gilgit	-0.2***	-0.2**	-0.3***	-0.2**	-0.1+	-0.3***	-0.4***
Bunji	Gilgit	-0.3***	-0.2**	-0.4***	-0.1	0.0	-0.5***	-0.5***
Saidu Sharif	Ghorband	0.1	-0.1	0.1	-0.1	0.3+	-0.2	-0.2
Bisham Qila	Ghorband	-0.01	0.15	-0.19+	0.20	-0.15	-0.31*	0.04
Precipitation (mm)								
Gupis	Gilgit	12.2**	3.0**	9.3***	0.2***	1.6*	4.4***	0.5**
Gilgit	Gilgit	5.8**	1.6**	5.3***	0.1***	-0.3	2.2***	1.4**
Bunji	Gilgit	0.6	-0.2*	1.6+	0.5+	-0.8	1.2	0.2
Saidu Sharif	Ghorband	28.2	-4.9	15.9	21.2+	-24.1	15.2	5.7
Bisham Qila	Ghorband	34.69	18.49	11.46	5.76	27.04	18.94	-6.35
Mean Flows (Cumeecs)								
Ghorband at Karora	Ghorband	-3.2***	-0.4	-5.9***	0.6	-7***	-5.6***	-0.6
Gilgit at Gilgit	Gilgit	2.1	0.5	3.8	0.4	10.4*	1.4	2.2
Maximum Flows (Cumeecs)								
Ghorband at Karora	Ghorband	-15.0***	-3.0	-21.0***	1.5	-22.1*	-22.1***	-2.2
Gilgit at Gilgit	Gilgit	-2.0	0.4	-2.0	0.6	18.2*	-31.9	1.6
Minimum Flows (Cumeecs)								
Ghorband at Karora	Ghorband	-0.8+	0.4	-1.9**	0.5	-2.8***	-1.3*	-0.1
Gilgit at Gilgit	Gilgit	2.9	0.4	5.6	0.0	3.4+	5.5	0.4

***Significance level <= 99.9%, **Significance level <= 99%. *Significance level <= 95%. +Significance level <= 90%.Bold = Negative Trend

5.8 FLOW DURATION CURVES

Time expedience data is required to represent time variability of river discharges. This information is used to plan a possible capacity sizing of a power plant if required to install. A Flow Duration Curve (FDC) represents relationship

between magnitude and frequency of daily, 10 daily or monthly stream flows for a particular river basin at a particular location. This provides estimation of cumulative percentage of time a given stream flow was equaled or exceeded over the given period of time. For the purpose of this study, 30 years of stream flow data Gilgit river at Gilgit and 26 years data Ghorband river at Karora has been analyzed on daily basis has and a Flow Duration Curve (FDC) has been prepared using daily flows. The FDC thus developed is presented in Figures 5.6 and 5.7 and the values obtained from the curve are given as under:

Table 5.2 Flows and percent of Time

Gilgit River at Gilgit		Ghorband River at Karora	
% of Time	Flows	% of Time	Flows
5%	1425	5%	41.33
10%	1080	10%	31.37
15%	877.3	15%	26.33
20%	727.3	20%	23.07
25%	607.1	25%	20.75
30%	492	30%	18.86
35%	373.6	35%	17.03
40%	263.9	40%	15.21
45%	211.7	45%	13.87
50%	168.8	50%	12.65
55%	140.8	55%	11.52
60%	120.8	60%	10.38
65%	108.1	65%	9.26
70%	94.9	70%	8.06
75%	83.9	75%	6.94
80%	73.5	80%	6.12
85%	65.9	85%	5.35
90%	60.1	90%	4.60
95%	55	95%	3.55
100%	49.9	100%	1.41

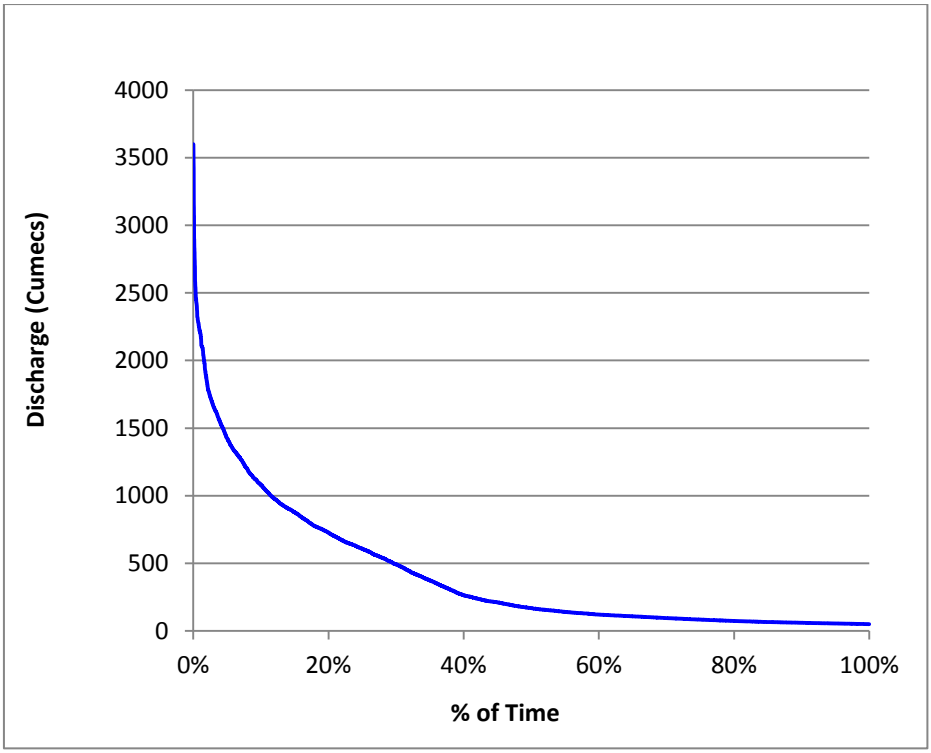

Fig. 5.6 Flow duration Curve Gilgit river at Gilgit

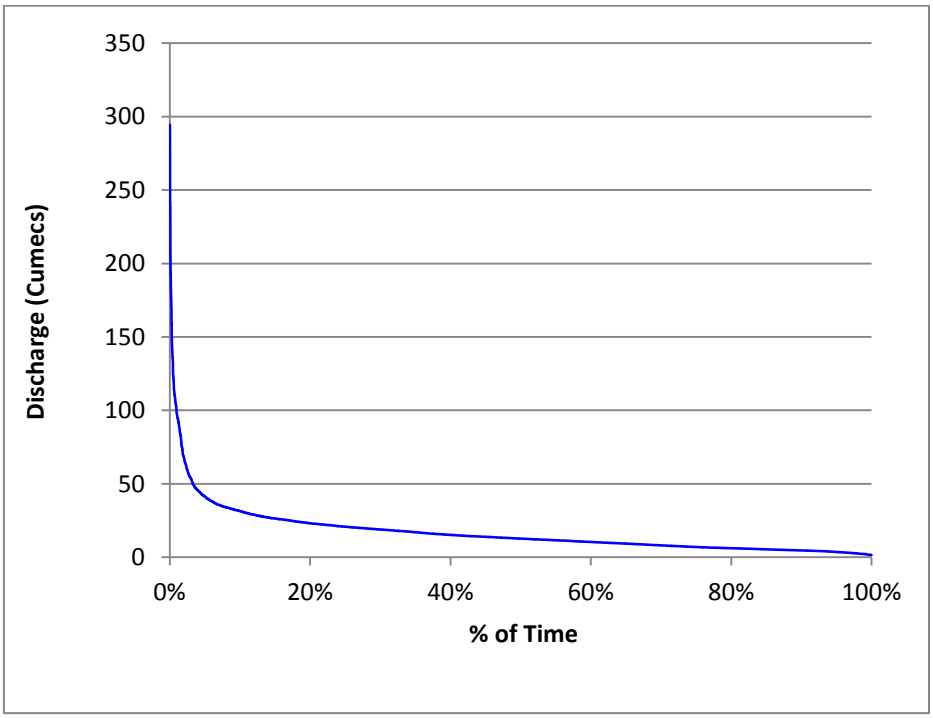

Fig. 5.7 Flow Duration Curve Ghorband River at Karora

5.9 SEDIMENT PATTERN IN GHORBAND RIVER AT KARORA AND GILGIT RIVER AT GILGIT

Per Decade sediment analysis has been performed for the Gilgit and Ghorband river. In Ghorband river per decade sediment yield is decreasing from 1980 to 2010 as shown in Table 5.3. The reduction in the sediment yield is a reduction of discharge in Ghorband river. In Gilgit river average annual sediment yield is increasing from 1990-2015 as shown in Figure 5.9. The increase in sediment yield is due to the increase in discharge in Gilgit river. In both rivers per decade sediment yield during the monsoon season is decreasing. It was also observed that percent of sediment yield is reducing during the monsoon season (June to September), per decade percent of sediment yield for the period 1980 to 1990 and 2000-2010 reduced from 98% to 92% which may be earlier melt of snow in Gilgit basin. Per decade sediment yield in Ghorband river also reduced form 50% to 37% as shown in Table 5.3.

Table 5.3 Percent of Sediment yield in monsoon (June to September)

Period	Gilgit river at Alam Bridge	Gilgit River at Gilgit	Ghorband River at Karora
1981-1990	97	98	50
1991-2000	96	94	49
2001-2010	95	92	37

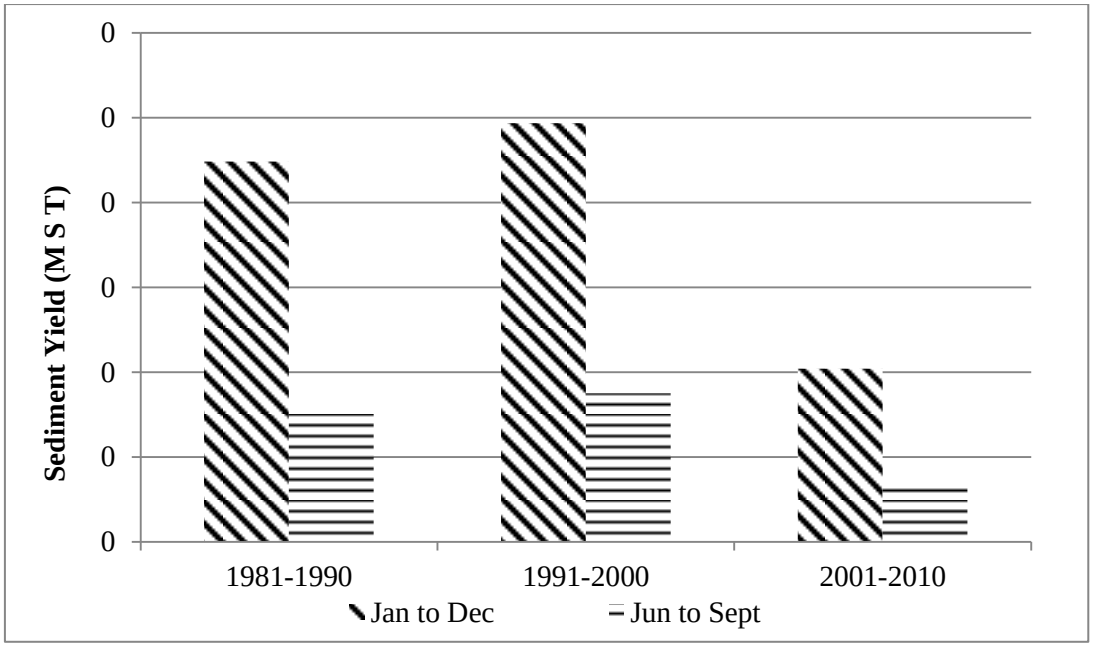

Fig. 5.8 Decade wise variation of sediment yield in Ghorband river at Karora

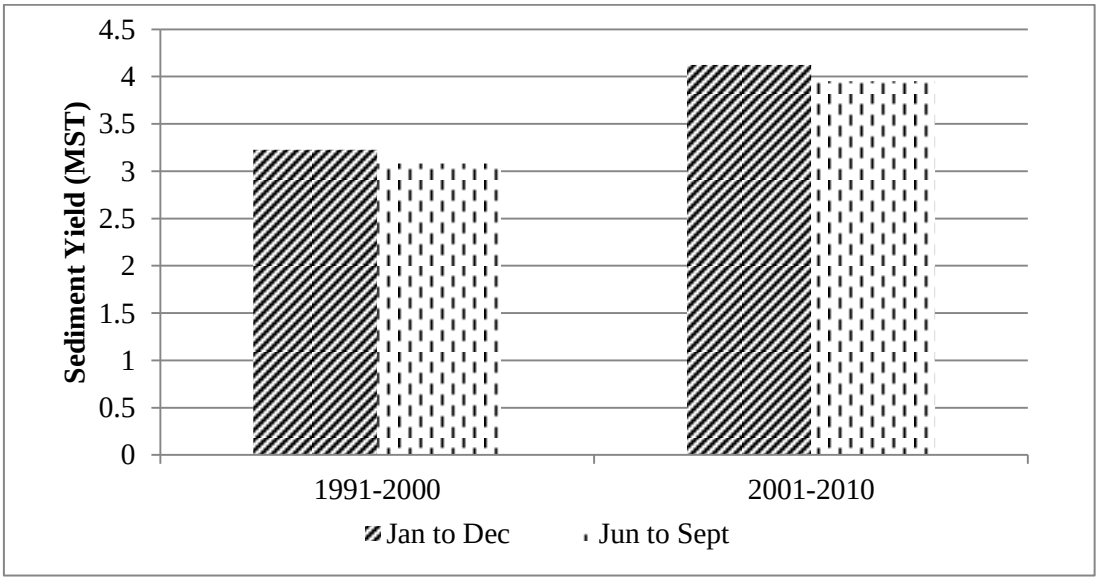

Fig. 5.9 Decade wise variation of sediment yield in Gilgit river at Gilgit

5.10 SNOW COVER ANALYSIS

The Moderate Resolution Imaging Spectroradiometer (MODIS) snow products were selected to calculate the percentage of snow cover area in the Gilgit and Gorband River Basins/Catchments. Several researchers have used the MODIS snow cover data as an input for the snow melt runoff modeling and snow cover area (e.g.,

Adnan et al, 2017, Tahir et al, 2011, Bookhagen and Burbank, 2010; Immerzeel et al., 2009; Prasad and Roy, 2005).

A month wise data set of MOD10A2 (V005) images are available from January 2001 to December 2016 and was downloaded from http://nsidc.org/cgi-bin/snowi/search.pl. The MODIS/Terra Snow Cover L3 Global 500 m Grid (MOD10A2), used for this study, contains data fields for maximum snow cover extent over an 30-day repeated period and has a resolution of approximately 500 m completely covering the Ghorband and Gilgit River basins. The available MODIS images were projected with the WGS 1984 UTM ZONE 43N projection system for the study area analysis. The Ghorband and Gilgit River Catchment /basin area was then extracted from this mosaicked scene to assess the percentage of snow and ice cover (cryosphere) in the study area. When the percentage of cloud cover exceeded 20% on a specific date, the record was removed and then the average snow cover was estimated on this date by interpolating linearly between the previous and the next available cloud-free images. Sixteen years (16) data was divided into four periods 2001-2004, 2005-2008, 2009-2012 and 2013-2016.

5.10.1 Snow Cover area Ghorband River Catchment

In Ghorband river catchment maximum snow cover area of 65% was observed during the month of January in the period 2009-2012 and minimum snow cover area is observed in the months of May to August. The percentage of snow cover area in the Ghorband River Catchment for the corresponding period is shown in Figure 5.10. Average four years Snow Cover area in Ghorband River Catchment (Sq.km) shown in Figure 5.11.

For the period 2001 to 2016 It is clear from the Table 5.4 maximum snow cover in the area is range between 50−65% during winter season and a minimum which about 10−15% during the summer season. December to February-snow accumulation period in the summer June to September-snow melt period, it is clear from the Figure 5.10 that annual and seasonal percentage of snow cover area is decreasing from the base period 2001-2016 which is reason of reduction in flow Ghorband river at karora.

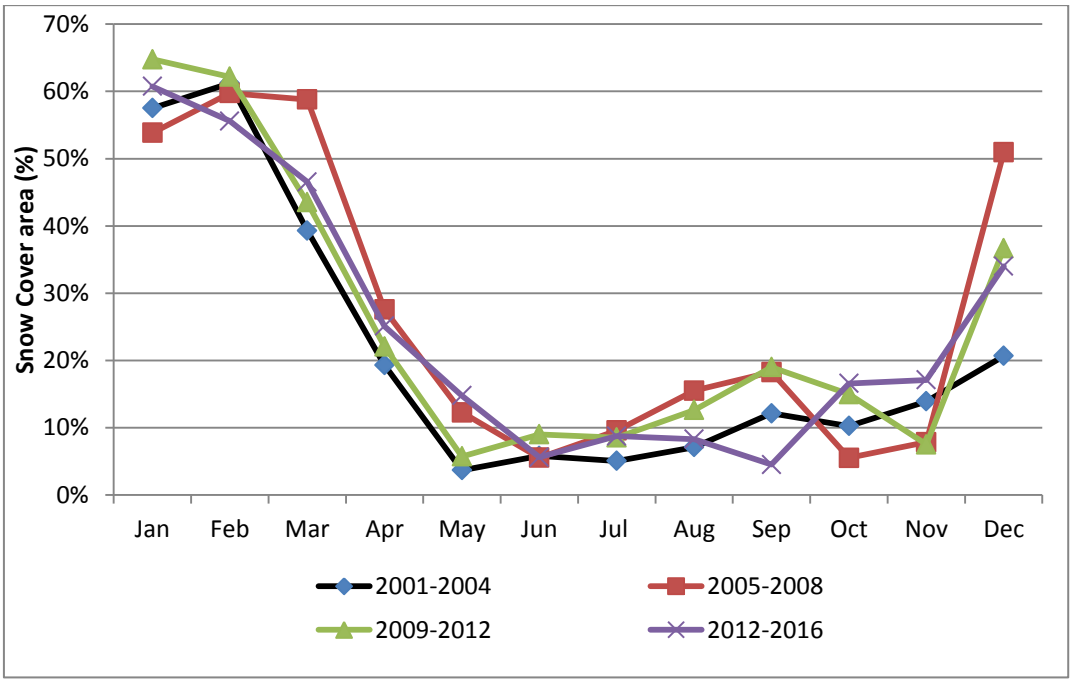

Fig. 5.10 Snow cover distribution in the Ghorband River Catchment over a period of 2001–2016. Snow cover area is estimated from the remotely sensed MODIS (MOD10A2) snow cover data

Table 5.4 Annual and Seasonal Snow Cover area in Ghorband River Catchment (Percent)

Period	Annual (J-D)	Winter (DJF)	Spring (MAM)	Summer (JJA)	Autumn (SON)
2001-2004	22%	46%	24%	6%	12%
2005-2008	25%	46%	33%	10%	11%
2009-2012	22%	45%	24%	10%	10%
2012-2016	21%	46%	21%	8%	9%

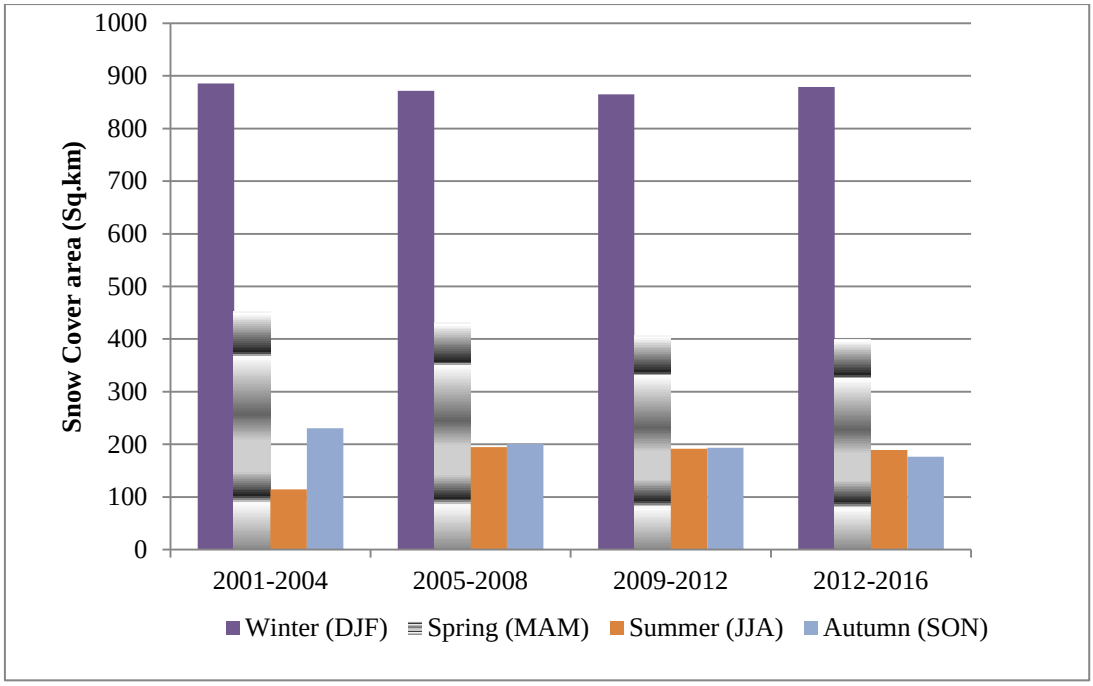

Fig. 5.11 Seasonal variation in Snow cover area in Ghroband river catchment

5.10.2 Snow Cover Area Gilgit River Catchment

In Gilgit river catchment maximum snow cover area of 55% was observed during the month of February in the period 2013-2016 and minimum snow cover area is observed in the months of August during the period of 2013-2016 as shown in Figures 5.12 and 5.13. Monthly percentage distribution of snow cover area in the Gilgit River basin for the corresponding period is shown in Table 5.5. Annual and season percentage variation of snow cover area is given in it is clear that annual and seasonal snow cover area is increasing as compared to the based period which is reason of increase in discharge of Gilgit river at Gilgit.

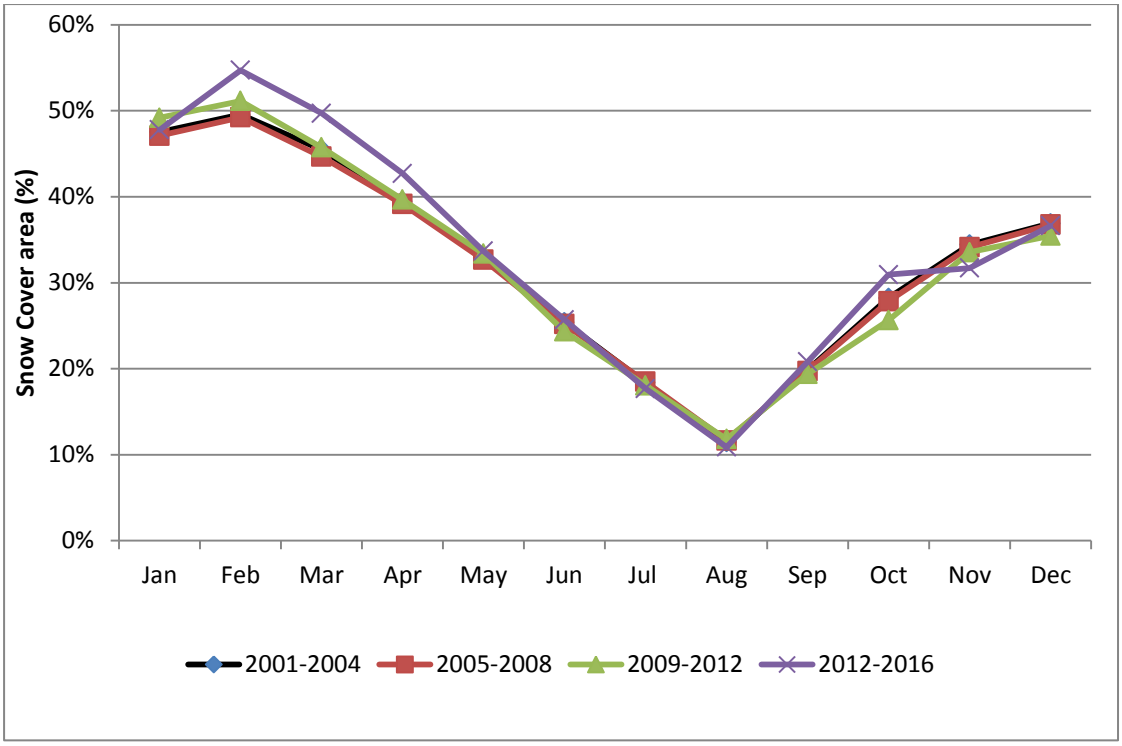

Fig. 5.12 Snow cover distribution in the Gilgit River Basin over a period of 2001–2016. Snow cover area is estimated from the remotely sensed MODIS (MOD10A2) snow cover data.

Table 5.5 Annual and Seasonal Snow Cover area in Gilgit River Catchment (Percent)

Period	Annual (J-D)	Winter (DJF)	Spring (MAM)	Summer (JJA)	Autumn (SON)
2001-2004	32%	45%	39%	18%	27%
2005-2008	32%	44%	39%	18%	27%
2009-2012	32%	45%	40%	18%	26%
2012-2016	34%	46%	42%	18%	28%

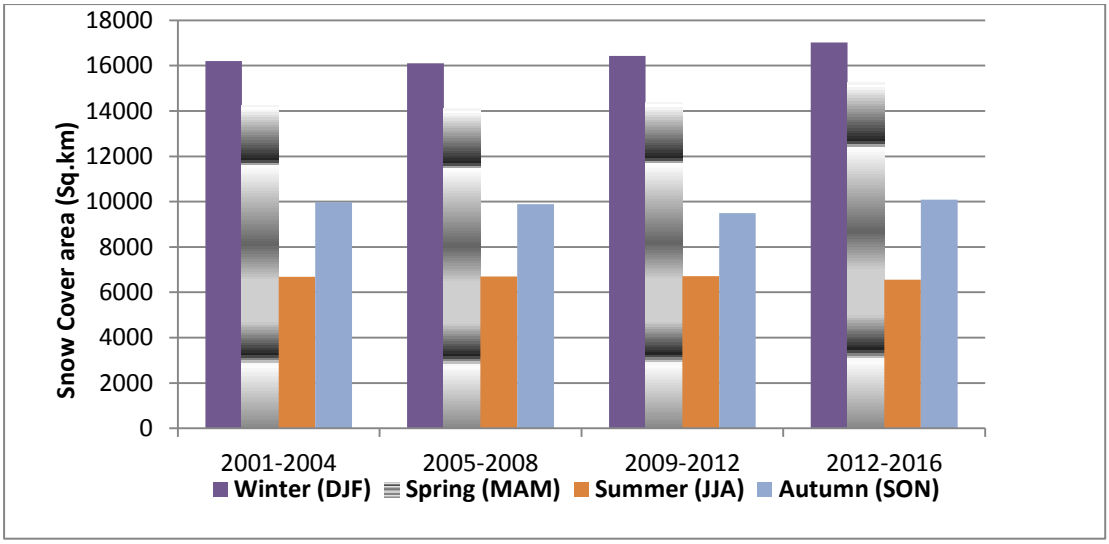

Fig. 5.13 Seasonal variation in Snow cover area in Gilgit river catchment

5.11 PROJECTION OF CLIMATE CHANGE

Statistical downscaling model (SDSM) has been applied on the climate station in and vicinity of Giligit and Ghorband catchments. For this purpose daily precipitation and temperature data seven (7) climate station are selected from 1984-2014.

5.11.1 Model Calibration and Validation (SDSM)

On the basis of available data set from 1984-2014 two data sets are made, 1984 to 2000 is used for the calibration and 2001-2014 has been used for validation of precipitation maximum and minimum temperature. SDSM was developed on the basis of selected NCEP predictors as shown in Table 5.6. The output of the model is daily temperature and precipitation data, the data was converted to monthly, seasonal and annual. These predictors have a good physical relationship with temperature and precipitation. In this study two predictors are selected (out of six) also mostly used in different studies (Wilby et al. 2002; Chu et al. 2010; Hashmi et al. 2011; Huang et al. 2011).

Table 5.6 Screening of most effective predictors

Sr. No.	Predictor	Description
1	necpshumas	Surface specific humidity
2	ncepp500as	500 hPa Geo-potential height
3	ncepp8_zas	850 hPa vorticity
4	Ncepp850as	850 hPa geopotential height
5	necptempas	Mean temperature at 2 m
6	necpp5_vas	500 hPa meridional velocity

Annual (SDSM-A) and monthly (SDSM-M) sub-models calibration for Tmax, Tmin and precipitation and comparison with observed data is shown in Table 5.7. It is clear from the table that both model SDSM-A and SDSM-M performed well in Tmax and Tmin, in case of precipitation SDSM-M perfoms better and simulates good results than SDSM-A, as R^2 value in SDSM-A is lower than SDSM-M. Statistical comparison of downscaled mean monthly precipitation, Tmax and Tmin with observed during the calibration for selected station validation parameters are given in Table 5.8. It is clear from the table that model performs well for both monthly and annual data series. The model calibration and validation has been done for all the selected seven stations (Gilgit, Gupis, Astore, Skerdu, Chilas, Saidu Sharif and Shahpur) here results of Astore are shown because in all the stations predictors in Figure 5.14 were most effective.

Table 5.7 Statistical comparison of downscaled mean monthly precipitation, Tmax and Tmin with observed during the calibration for selected station (1984-200)

		R^2	RMSE (^{0}C/mm)
Tmax	Observed		
	NCEP-A	0.940	1.70
	NCEP-M	0.988	0.07
Tmin	Observed		
	NCEP-A	0.975	1.000.18
	NCEP-M	0.998	
Precipitation	Observed		
	NCEP-A	0.701	33.47
	NCEP-M	0.899	10.8

R^2 = Coefficient of determination, RMSE= Room mean square error

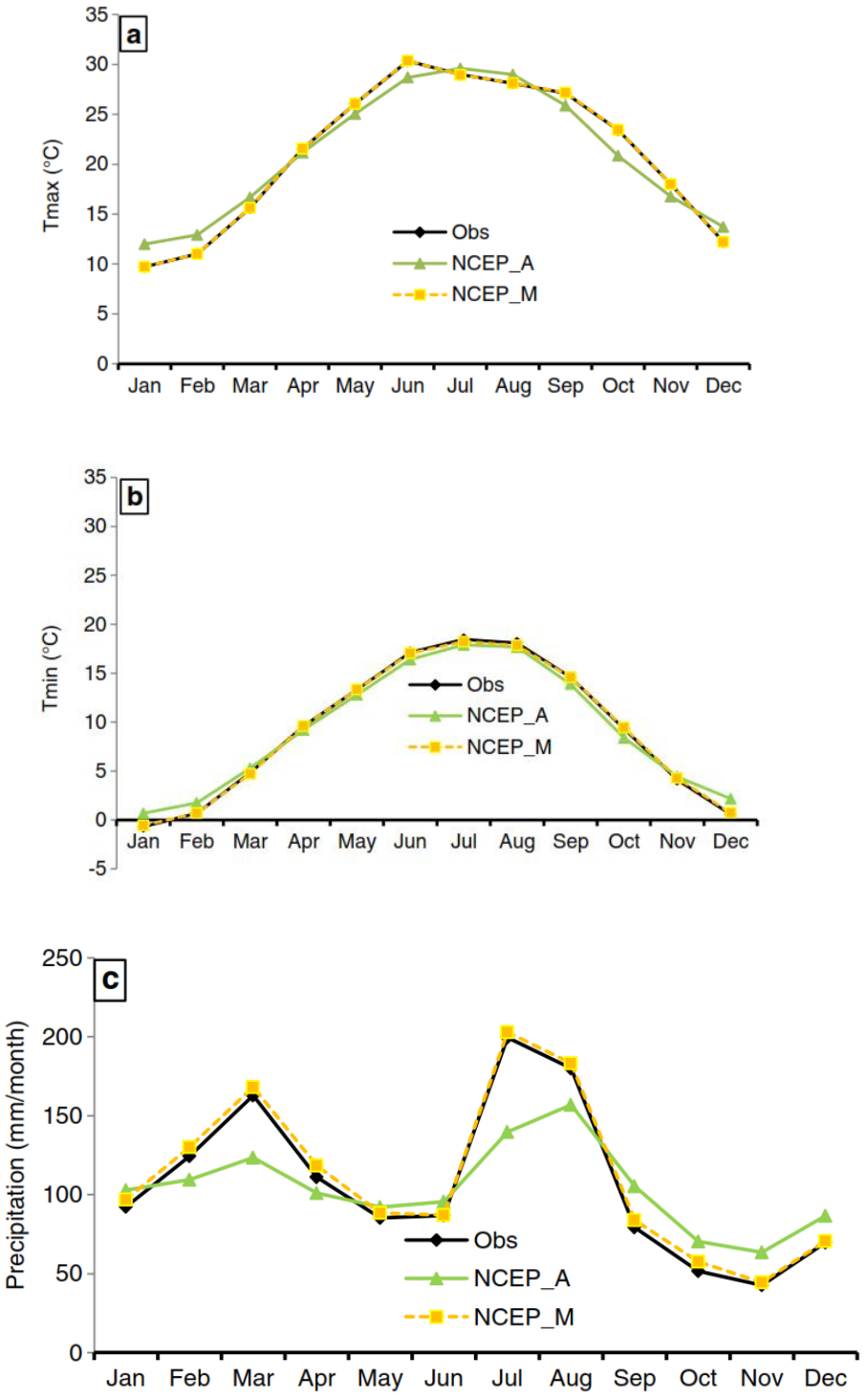

Fig. 5.14 Observed and simulated mean monthly (a) Tmax (b) Tmin and (c) precipitation for the calibration for Gilgit and Ghorband Basin (1984-2000)

Table 5.8 Statistical comparison of downscaled mean monthly precipitation, Tmax and Tmin with observed during the validation for selected station (2001-2014)

		R^2	RMSE (^{0}C/mm)
Tmax	Observed		
	NCEP-A	0.935	1.83
	H3A2_A	0.936	2.06
	NCEP-M	0.983	0.93
	H3A2_M	0.980	1.04
Tmin	Observed		
	NCEP-A	0.943	1.58
	H3A2_A	0.939	1.97
	NCEP-M	0.988	0.93
	H3A2_M	0.967	1.09
Precipitation	Observed		
	NCEP-A	0.691	39.91
	H3A2_A	0.561	46.88
	NCEP-M	0.81	20.34
	H3A2_M	0.702	37.63

1.1.2 **R^2 = Coefficient of determination, RMSE= Room mean square error**

1.1.3

1.1.4 **5.11.2**

Downscaling of Climate

1.1.5 After the model calibration and validation climate parameters (Tmax, Tmin, precipitation) has been projected at the end of 21th century (2099). Three data sets 2015-20140, 2041-20170 and 2071-2099 were made of projected rainfall and temperature for the selected seven stations, their comparison were made with the base period 1984-2014. The selection of the climate station was made in such a way that the climate station near the catchment/ basin was also used for analysis**.**

5.11.2.1 Projection of Mean Maximum Temperature (Tmax)

To analyze the future hydrological conditions of Tmax, scenarios generated by climate model using GCM output were analyzed on annual and seasonal scale i.e. Winter DJF(December, January, February), Spring MAM (March, April, May), Summer JJA (June, July, August) and Autumn SON (September, October, November) as shown in Table 5.9. As per Table 5.9 it is clear that mean annual, winter, summer

and spring maximum temperature is continuously increasing Gilgiit, Gupis, Astore, Chilas, Skardu and Saidu sharif. At the end of 21th century (2099) annual Tmax at Gilgiit, Gupis, Astore, Chilas, Skardu and Saidu sharif. is expected to increase 1.98, 2.34, 1.76, 1.56, 1.82 and 1.94 as shown in Figure 5.15. During the winter season at the end of 21th century (2099) mean Tmax at Gilgiit, Gupis, Astore, Chilas, Skardu and Saidu sharif. is expected to increase 1.08, 1.96, 1.62, 0.29, 0.62 and 1.68 as shown in Figure 5.15. During the spring season at Gupis, Chilas and Skardu stations projected mean Tmax for period 2015-2040 deceased 0.30, 0.16 and 0.46 ^{0}C from the based period 1984-2014 and then increased form 2041-2099 respectively as shown in Figure 5.15. At the end of 21th century (2099) spring season mean Tmax at Gilgiit, Gupis, Astore, Chilas, Skardu and Saidu sharif. is expected to increase 1.33, 1.40, 0.98, 0.56, and 0.95 as shown in Figure 5.15. At the end of 21th century (2099) summer season temperature is also increasing at mean Tmax at Gilgiit, Gupis, Astore, Chilas, Skardu and Saidu sharif. is expected to increase 3.23, 2.61, 2.70, 2.88, 3.12 and 2.69 respectively. At the end of 21th century (2099) spring season temperature is also increasing at mean Tmax at Gilgiit, Gupis, Astore, Chilas, Skardu and Saidu sharif. is expected to increase 2.27, 3.41, 1.73, 2.54, 2.58 and 1.25 respectively.

Table 5.9 Increase mean maximum temperature, Tmax (^{0}C) at the end of 21th century (2099) from the base period 1984-2014

Sr. No	Station	Annual	Winter (DJF)	Spring (MAM)	Summer (JJA)	Autumn(SON)
Stations in and vicinity of Giigit basin						
1	Gilgit	1.98	1.08	1.33	3.23	2.27
2	Gupis	2.34	1.96	1.40	2.61	3.41
3	Astore	1.76	1.62	0.98	2.70	1.73
4	Chilas	1.56	0.29	0.56	2.88	2.54
5	Skardu	1.82	0.62	0.95	3.12	2.58
Stations in Ghorband catchment						
1	Saidu Sharif	1.94	1.68	2.15	2.69	1.25

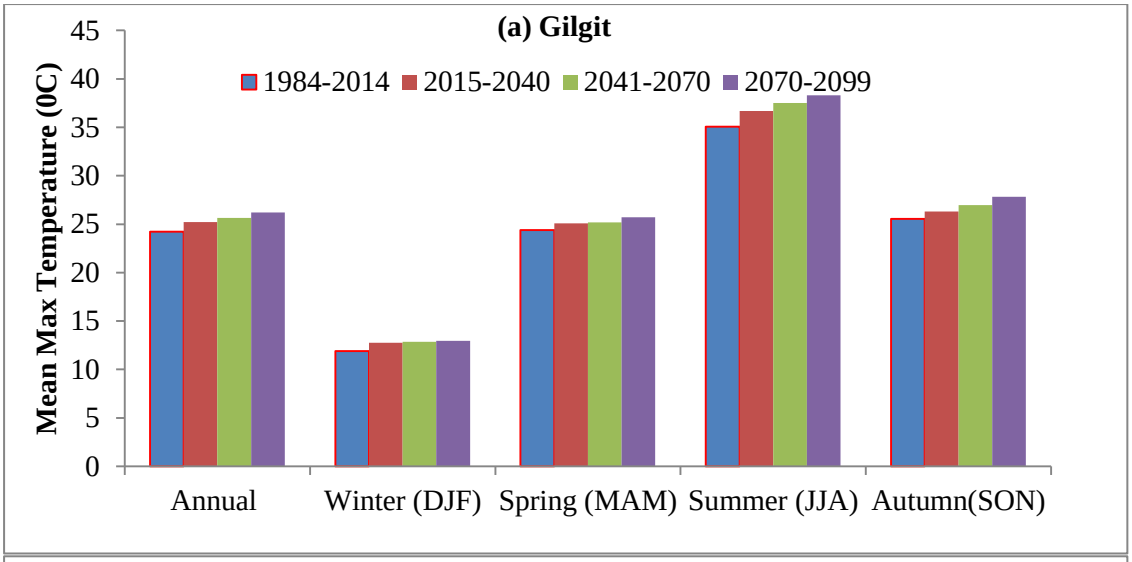
(a) Gilgit
1984-2014
2015-2040
2041-2070
2070-2099
Mean Max Temperature (0C)
45
40
35
30
25
20
15
10
5
0
Annual
Winter (DJF)
Spring (MAM)
Summer (JJA)
Autumn(SON)

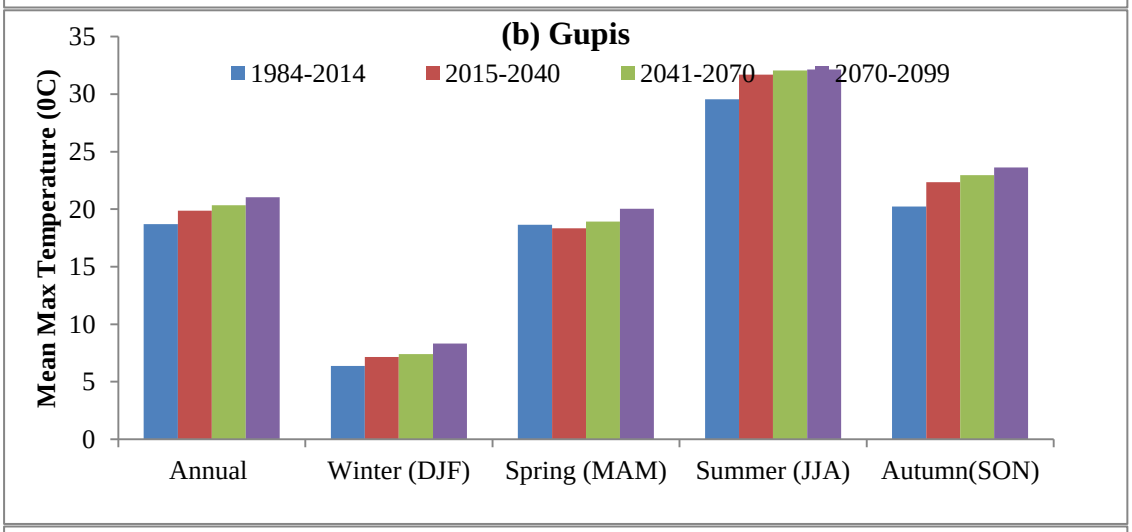
(b) Gupis
1984-2014
2015-2040
2041-2070
2070-2099
Mean Max Temperature (0C)
35
30
25
20
15
10
5
0
Annual
Winter (DJF)
Spring (MAM)
Summer (JJA)
Autumn(SON)

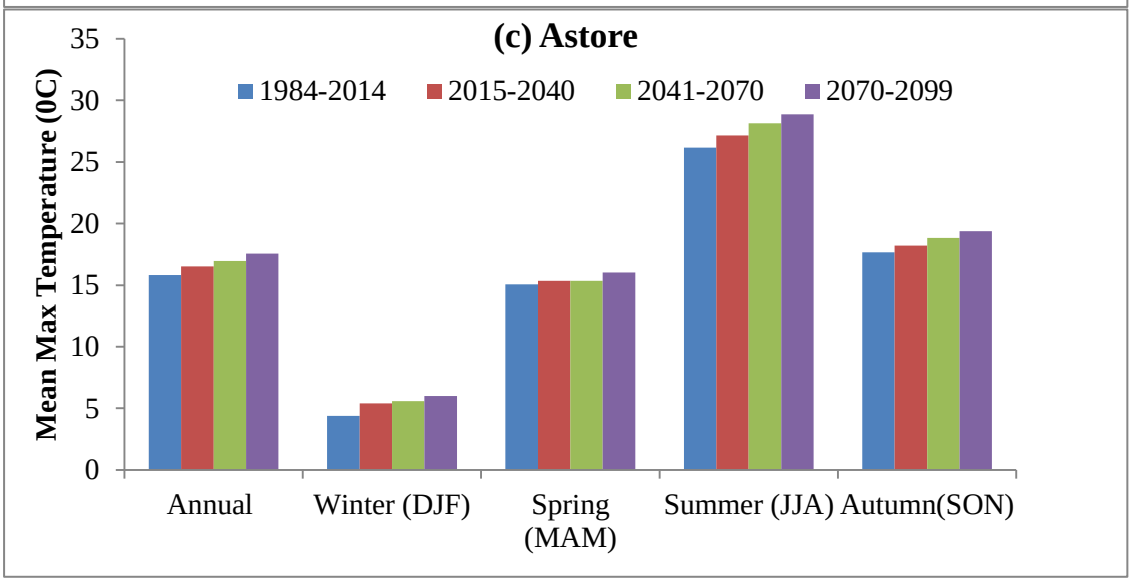
(c) Astore
1984-2014
2015-2040
2041-2070
2070-2099
Mean Max Temperature (0C)
35
30
25
20
15
10
5
0
Annual
Winter (DJF)
Spring (MAM)
Summer (JJA)
Autumn(SON)

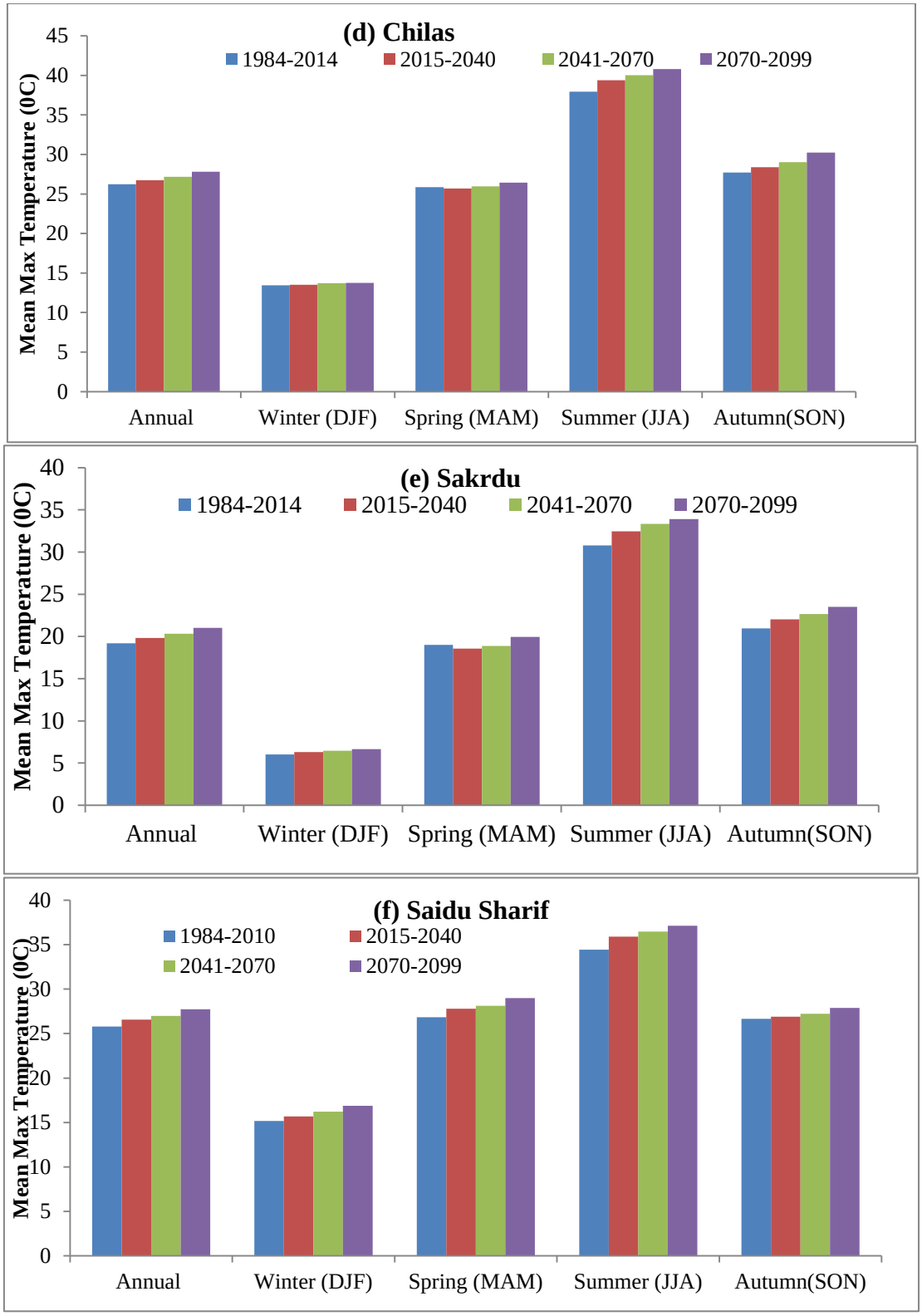

Fig. 5.15 Comparison of Baseline (1984-2014) and Projected (SDSMHadCM3) mean maximum temperature (0C) of (a) Gilgit (b) Gupis (c) Astore (d) Chilas (e) Sakrdu and (f) Saidu Sharif

511.2.2 Projection of Minimum Temperature (Tmin)

To analyze the future hydrological conditions of Tmin, scenarios generated by climate model using GCM output were analyzed on annual and seasonal scale i.e. Winter DJF(December, January, February), Spring MAM (March, April, May), Summer JJA (June, July, August) and Autumn SON (September, October, November) as shown in Figure 5.16. As per Figure 5.16 it is clear that mean annual, winter, summer and spring mean minimum temperature Tmin is continuously increasing Gilgiit, Gupis, Astore, Chilas, Skardu and Saidu sharif. At the end of 21th century (2099) annual Tmin at Gilgiit, Gupis, Astore, Chilas, Skardu and Saidu sharif. is expected to increase 0.85, 0.44, 1.14, 1.54, 2.27 and 1.99 as shown in Table 5.10 respectively. During the winter season at the end of 21th century (2099) mean Tmax at Gilgiit, Gupis, Astore, Chilas, Skardu and Saidu sharif. is expected to increase 0.95, 0.77, 0.39, 1.18, 1.48 and 0.91 as shown in Table 5.10respectively. The results of the study indicates that during winter season at chilas station mean Tmin for period 2015-2040 increased 1 ^{0}C from the based period 1984-2014 and then decreased 0.5 ^{0}C during 2041-2070 form 2015-2040 as shown in Figure 5.16.

At the end of 21th century (2099) spring season mean Tmin at Gilgiit, Gupis, Astore, Chilas, Skardu and Saidu sharif. is expected to increase 0.54, 0.22, 0.49, 0.22, 1.62 and 2.46 as shown in Table 5.11 respectively. During the spring season at Gilgit Gupis,and Chilas stations projected mean Tmax for period 2015-2040 deceased 0.17, 0.48 and 0.31 ^{0}C from the based period 1984-2014 and then increased form 2041-2099 respectively as shown in Figure 5.16. At the end of 21th century (2099) summer season temperature is also increasing at mean Tmax at Gilgiit, Gupis, Astore, Chilas, Skardu and Saidu Sharif is expected to increase 0.36, 0.71, 1.78, 2.86, 3.46 and 2.11

respectively. At the end of 21th century (2099) spring season temperature is also increasing at mean Tmax at Gilgiit, Gupis, Astore, Chilas, Skardu and Saidu sharif. is expected to increase 1.56, 2.01, 1.90, 2.52 and 2.48 respectively.

Table 5.10 Increase mean minimum temperature (^{0}C) at the end of 21st century (2099) form the base period 1984-2014

Sr. No	Station	Annual	Winter (DJF)	Spring (MAM)	Summer (JJA)	Autumn (SON)
Stations in and vicinity of Giigit basin						
1	Gilgit	0.85	0.95	0.54	0.36	1.56
2	Gupis	0.44	0.77	0.22	0.71	2.01
3	Astore	1.14	0.39	0.49	1.78	1.90
4	Chilas	1.54	1.18	0.22	2.86	1.90
5	Skardu	2.27	1.48	1.62	3.46	2.52
Stations in Ghorband catchment						
1	Saidu Sharif	1.99	0.91	2.46	2.11	2.48

5.11.2.3 Projection of Precipitation

Future hydrological projections/ scenarios generated for the precipitation by climate model using GCM output were analyzed on annual and seasonal scale i.e. Winter DJF(December, January, February), Spring MAM (March, April, May),

Summer JJA (June, July, August) and Autumn SON (September, October, November) as shown in Figure 5.17.

As per Figure 5.16, it is clear that mean annual, winter, summer and spring precipitation is continuously increasing Gilgit, Gupis, Astore, Chilas, Skardu and Saidu sharif. At the end of 21th century (2099) annual precipitation at Gilgit, Gupis, Astore, Chilas, Skardu, Saidu sharif.and Shahpur is expected to increase 0.85, 32, 18, 22, 24, 22, 12 and 7% as shown in Table 5.11 respectively. At the station skardu increase in mean annual precipitation for the period 2070-2099 is less as compared to increase 2040-2070 form the base period 1984-2014 as shown in Figure 5.17. During the winter season at the end of 21th century (2099) mean annual precipitation at Gilgit, Gupis, Astore, Chilas, Skardu Saidu sharif.and shahpur is expected to increase 43, 22, 20, 7, 24, 17, and 8% as shown in Table 5.11 respectively. At the end of 21th century (2099) spring season mean annual precipitation at Gilgit, Gupis, Astore, Chilas, Skardu Saidu Sharif and shahpur.is expected to increase 34, 27, 20, 28,1 9, 2 and 2% as shown in Table 5.11 respectively. Mean annual precipitation is also increasing at Gilgit, Gupis, Chilas, Skardu, Saidu sharif.and shahpur is expected to increase 19, 22, 29, 31, 28, 18 and 9% in 2099 respectively. Spring season precipitation is also increasing at the stations.

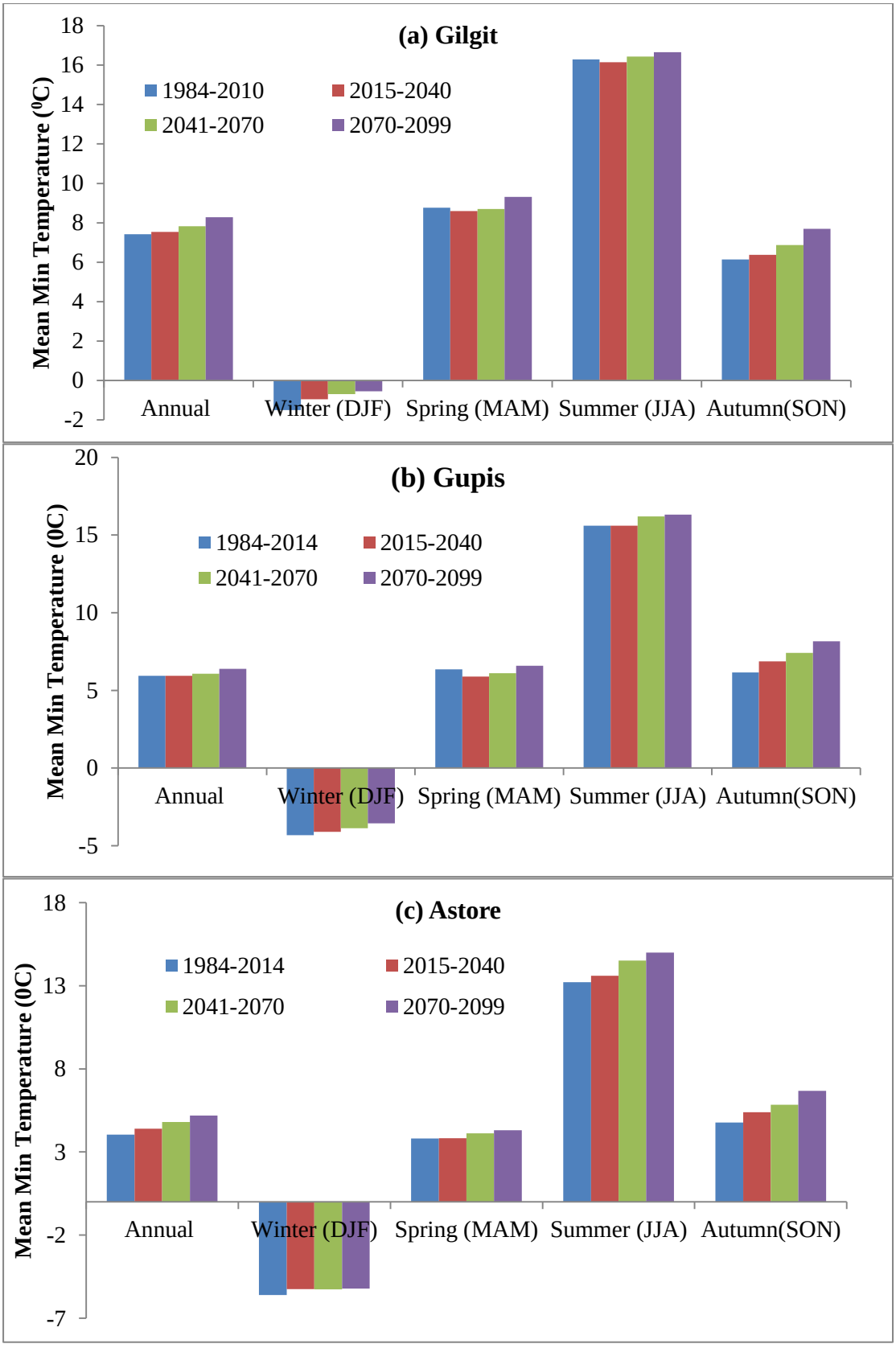
(a) Gilgit
Mean Min Temperature (⁰C)
18
16
14
12
10
8
6
4
2
0
-2
1984-2010
2015-2040
2041-2070
2070-2099
Annual
Winter (DJF)
Spring (MAM)
Summer (JJA)
Autumn(SON)
(b) Gupis
Mean Min Temperature (0C)
20
15
10
5
0
-5
1984-2014
2015-2040
2041-2070
2070-2099
Annual
Winter (DJF)
Spring (MAM)
Summer (JJA)
Autumn(SON)
(c) Astore
Mean Min Temperature (0C)
18
13
8
3
-2
-7
1984-2014
2015-2040
2041-2070
2070-2099
Annual
Winter (DJF)
Spring (MAM)
Summer (JJA)
Autumn(SON)

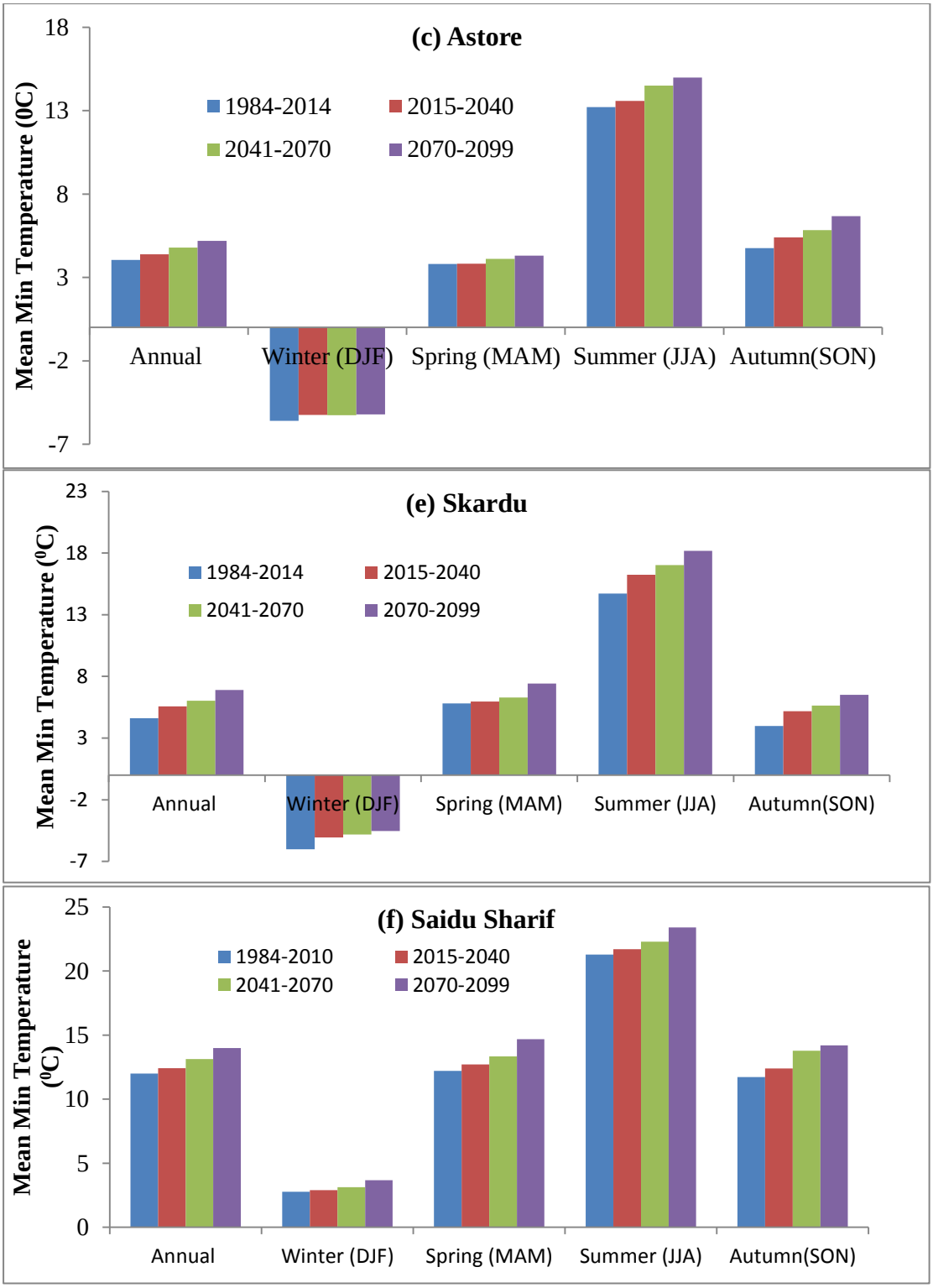

Fig. 5.16 Comparison of Baseline (1984-2014) and Projected (SDSMHadCM3) mean minimum temperature (^{o}C) of (a) Gilgit (b) Gupis (c) Astore (d) Chilas (e) Sakrdu and (f) Saidu Sharif

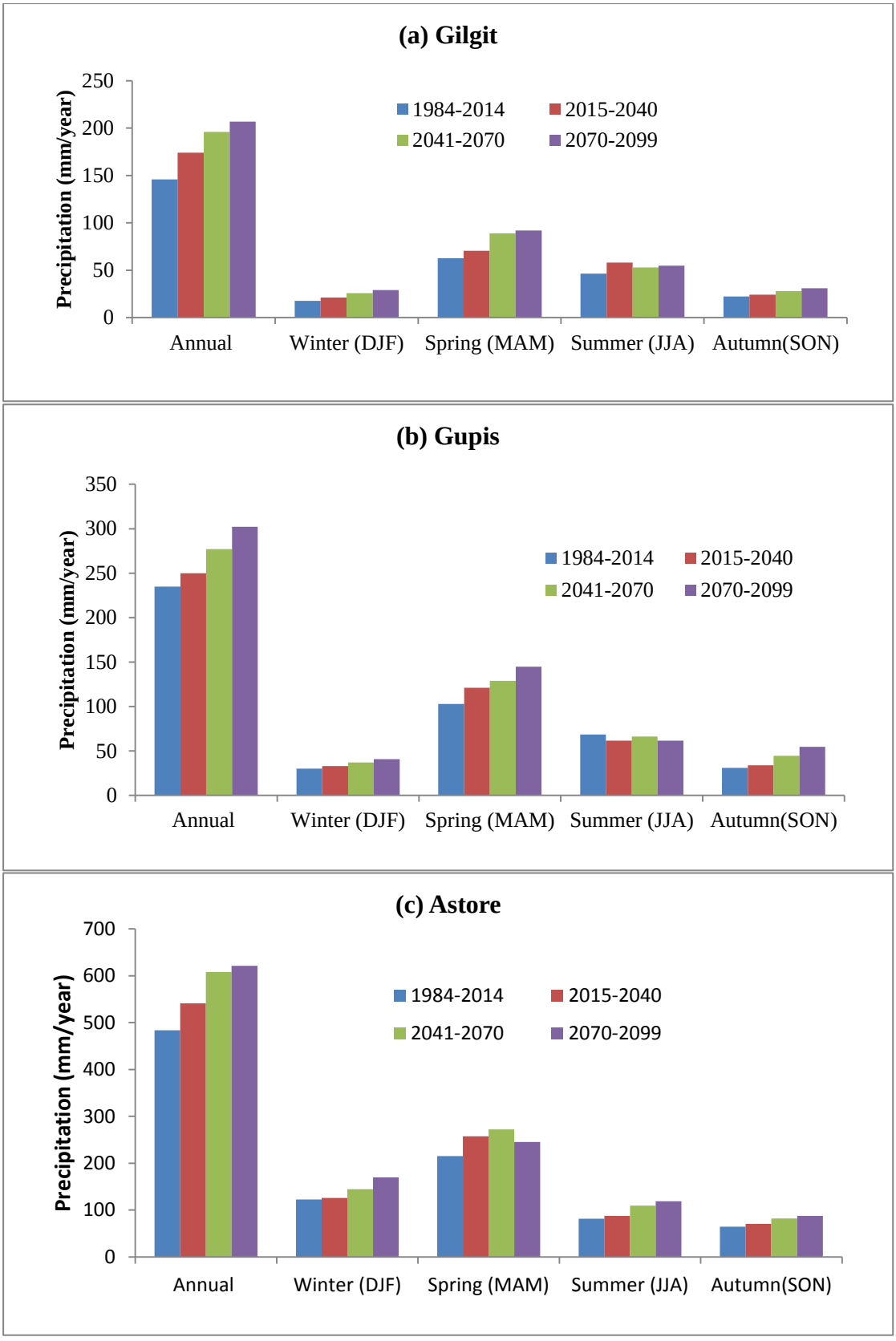
(a) Gilgit
Precipitation (mm/year)
250
200
150
100
50
0
1984-2014
2015-2040
2041-2070
2070-2099
Annual
Winter (DJF)
Spring (MAM)
Summer (JJA)
Autumn(SON)
(b) Gupis
Precipitation (mm/year)
350
300
250
200
150
100
50
0
1984-2014
2015-2040
2041-2070
2070-2099
Annual
Winter (DJF)
Spring (MAM)
Summer (JJA)
Autumn(SON)
(c) Astore
Precipitation (mm/year)
700
600
500
400
300
200
100
0
1984-2014
2015-2040
2041-2070
2070-2099
Annual
Winter (DJF)
Spring (MAM)
Summer (JJA)
Autumn(SON)

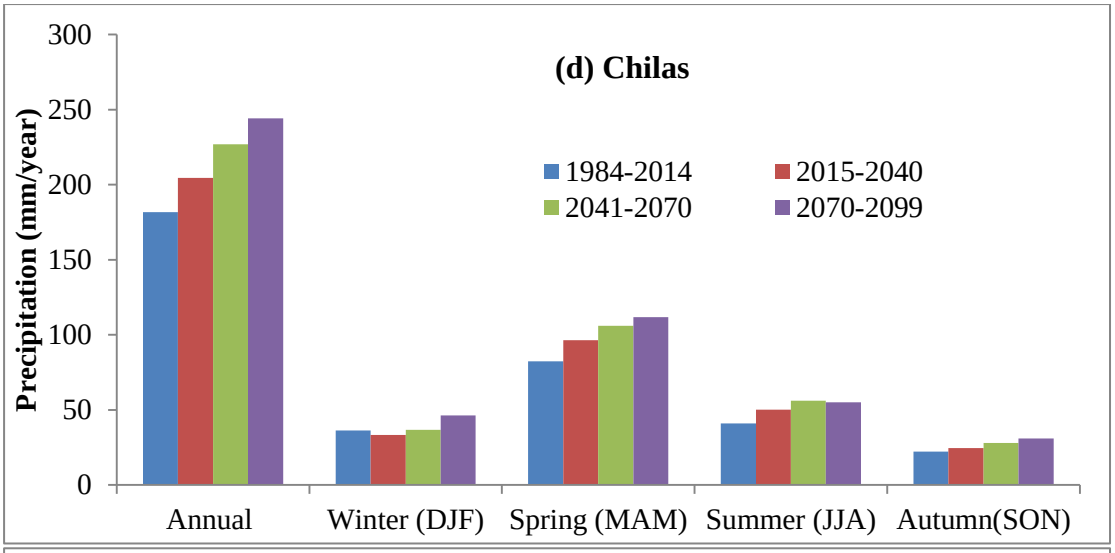
(d) Chilas
Precipitation (mm/year)
300
250
200
150
100
50
0
1984-2014
2015-2040
2041-2070
2070-2099
Annual
Winter (DJF)
Spring (MAM)
Summer (JJA)
Autumn(SON)

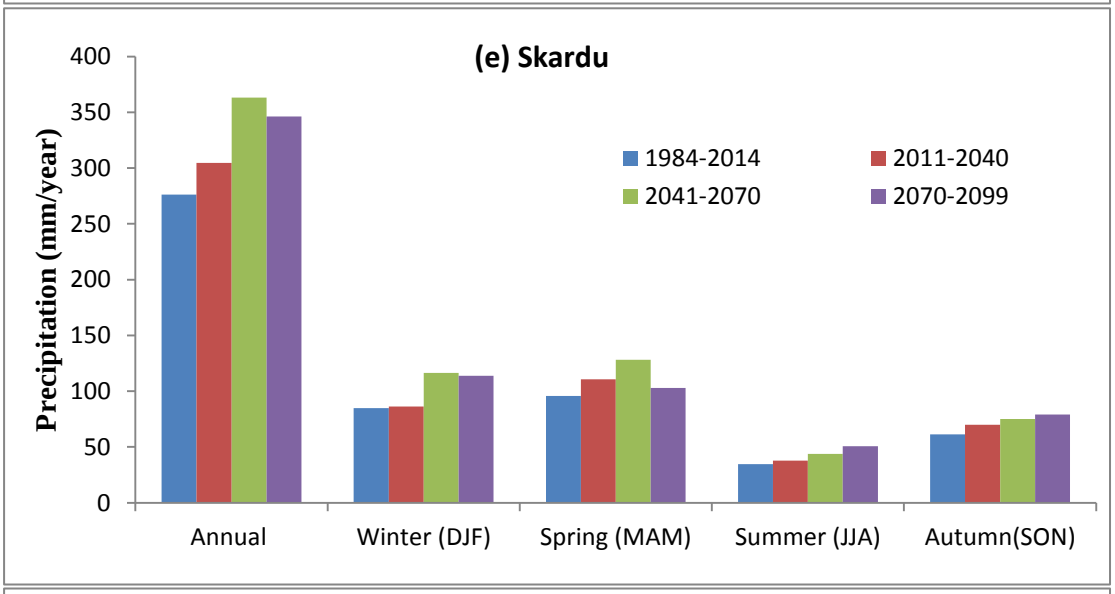
(e) Skardu
Precipitation (mm/year)
400
350
300
250
200
150
100
50
0
1984-2014
2011-2040
2041-2070
2070-2099
Annual
Winter (DJF)
Spring (MAM)
Summer (JJA)
Autumn(SON)

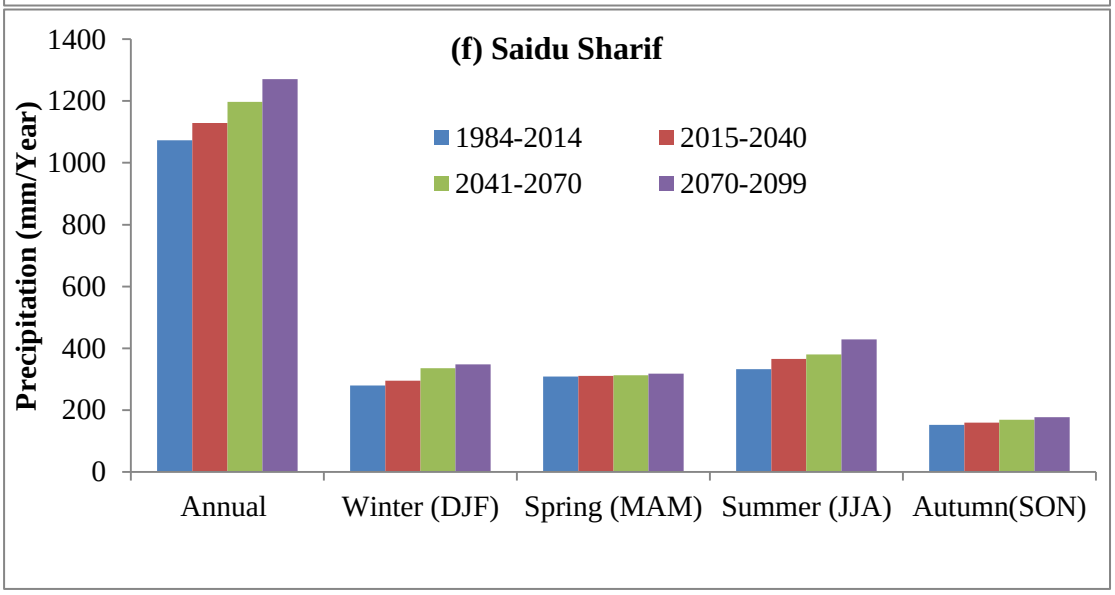
(f) Saidu Sharif
Precipitation (mm/Year)
1400
1200
1000
800
600
400
200
0
1984-2014
2015-2040
2041-2070
2070-2099
Annual
Winter (DJF)
Spring (MAM)
Summer (JJA)
Autumn(SON)

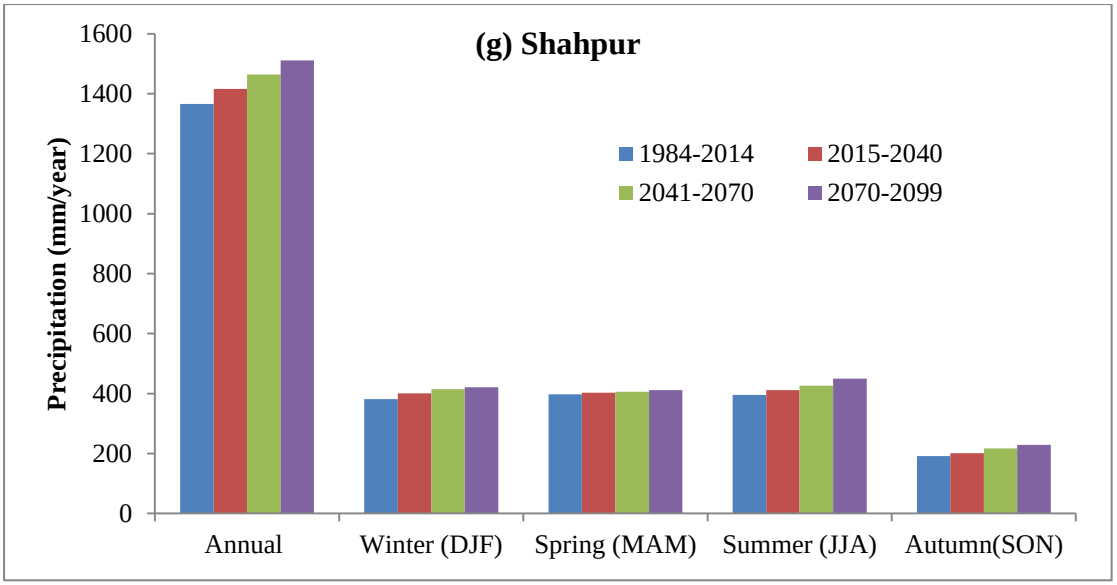

Fig. 5.17 Comparison of Baseline (1984-2014) and Projected (SDSMHadCM3) precipitation (mm/year) of (a) Gilgit (b) Gupis (c) Astore (d) Chilas (e) Sakrdu (f) Saidu Sharif and (g) Shahpur

Table 5.11 Percent increase in rainfall at the end of 21th century (2099) from the base period 1984-2014

Sr. No	Station	Annual	Winter (DJF)	Spring (MAM)	Summer (JJA)	Autumn (SON)
Stations in and vicinity of Giigit basin						
1	Gilgit	32%	43%	34%	19%	24%
2	Gupis	18%	22%	28%	22%	44%
3	Astore	22%	20%	20%	29%	24%
4	Chilas	24%	7%	27%	31%	26%
5	Skardu	22%	24%	19%	28%	22%
Stations in and vicinity of Ghorband catchment						
1	Saidu Sharif	12%	17%	2%	18%	11%
2	Shahpur	7%	8%	2%	9%	12%

5.12 HYDROLOGICAL MODELING

Different researcher and scientist have used SWAT model for stream flow and sediment modeling (Yasin 2016, Haguma t al., 2014, Mukudan et al, 2013, Rahman et al., 2013 and Rehman et al (2012). In this study stream flow and sediment modeling has been done for the period of 1984 to 2014 for the Gilgit and Ghorband river catchments. Model calibration, validation and sensitivity analysis has been performed. Future climate modeling has been also performed at the end of 21st century (2099).

1.1.6

1.1.7 **5.12.1** **SWAT**

Model Calibration and Validation

Model calibration and validation is done for both Gilgit and Ghorband river. Calibration is the process to get the optimum set of parameters that gives the best match between observed the simulated discharge. Initially model run in daily time step using Arcgis then SWAT Cup was used for calibration; SWAT Cup is computer software that can be used for auto-calibration. For Giligit river calibration of model was done for 1984-1994 and validation was done 1995-2014 and For ghorband river calibration of model was done for 1984-1991 and validation was done 1991-2010.[7]. The parameters used for the calibration are shown in Table 5.12. The snow and curve number parameters were found most sensitive for simulation of discharge. ADJ_PKR, SPCON and SPEXP parameters were found sensitive simulating sediment yield.

[7] Guage was closed by SWHP after 2010.

Table 5.12 Calibrated Parameters of SWAAT model used Gilgit and Ghorband rivers

Sr. No	Parameter	Initial Range	Final parameter Range	Gilgit	Ghorband
1	SOL_AWC	0-1	0.01	0.01	0.01
2	ALPHA_BF	0-1	0.007	0.007	0.007
3	PLAPS	−500,+500	500	500	500
4	SFTMP	−20,+20	2.2-3.7	2.2	3.7
5	SMTMP	−20,+20	4.6-5.1	4.6	5.1
6	SMFMN	0-20	0.72-0.82	0.72	0.82
7	SMFMX	0-20	0.72-3.7	0.72	3.7
8	TIMP	0,1	1	1	1
9	GWQMN	0-5000	0	0	0
10	SPCON	0.0001-0.01	0.00023	0.00023	0.00023
11	SPEXP	1-1.5	1.45	1.45	1.45
12	USLE_P	0-1	0.0051-0.36	0.0051	0.36
13	TLAPS	−10,+10	-10	-10	-10
14	CN	34-99	82-85	82	85
15	ADJ_PKR	0.6-2	2	2	2

The model successfully simulated the daily discharge and annual sediment yield. The model can simulate the low medium and peak flows efficiently. Calibration and validation for the Gilgit river at gilgit is shown Figures 5.18 and 5.19 respectively. Calibration and validation for the Ghorband river at Karora river is shown in Figures 5.20 and 5.21 respectively. SWAT model calibration and validation has showed a

reasonable match between observed and simulated discharge. To check the model performance of statistical analysis was also performed as shown in Table 5.13 for discharge and Table 5.14 for sediment. For Gilgit river coefficient of determination R^2 for calibration 0.818 and 0.74 for validation, Nash-Sutcliffe Efficiency, NSE for calibration 0. 712, and for validation 0.671, percent bias, PBIAS for Calibration -8.5 and for validation 5 . For Ghorband river coefficient of determination R^2 for calibration 0.797 and 0.68 for validation, Nash-Sutcliffe Efficiency, NSE for calibration 0. 586 and for validation 0.548, percent bias, PBIAS for Calibration -10.6 and for validation 11. The results of SWAT model simulations show that model is capable of simulating sediment yield. For Gilgit river coefficient of determination R^2 for calibration 0.93 and 0.85 for validation, Nash-Sutcliffe Efficiency, NSE for calibration 0. 91, and for validation 0.90, percent bias, PBIAS for Calibration 12 and for validation -7.8. For Ghorband river coefficient of determination R^2 for calibration 0.96 and 0.90 for validation, Nash-Sutcliffe Efficiency, NSE for calibration 0.92 and for validation 0.90, percent bias, PBIAS for Calibration 10 and for validation -8.

Table 5.13 Statistical parameter for evaluation of model performance for discharge

	R^2	NSE	PBIAS
Gilgit Watershed			
Calibration	0.818	0.712	-8.5
Validation	0.74	0.671	5
Ghorband Watershed			
Calibration	0.797	0.586	-10.6
Validation	0.68	0.548	11

R^2= Coefficient of determination
NSE= Nash-Sutcliffe Efficiency
PBIAS = Percent Bias

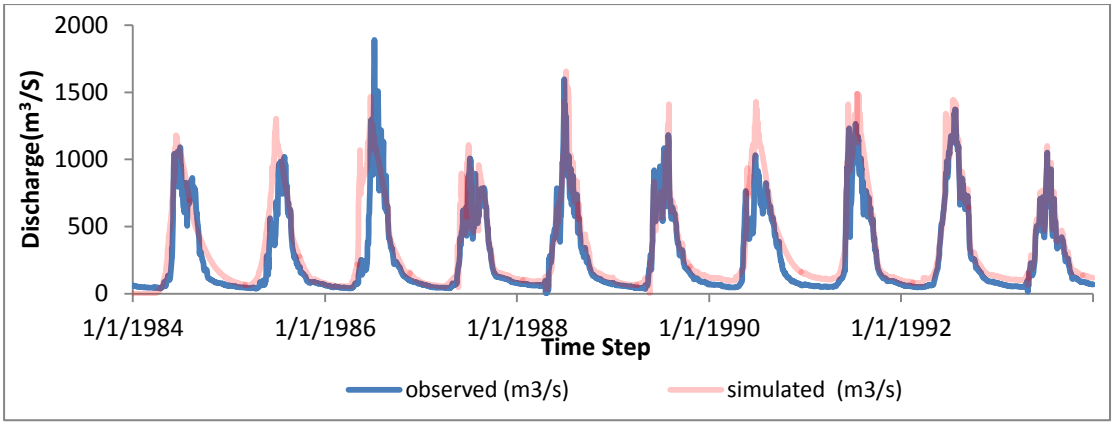

Fig. 5.18 Discharge at Gilgit river observed and simulated calibration period 1984-1993

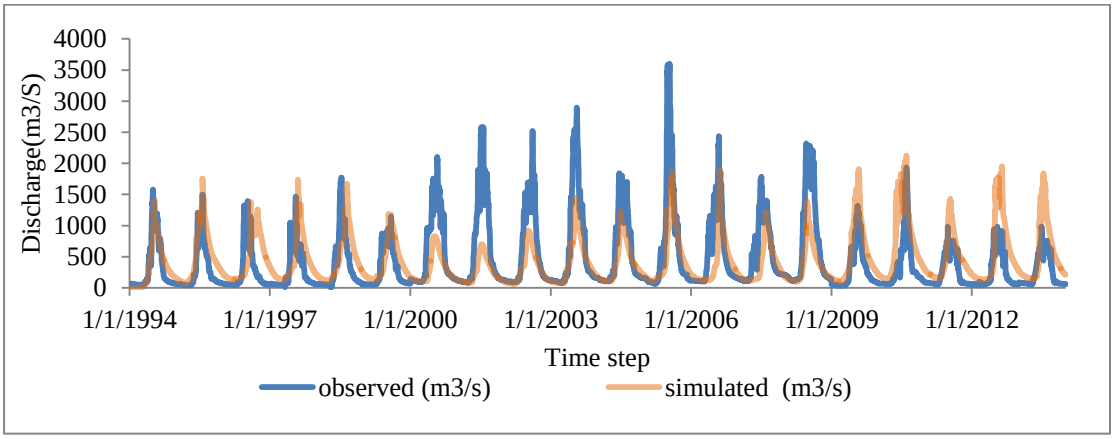

Fig. 5.19 Discharge at Gilgit river observed and simulated validation period 1995-2014

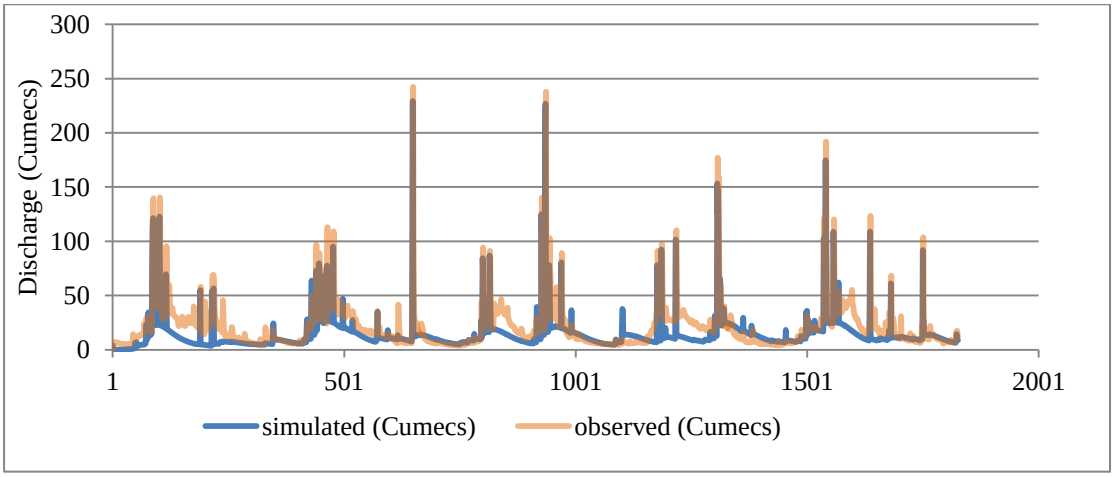

Fig. 5.20 Discharge at Ghorband river observed and simulated calibration period 1984-1991

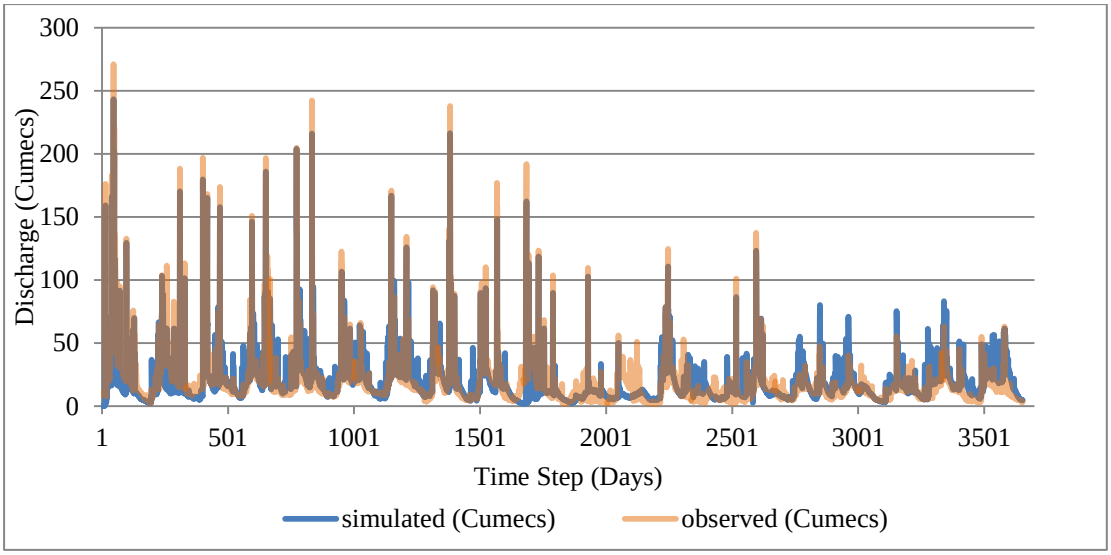

Fig. 5.21 Discharge at Ghorband river observed and simulated validation period 1992-2010

Table 5.14 Statistical parameter for evaluation of model performance for sediment

	R^2	NSE	PBIAS
Gilgit Watershed			
Calibration	0.93	0.849	12
Validation	0.96	0.903	-7.8
Ghorband Watershed			
Calibration	0.91	0.81	10
Validation	0.92	0.90	-8

R^2= Coefficient of determination
NSE= Nash-Sutcliffe Efficiency
PBIAS = Percent Bias

The statistical parameters to check the performance of the model show the agreement of observed and simulated values of flow and sediment yield, therefore we can say that the model results are reasonable and realistic. The main source of runoff in the Gilgit river basin is snowmelt, the main source of runoff in Ghorband river is rainfall.

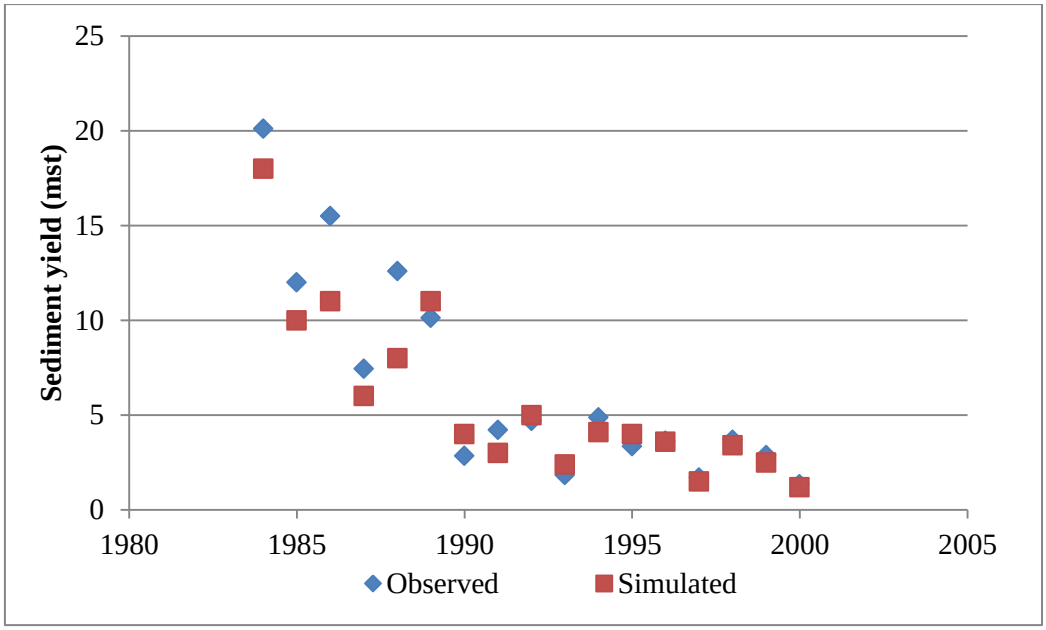

Fig. 5.22 Observed and Simulated sediment yield in Gilgit river at Gilgit for calibration period 1984-2000

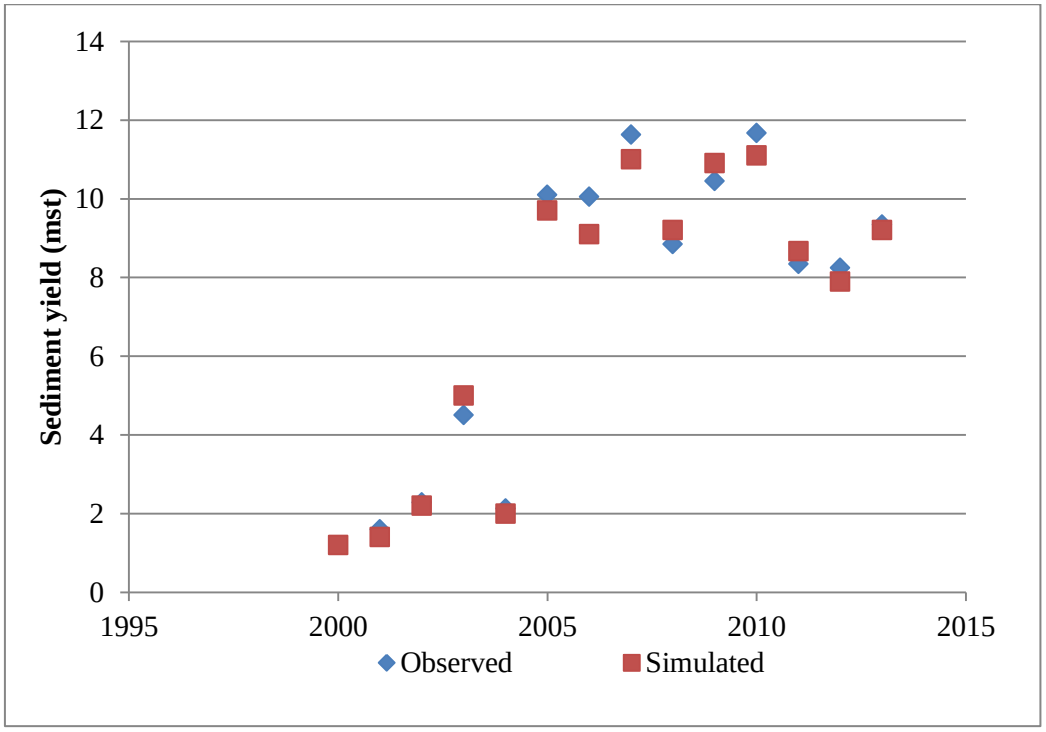

Fig. 5.23 Observed and Simulated sediment yield in Gilgit river at Gilgit for validation period 1984-2000

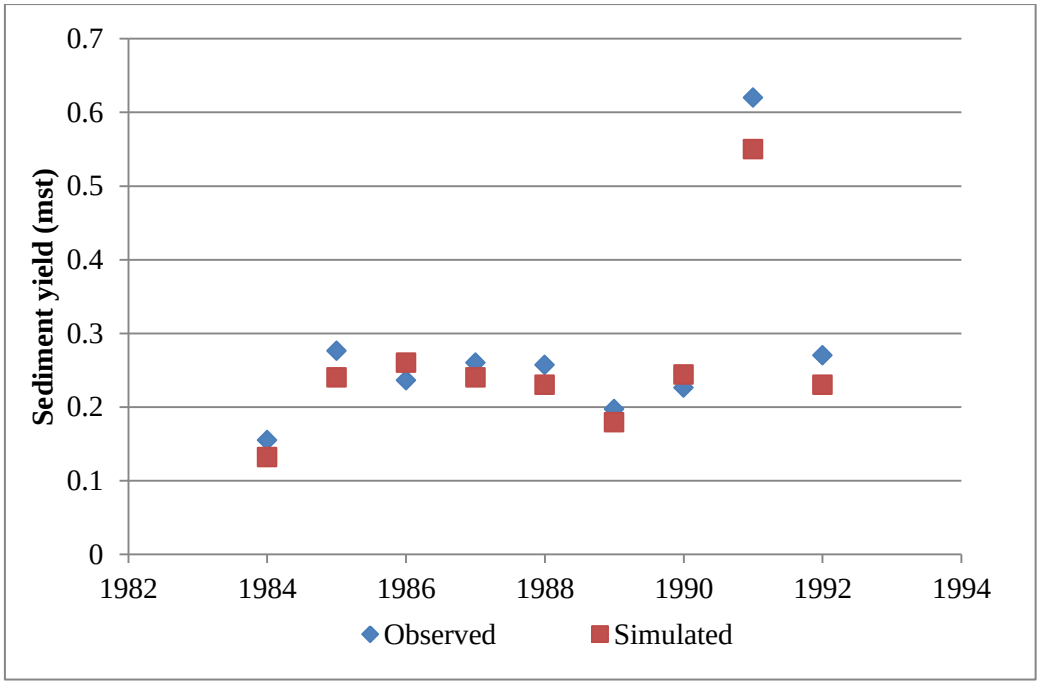

Fig. 5.24 Observed and Simulated sediment yield in Gilgit river at Gilgit for calibration period 1984-1992

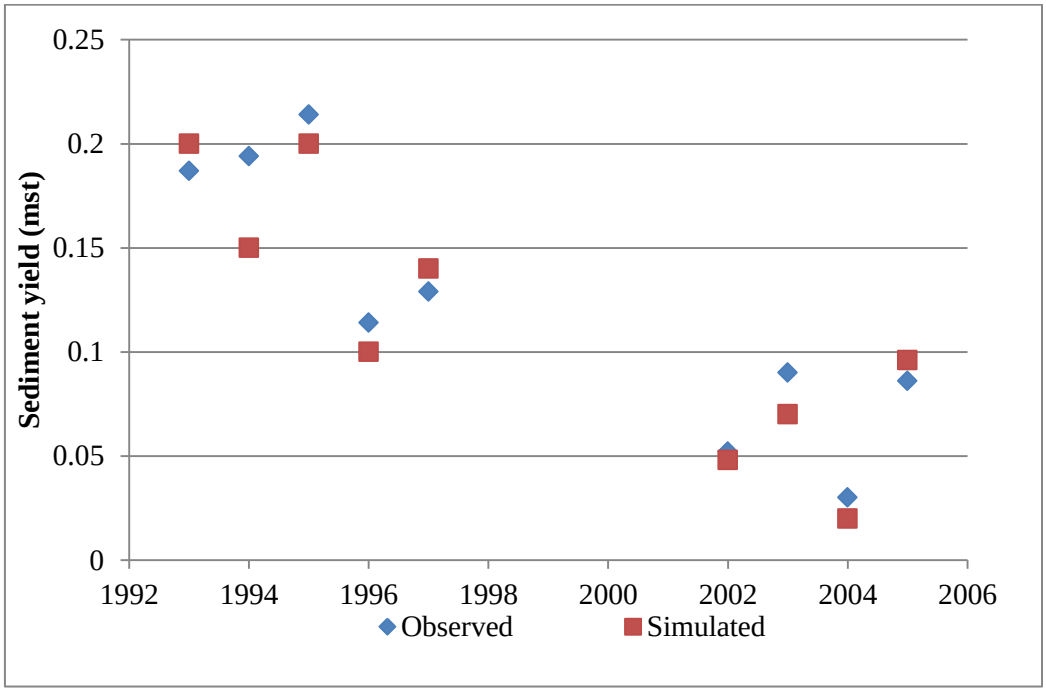

Fig. 5.25 Observed and Simulated sediment yield in Gilgit river at Gilgit for validation period 1993-2005 (1998-2001 period not measured by SWHP, WAPDA)

The results of studies shows that Per decade average annual sediment yield in in Gilgit river is increasing as shown in Figure 5.26. Per decade average annual sediment yield Ghorband river at Karora is increased for the period 1991-2000 as compared to the period 1981-1990 and then reduces 2001-2010 as shown in Figure 5.27. The reduction in sediment yield is due to the reduction in in average annual discharge. It was observed that percent of sediment is reducing during the monsoon period in Gilgit and Ghorband river as shown in Table 5.15.

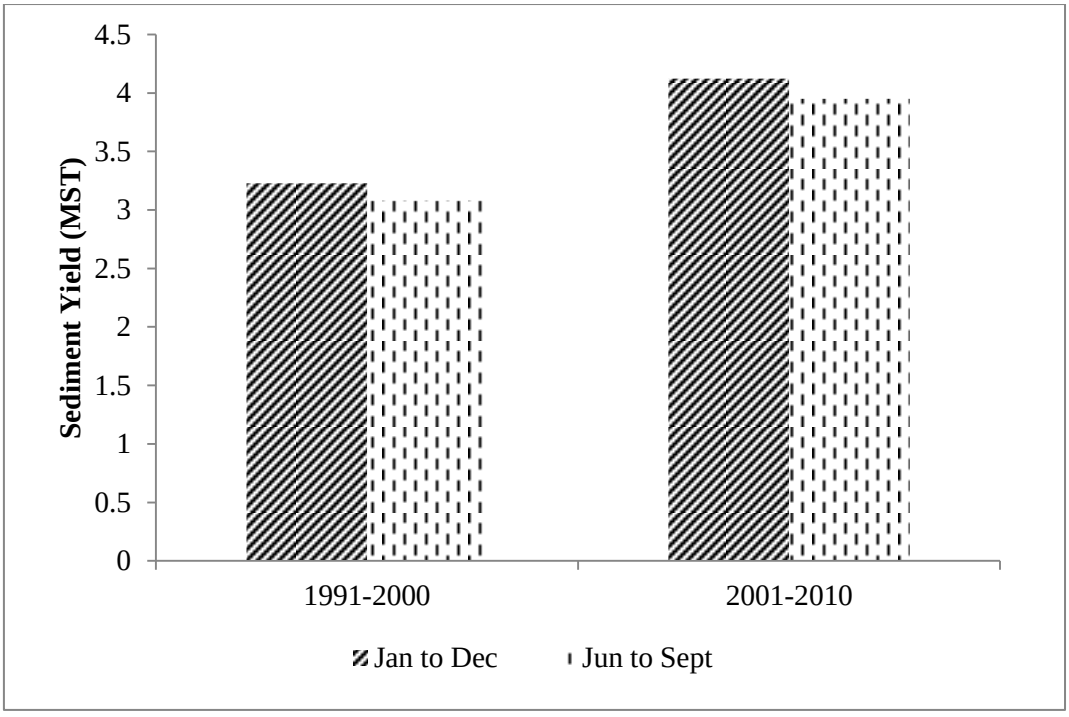

Fig. 5.26 Per Decade Variation in Sediment Yield Gilgit River at Gilgit (1991-2010)

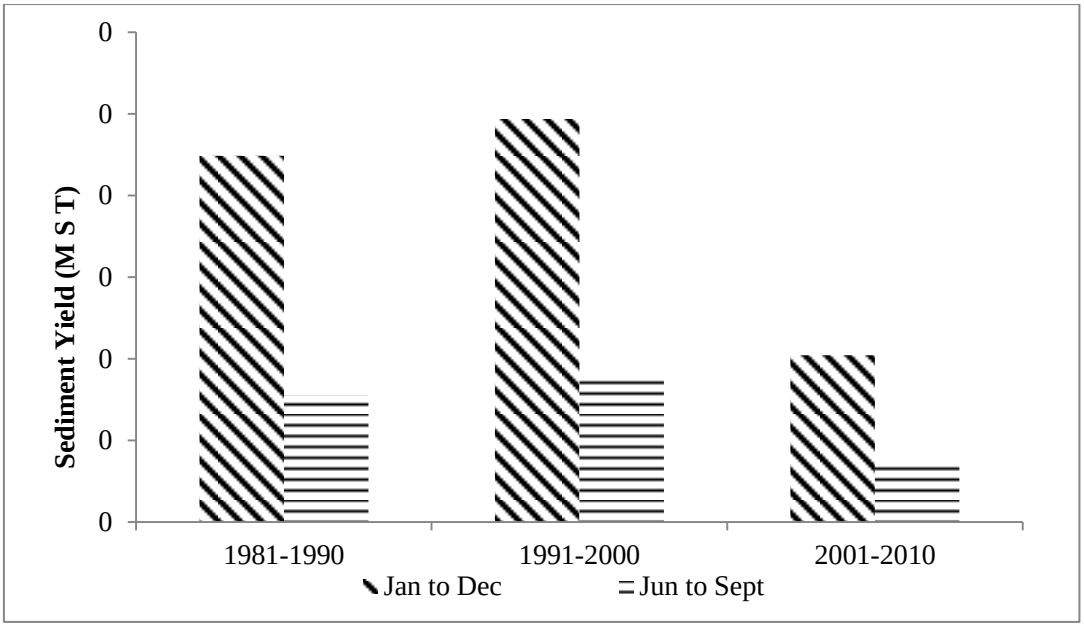

Fig. 5.27 Per Decade Variation in Sediment Yield Ghorband River at Karora (1981-2010)

In Gilgit river percent per decade sediment yield has been reduced from 98% to 92% for the 1981-1990 to 2001-2010 respectively. On the other hand in Ghorband river at karora percent per decade sediment yield has been reduced from 50% to 37% for the 1981-1990 to 2001-2010. The reduction in sediment yield is an indication of shift of the flow pattern from monsoon season.

Table 5.15 Percent of Average Sediment yield in monsoon (June to September)

Period	Gilgit river at Alam Bridge	Gilgit River at Gilgit	Ghorband River at Karora
1981-1990	97	98	50
1991-2000	96	94	49
2001-2010	95	92	37

1.1.8 **5.12.2 Impact of Projected Climate on Discharge and Sediment Yield**

It was observed that average annual discharge in Gilgit river at Gilgit form 1963 to 1983 and 1984-2014 is 267.26 and 290.87 cumecs respectively. It is clearly noted that for period thirty (1984-2013) 23.61 cumecs (9 percent) increase in discharge has been observed. The projected annual percentage change in discharge and sediment, relative to the baseline (1984-2014) in the Gilgit river basin has presented in

. The results of the study indicates that average annual discharge for the period 2015-2040, 2041-2070 and 2071-2099 is expected to increase 17, 19 and 7% respectively. Average annual sediment yield for the period 2015-2040, 2041-2070 and 2071-2099 is expected to increase 27, 30 and 13% respectively. At the end of 21th century (2099) 14% increase in average discharge is expected to increase and average annual sediment yield will increase upto 24%. The increase in the future discharge in the Northern part of Pakistan is also confirmed by Ali et al. (2015) who reported an increase specifically in the winter months in the upper Indus basin

Table 5.16 Projected upto 2099 increase in discharge and sediment yield in Gilgit river basin

Year	Average annual Discharge (Cumees)	Percent increase in Discharge	Average annual Sediment yield (m.s.t)	Percent increase sediment yield
2015-2040	334.37	17%	11.91	27%
2041-2070	340.32	19%	12.20	30%
2071-2099	306.45	7%	10.58	13%
2015-2099	327.28	14%	11.57	24%

It was observed that average annual discharge in Ghorband river at Gilgit form 1984 to 2010 18.47 cumecs average annual sediment yield 0.656 mst. The projected annual percentage change in discharge and sediment, relative to the baseline (1984-2014) in the Gilgit river basin has presented in Table 5.17. The results of the study indicates that average annual discharge for the period 2011-2040, 2041-2070 and 2071-2099 is expected to increase 12, 12 and 16% respectively. Average annual sediment yield for the period 2015-2040, 2041-2070 and 2071-2099 is expected to increase 17, 19 and 24% respectively. At the end of 21th century (2099) 13% increase in average discharge is expected to increase and average annual sediment yield will increase upto 20%.

Table 5.17 Projected upto 2099 increase in discharge and sediment yield in Ghorband river

Year	Average annual Discharge (Cumees)	Percent increase in Discharge	Average annual Sediment yield (m.s.t)	Percent increase sediment yield
2011-2040	20.65	12%	0.769	17%
2041-2070	20.78	12%	0.781	19%
2071-2099	21.40	16%	0.811	24%
2015-2099	20.94	13%	0.787	20%

CHAPTER 6
SUMMARY, CONCLUSIONS AND RECOMMENDATION

In this chapter, summary and conclusions are drawn from the results of the research are presented. It further highlights the recommendations for future researchers.

6.1 SUMMARY

Climate is globally changing at an alarming rate and the river flows are directly affected by the rainfall patterns and snowmelt. The discharge in the river, rainfall intensity, and rainfall erodibility affect the soil erosion and sedimentation. The soil which erodes from one place transports with the water and settle down and other areas and adversely affect the water availability, reducing the storage capacity of reservoirs. As per Intergovernmental Panel on Climate Change (IPCC) (IPCC, 2008), the global average surface temperature has increased by 0.074°C (± 0.018°C) and 0.13°C (± 0.03°C) per decade over the past 100 years (1906–2005) and 50 (1956-2005) years respectively. Since 1981, the rate of warming is faster, with a value of approximately 0.177 °C (±0.052°C) per decade This makes it necessary to project the sediment yield that a certain river basin is expecting, especially if there is an important hydraulic structure located in that river.

The purpose of the study was to assessment of change in Climate parameters i.e Precipitation, Temperature and their impact on land use changes. Modeling in climate change impact on runoff and sediment yield in selected basins/catchments of upper Indus basin (Gilgit and Ghorband river cacthments) then projection of climate change scenarios for potential change in Snow cover, Glaciers and sediment flows of

selected area and management options under changed climate conditions. For this purpose fifty-four years (54) (1961-2014) year's temperature, precipitation and stream flow data of 25 climatic and thirty-five (35) hydrometric stations historic data has been collected and trend analysis was performed using a non-parametric approach man-kandal statistical test. Results indicates that the overall increase in annual mean and maximum temperature in UIB for the selected period and mean annual temperature in lower part of upper Indus basin has decreased. Annual rainfall in upper Indus basin is increasing where as in low elevated area it is decreasing. During the winter and summer season at 81% and 83% of stations rainfall is increasing respectively. Average annual flows in highly elevated areas (Snow Cover) tributaries are increasing and in low elevated region it is decreasing. MODIS (MOD10A2) data for the period 2001-2016 has been used to estimate the variation in the snow and glacier cover area in Gilgit and Ghorband catchments. Results indicate that annual and seasonal snow cover area has been decreased in Ghorband river catchment whereas annual and seasonal snow cover area has been increased in Gilgit river basin. Statistical downscaling model (SDSM) model was used downscale climate variables (precipitation and temperature). Historical data of thirty years (1984-2014) of seven climate stations were used to develop the relationship between large scale variables with local scale variables and a quantitative approach was used to select the most dominant predictors. In Gilgit river basin at the end of 21^{th} century mean annual maximum and minimum temperature is expected to increase 2.33 ^{0}C and 1.25 ^{0}C respectively. Seasonal temperature will also increasing i.e. Winter DJF(December, January, February), Spring MAM (March, April, May), Summer JJA (June, July, August) and Autumn SON (September, October, November) Tmax 1.1, 1.04, 2.9 and 2.5, Tmin 0.9, 0.62, 1.84 and 1.98 ^{0}C respectively. In Ghorband river catchment at the

end of 21th century (2099) mean annual maximum and minimum temperature will expected to increase 1.94 ^{0}C and 1.99 ^{0}C respectively. Seasonal temperature will also increasing i.e. Winter, Spring, Summer and Autumn Tmax 1.68,2.15, 2.69 and 1.25, Tmin 0.91, 2.46, 2.41 and 2.48 ^{0}C respectively. Average annual and seasonal (winter, spring, summer and autumn) precipitation in Gilgit river basin will increase 24, 23, 26, 20 and 28% respectively. Average annual and seasonal (winter, spring, summer and autumn) precipitation in Ghorband river basin will increased 9, 12, 2, 13 and 12% respectively.

The baseline temperature and precipitation data, historical landuse and soil data are then used to formulate integrated models of Gilgit river and Ghorband river in Arc SWAT 2012. The output of the model are discharge and sediment yield. The results of discharge and sediment yield were compared with the observed discharge and sediment yield data, and model parameters are adjusted to get an agreement between simulated and observed values of discharge and sediment. Model performance was evaluated by co-efficient of determination (R^2), Nash Sutcliffe efficiency coefficient (NSE) and PBIAS (percentage bias). The model, once calibrated, was fed with the future climate data from the SDSM . Percent increase in discharge Gilgit river at Gilgit from the base period (1984-2014) for period 2015 2040, 2041-2070 and 2071-2099 is 27, 30, 13% respectively and overall increase in discharge from 2015 to 2099 is 14%. Percent increase in sediment yield Gilgit river at Gilgit from the base period (1984-2014) for period 2015-2040, 2041-2070 and 2071-2099 will 27, 30, 13% respectively and overall increase in discharge from 2015 to 2099 is 24%. Percent increase in discharge Ghorband river at karora from the base period (1984-2010) for period 2011 2040, 2041-2070 and 2071-2099 will 12, 12, 16%

respectively and overall increase in discharge from 2011 to 2099 is 13%. Percent increase in sediment yield Ghorband river at karora from the base period (1984-2010) for period 2011-2040, 2041-2070 and 2071-2099 will 17, 19, 24% respectively and overall increase in discharge from 2015 to 2099 is 20%.

Two sediment management options, i.e., check dam and sediment basin; and two erosion reduction options, i.e., filter strip and grassed waterways; are provided in the SWAT model and the resulting sediment yield after each case was observed. It was found out that the most efficient option is to provide sediment basin in the high sediment yield areas and that can reduce the sediment yield up to 65% of the total sediment yield in the basin. Other options, check dam, filter strip and grassed waterway reduce the sediment yield by 58, 54 and 48% of the total generated sediment yield in the basin, therefore, providing sediment basin the best alternative.

6.2 CONCLUSIONS

After analysis of available historical climate data and projection of future scenario following conclusions have been drawn.

1. In upper region (snow covered) of UIB the annual maximum temperature is increasing whereas in lower region it is decreasing. In high elevated snow covered region, per decade mean and maximum temperature is increasing, whereas in low elevated areas minimum temperature has decreasing trends. Tmax is increasing more than Tmin. Winter and spring season temperature is also increasing at most of the stations.

2. Annual and seasonal Precipitation in the region is increasing; It increases with the increase in elevation and deceasing with decease in elevation. Majority (81%) of stations has the increasing trends during the winter precipitation, during the spring season 50% of stations have the increasing trends, during the summer season at the 83% of stations precipitation trends are increasing significantly and during the autumn season at the higher elevated areas precipitation is increasing significantly.

3. Average Annual flows in Highly elevated areas (Snow Cover) tributaries is increasing and in low elevated region it is decreasing, whereas during the winter and spring monthly flow is increasing due to the increase in temperature (earlier melt of snow), during the summer it is decreasing due the decrease in temperature during the summer season.

4. Results indicate that annual and seasonal snow cover area is decreasing in Ghorband river catchment and annual and seasonal snow cover area is increasing in Gilgit river basin.

5. At the end of 21^{th} century in Gilgit river basin mean annual maximum and minimum temperature is expected to increase 2.33 ^{0}C and 1.25 ^{0}C respectively, and in Ghorband river catchment Tmax and Tmin expected to increase 1.94 and 1.99 ^{0}C.

6. As a result of increase in temperature average annual discharge and sediment yield in Gilgit has is expected to increase 14 and 24%, where as in Ghorband river discharge and sediment yield is also expected to increase 13 and 20% respectively.

7. Options for the reduction of erosion and consequent sediment origination control were simulated and compared. which lead to the primary outcome of this research, that the provision of sediment basin for management of sediment yield in the Gilgit and Ghorband river basin can reduce sediment yield 65%.

8. Analysis of temperature, precipitation and stream flow that the phenomenon of the climate change is occurring in the upper Indus basin, it is alarming for the planner and water experts to guide and adopt the Integrated Watershed Management to fulfill the fore coming food and water demands.

6.3 RECOMMENDATION

1. As per WMO (1994) for hilly areas, minimum rain gauge density for the non-recording is 250 Km^2 and for recording 2500 Km^2 so more climatic stations should be installed in the Gilgit and Ghorband river basins as they are currently insufficient and do not meet the WMO gauge density criterion for the minimum number of gauges in a hilly area.

2. The study has been conducted using SDSM, future Scenario's for Temperature and precipitation can be generated by using dynamic down scaling models

3. Climate change has a significant effect on temperature, precipitation and stream flows of mountainous watershed so it is recommended that climate change study should preferably be made prior to the construction of water resources & agriculture related projects

4. Snow cover analysis has been performed using MODIS satellite data, the analysis can be performed using finer resolution satellite data

REFERENCE

Adnan M, Nabi G and et al. (2017). "Snowmelt runoff prediction under changing climate in the Himalayan cryosphere: A case of Gilgit River Basin Elsevier Geoscience Frontiers 8 (2017) 941-949.

Ahmad W., Fatima A., Awan U K., and Anwar A., (2014). "Analysis of long term meteorological trends in the middle and lower Indus Basin of Pakistan—A non-parametric statistical approach" Global and Planetary Change 122 (2014) 282–291.

Ahmad Z., Hafeez M., and Ahmad I., (2012). "Hydrology of mountainous areas in the upper Indus Basin, Northern Pakistan with the perspective of climate change" Environ Monit Assess (2012) 184:5255–5274 DOI 10.1007/s10661-011-2337-7.

Ali, S., Li, D., Congbin, F., & Khan, F. (2015). "Twenty first century climatic and hydrological changes over Upper Indus Basin of Himalayan region of Pakistan". Environmental Research Letters, 10(1), 014007.

Amene, L. (2005). "Reservoir Siltation in the Dry lands of Northern Ethiopia: Causes, Source Areas and Management Options" (Doctoral dissertation, Pub).

Arnold, J. G., Srinivasan, R., Muttiah, R. S., and William, J. R. (1998). "Large area hydrologic modeling and assessment-Part I: model development". Water Resources Association, 34(1), 73 –89 (1998).

Bates B. C., Kundzewicz Z. W., Wu S. and Palutikof J. (2008). "Climate Change and Water. Technical Paper of the Intergovernmental Panel on Climate Change", IPCC Secretariat, Geneva.

Bavay M., Grünewald T. and Lehning L., (2013). "Response of snow cover and runoff to climate change in high Alpine catchments of Eastern Switzerland" Advances in Water Resources 55 (2013) 4–16.

Bewley D., Alila Y., and Varhola A., (2010). "Variability of snow water equivalent and snow energetics across a large catchment subject to Mountain Pine Beetle infestation and rapid salvage logging" Journal of Hydrology 388 (2010) 464–479.

Bhatti A M., Koike T., and Shrestha M., (2016). "Climate change impact assessment on mountain snow hydrology by water and energy budget-based distributed hydrological model" Journal of Hydrology 543 (2016) 523–541.

Chang H., and Jung W., (2010). "Spatial and temporal changes in runoff caused by climate change in a complex large river basin in Oregon" Journal of Hydrology 388 (2010) 186–207.

Chen j., and et al (2014). “Variability and trend in the hydrology of the Yangtze River, China: Annual precipitation and runoff” Journal of Hydrology 513 (2014) 403–412.

Chu J, Xia J, Xu CY, Singh, V. (2010). “Statistical downscaling of daily mean temperature, pan evaporation and precipitation for climate change scenarios in Haihe River, China”. Theor Appl Climatol 99 (1):149–161. doi:10.1007/s00704-009-0129-6.

Cousino K L., Becker R H., Zmijewski K A., (2015). “Modeling the effects of climate change on water, sediment,and nutrient yields from the Maumee River watershed Luke” Journal of Hydrology: Regional Studies xxx (2015) xxx–xxx.

D. Serpa D., Nunes J.P., Santos J., Sampaio E., Jacinto R., Veiga S., Lima J.C., Moreira M., Corte-Real J., Keizer J.J., and Abrantes N., (2015). “Impacts of climate and land use changes on the hydrological and erosion processes of two contrasting Mediterranean catchments” Science of the Total Environment 538 (2015) 64–77.

Ding Y, Ren G, Zhao Z, Xu Y, Luo Y, Li Q, Zhang J. (2007). “Detection, causes and projection of climate change over China: an overview of recent progress”. Advances in Atmospheric Sciences 24: 954–971.

“Ethiopian Highlands”. (2016). Journal of Agricultural and Biological Engineering September 2016.

Fischer T., Gemmer M., Liu L.,and Su B., (2010). “Trends in Monthly Temperature and Precipitation Extremes in the Zhujiang River Basin, South China (1961-2007)” National Climate Center, China Meteorological Administration, Beijing 100081, China, Advances in Climate Change Research 1(2): 63-70, 2010.

Gautam M. R., a, Acharya K., and Mohan K. Tuladhar M. K., (2010), “Upward trend of streamflow and precipitation in a small, non-snow-fed, mountainous watershed in Nepal” Journal of Hydrology 387 (2010) 304–311.

Haguma, D., Leconte, R., Cote, P., Krau, S., & Brissette, F. (2014). “Optimal Hydropower Generation Under Climate Change Conditions for a Northern Water Resources System”. Water Resources Management, 28(13), 4631-4644.

Hall, D., Riggs, G. and Salomonson, V., (2006). “Updated weekly, MODIS/Terra Snow Cover 8-Day L3 Global 500m Grid V005, [March 2000 to December 2009]. Boulder, Colorado USA: National Snow and Ice Data Center. Digital media.

Hall, D., Riggs, G., Salomonson, V.V., DiGirolamo, N. and Bayr, K. (2002). “MODIS snow-cover products. Remote-sensing of Environment”, 83: 181 - 94.

Hannaford J., and Buys G., (2012). “Trends in seasonal river flow regimes in the UK” Journal of Hydrology 475 (2012) 158–174.

Hashmi M, Shamseldin A, Melville B (2011). “Comparison of SDSM and LARS-WG for simulation and downscaling of extreme precipitation events in a watershed”. Stoch Env Res Risk A 25 (4):475–484. doi:10.1007/s00477-010-0416-x

Huang J, Zhang J, Zhang Z, Xu C, Wang B, Yao J. (2011). "Estimation of future precipitation change in the Yangtze River basin by using statistical downscaling method". Stoch Env Res Risk A 25(6):781–792. doi:10.1007/s00477-010-0441-9.

Iida T., Kajihara A., OkuboH., and Okajima K. (2012). "Effect of seasonal snow cover on suspended sediment runoff in a mountainous catchment" Journal of Hydrology 428–429 (2012) 116–128.

IPCC AR4 (Intergovernmental Panel on Climate Change Fourth Assessment Report), (2008). "Climate change and water 2007". IPCC Technical paper VI (htt://www.ipcc.ch/pdf). [Accessed 20 June 2008].

Kahlown, M. A., Raoof, A., Zubair, M., and Kemper, W. D., (2007). "Water use efficiency and economic feasibility of growing rice and wheat with sprinkler irrigation in the Indus Basin of Pakistan". Agriculture Water Management. 87, 292-298.

Khadka D., Babel M S., Shrestha S., and Tripathi N K., (2-14). "Climate change impact on glacier and snow melt and runoff in Tamakoshi basin in the Hindu Kush Himalayan (HKH) region" Journal of Hydrology 511 (2014) 49–60.

Kumar S., and et al (2009). "Stream flow trends in Indiana: Effects of long term persistence, precipitation and subsurface drains" Journal of Hydrology 374 (2009) 171–183.

Lida T., Kajihara A., Okubo H., and Okajima K., (2012). "Effect of seasonal snow cover on suspended sediment runoff in a mountainous catchment" Journal of Hydrology 428–429 (2012) 116–128.

Lorenzo-Lacruz J., Vicente-Serrano S M., López-Moreno J.I., Morán-Tejeda E., and Zabalza J., (2012). "Recent trends in Iberian stream flows (1945–2005)" Journal of Hydrology 414–415 (2012) 463–475.

Luo Y. Ficklin D L., Liu X., and Zhang M., (2013). "Assessment of climate change impacts on hydrology and water quality with a watershed modeling approach". Science of the Total Environment 450–451 (2013) 72–82.

Mahmood R., Babel M S., JIA S., (2015). "Assessment of temporal and spatial changes of future climate in the Jhelum river basin, Pakistan and India" Weather and Climate Extremes 10(2015)40–55.

Mukundan R., and et al (2013). "Suspended sediment source areas and future climate impact on soil erosion and sediment yield in a New York City water supply watershed, USA" Geomorphology 183 (2013) 110–119.

National Climate Change Policy (2012). "A report published by Ministry of Climate Change". Government of Pakistan September 2012.

Neitsch, S.L., J.G. Arnold, J.R. Kiniry, R. Srinivasan, and J.R. Williams (2002). "Soil and Water Assessment Tool: User Manual, Version 2000", TWRI Rep. TR-192, 455 pp., Texas Water Resources Institute, College Station, TX.

Okalp, K. (2005). "Soil erosion risk mapping using geographic information systems: a case study on Kocadere creek watershed", Izmir (Doctoral dissertation, Middle East Technical University).

Panday, P.K., Brown, M.E., (2010). "Snowmelt Runoff Modeling in the Tamor River Basin in the Eastern Nepalese Himalaya". Department of Geography, Clark University, Worcester, U.S.A.

Rahman K., Maringanti C., Beniston M., Widmer F., Abbaspour K., and Lehmann A., (2012). "Streamflow Modeling in a Highly Managed Mountainous Glacier Watershed Using SWAT: The Upper Rhone River Watershed Case in Switzerland" Water Resource Manage DOI 10.1007/s11269-012-0188-9.

Rahman, K., Maringanti, C., Beniston, M., Widmer, F., Abbaspour, K., & Lehmann, A. (2013). "Streamflow Modeling in a Highly Managed Mountainous Glacier Watershed Using SWAT: The Upper Rhone River Watershed Case in Switzerland". Water Resources Management, 27(2), 323-339.

S.D. Nerantzaki S D., Giannakis G V., Efstathiou D., Nikolaidis N.P., Sibetheros I.A., Karatzas G.P., Zacharias I., (2015). "Modeling suspended sediment transport and assessing the impacts of climate change in a karstic Mediterranean watershed". Science of the Total Environment 538 (2015) 288–297.

Schober J., Schneider K., Helfricht K., Schattan P., Achleitner S., Schöberl F., Kirnbauer R., (2014). "Snow cover characteristics in a glacierized catchment in the Tyrolean Alps - Improved spatially distributed modelling by usage of Lidar data "Journal of Hydrology 519 (2014) 3492–3510.

Shannak S., (2017). "Calibration and validation of SWAT for sub-hourly Time steps using Swat-Cup". International journal of sustainable water and Environment systems Vol 9 No.1 (2017) pp 21-27.

Sonali P., and Kumar D N., (2013). "Review of trend detection methods and their application to detect temperature changes in India" Journal of Hydrology 476 (2013) 212–227.

Sun W., and et al (2016). "Changes in extreme temperature and precipitation events in the Loess Plateau (China) during 1960–2013 under global warming" Atmospheric Research 168 (2016) 33–48.

Tahir A A., Chevallier P., Arnaud Y., Neppel L., and Ahmad B., (2011). “Modeling snowmelt-runoff under climate scenarios in the Hunza River basin, Karakoram Range, Northern Pakistan” Journal of Hydrology 409 (2011) 104–117

Tao H., Gemmer b M., Bai c Y., Su b B., Mao d W., (2011). “Trends of streamflow in the Tarim River Basin during the past 50 years: Human impact or climate change?” Journal of Hydrology 400 (2011) 1–9.

Wilby RL, Dawson CW, Barrow EM (2002). “SDSM—a decision support tool for the assessment of regional climate change impacts”. Environ Model Software 17(2):145–157. doi:10.1016/s13648152(01)00060-3

Winchell M. and et al (2013). “User’s Guide Arcswat Interface for Swat2012 Blackland Research and Extension Center, Texas Agri-life Research, 720 East Blackland Road - Temple, Texas 76502, Grassland, Soil and Water Research Laboratory, USDA Agricultural Research Service, 808 East Blackland Road - Temple, Texas 76502.

Wing H. Cheung, W. H., Senay, G. B. and Singha, A. (2008). “Trends and spatial distribution of annual and seasonal rainfall in Ethiopia”. Int. J. Climatol. 28: 1723–1734.